Fluoropolymer Nanoparticles Synthesized via Reversible-Deactivation Radical Polymerizations and Their Applications

Zexi Zhang, Kaixuan Chen, Bruno Ameduri, Mao Chen

Fluoropolymer Nanoparticles Synthesized via Reversible-Deactivation Radical Polymerizations and Their Applications

Journal:	*Chemical Reviews*
Manuscript ID	Draft
Manuscript Type:	Review
Date Submitted by the Author:	n/a
Complete List of Authors:	Zhang, Zexi ; Fudan University Chen, Kaixuan; Fudan University, Department of Macromolecular Science Ameduri, Bruno; University of Montpellier Chen, Mao; Fudan University, Department of Macromolecular Science

Fluoropolymer Nanoparticles Synthesized via Reversible-Deactivation Radical Polymerizations and Their Applications

Zexi Zhang,[a] Kaixuan Chen,[a] Bruno Ameduri,*[b] Mao Chen*[a]

[a]Department of Macromolecular Science, State Key Laboratory of Molecular Engineering of Polymers, Fudan University, Shanghai 200438, China

[b]Institute Charles Gerhardt of Montpellier (ICGM), CNRS, University of Montpellier, ENSCM Montpellier, France

Outline

Abstract

Fluorinated polymeric nanoparticles (FPNPs) combine unique properties of fluoropolymers and polymeric nanoparticles, stimulating massive interests in academia and industries for decades. However, fluoropolymers are not directly available from natural sources, resulting in developments of conventional techniques to obtain FPNPs based on free radical polymerizations. Recently, while increasing areas demand tailored FPNPs of complicated architectures and/or compositions as motivated by cutting-edge areas, such materials are difficult to be prepared through conventional approaches. During the past few years, reversible-deactivation radical polymerizations (RDRPs) have become powerful methods to afford well-defined polymers. Researchers have applied RDRPs to the fabrication of FPNPs, enabling the construction of particles with improved complexity in terms of structure, composition, morphology, functionality and so on. Such examples are classified into three categories. First, well-defined fluoropolymers synthesized via RDRPs have been utilized as precursors to form FPNPs. For example, self-folding, solution self-assembly have been developed for fluoropolymers of various sequences. Second, thermal- and photo-initiated RDRPs have been explored to realize in-situ preparations of FPNPs, facilitating the direct synthesis via polymerization-induced self-assembly, cross-linking copolymerization to afford FPNPs of varied morphologies. Third, grafting from inorganic nanoparticles has been investigated based on RDRPs. Importantly, these synthetic advancements have promoted investigations toward promising applications, including magnetic resonance imaging, biomedical delivery, energy storage, adsorption of perfluorinated alkyl substances, photosensitizers and so on. This review should present useful knowledge to researchers in polymer science and nanomaterials, and inspire innovative ideas for the synthesis of FPNPs and expand their applications.

Keywords

fluoropolymer, nanoparticle, polymer synthesis, reversible-deactivation radical polymerization

1. INTRODUCTION

Polymeric nanoparticles (PNPs) play an important role in nanomaterials due to their interesting physical and chemical properties caused by high relative surface area, quantum size effects, as well as characteristics brought from polymers (e.g., mechanical strength, chemical structure, polarity, solubility).[1-6] Fluorinated polymeric nanoparticles (FPNPs) combine attributes of both PNPs and unique properties of fluoropolymers, such as outstanding chemical and temperature stability, high hydrophobicity, low surface energy, low refractive index and others, and have stimulated massive interests in both academia and industries.[7-10] However, fluoropolymers are not available from natural sources. As a result, people have developed various synthetic approaches to obtain

FPNPs, leading to fluorinated materials of many applications in coatings, paintings, additives, electronics, photonics, and so forth during past decades.[9, 11, 12]

Conventionally, the most important strategy for the synthesis of FPNPs relies on free radical polymerization mechanism, which is compatible with water and has been largely employed in industry. A variety of synthetic techniques, such as emulsion polymerization, mini-emulsion polymerization, micro-emulsion polymerization, polymerization in supercritical fluids, have been developed to afford FPNPs of different morphologies, sizes and compositions, as well as FPNP-based mixtures (e.g., emulsions) of desirable formulations, concentrations and other features through free radical processes.[13-20] Fluorinated monomers including semi-fluorinated (meth)acrylates, tetrafluoroethylene (TFE), chlorotrifluoroethylene (CTFE), vinylidene fluoride (VDF), trifluoroethylene (TrFE) have been successfully adopted to yield FPNPs in water and organic solvents. FPNPs of different types have also been engineered to broaden their application scope.[21, 22] For example, people have synthesized matrix particles, whose entire compositions are almost the same fluoropolymers, and core-shell particles that contain non-fluorinated and fluorinated polymers, simultaneously.[19, 20, 23-25] However, free radical polymerizations lack control over chain growth, which frequently yield polymers of unpredictable chain lengths, broad dispersities, and are difficult to approach polymer sequences, topologies of increased complexity. In recent years, while more and more investigations have disclosed the importance of preparing well-defined polymers to achieve interesting properties, and revealed the necessities of macromolecular engineering in cutting-edge areas,[26-29] it is desirable to develop novel synthetic pathways to tailor FPNPs and explore properties of those customized materials.

During the past two decades, reversible-deactivation radical polymerizations (RDRPs) have become powerful methods to afford polymers of predefined molar masses, low dispersities and well-defined structures.[27, 30-33] For example, atom transfer radical polymerization (ATRP),[34, 35] reversible addition-fragmentation chain transfer (RAFT) polymerization,[36-38] nitroxide-mediated polymerization (NMP),[39] iodine transfer polymerization (ITP)[40, 41] have been systematically developed, and widely employed for controlled polymer synthesis. With those methods, polymer sequences (e.g., block, random, alternating), topologies (e.g., (hyper)branch, brush) could be finely tuned via rational design of (macro)initiators, chain transfer agents (CTAs), catalysts, reaction strategies (e.g., graft polymerization, gradual addition of agent), and/or combination with suitable monomers.

Motivated by the synthetic advantages, RDRPs have been applied to the synthesis of fluoropolymers,[28] which enable the construction of FPNPs with improved complexity in terms of chemical composition, morphology, functionality and so on. The synthetic methods could be mainly classified into two categories (Scheme 1). First, well-defined polymers synthesized via RDRPs have been utilized as precursors to yield FPNPs (section 2). In this category, the solution self-assembly of diblock, multi-block copolymers with fluorinated segments provides an important pathway to create FPNPs with attractive architectures, properties and functions. Beyond the aggregation of many macromolecular chains, it has been reported that the self-folding strategy of single fluorinated chains of block, even random sequences, could be highly reversible under folding/unfolding conditions. Second, FPNPs are directly generated during the process of RDRPs

under thermal or light-irradiation reaction conditions (section 3). Macroinitiators of controlled chain length, customized side groups are adopted for chain-extensions via RDRPs, leading to polymerization-induced self-assembly (PISA) that enables the in-situ formation of a series of morphologies such as spheres, worms, cylinders, vesicles and others at variable mass fractions. To enhance the stability of particles, transformations with small molecular cross-linkers are also examined to generate covalently cross-linked polymeric networks mediated by RDRPs. Additionally, with inorganic nanoparticles as substrates, surface-initiated RDRPs (SI-RDRPs) have been developed with fluorinated monomers to yield nanoparticles with fluoropolymer coatings (section 4). Based on the synthetic advancements, FPNPs have been investigated for a variety of potential applications (section 5) including magnetic resonance imaging (MRI), delivery of drugs, genes and proteins, energy materials, adsorption of perfluoroalkyl substances (PFASs), photodynamic therapy (PDT) and so on.

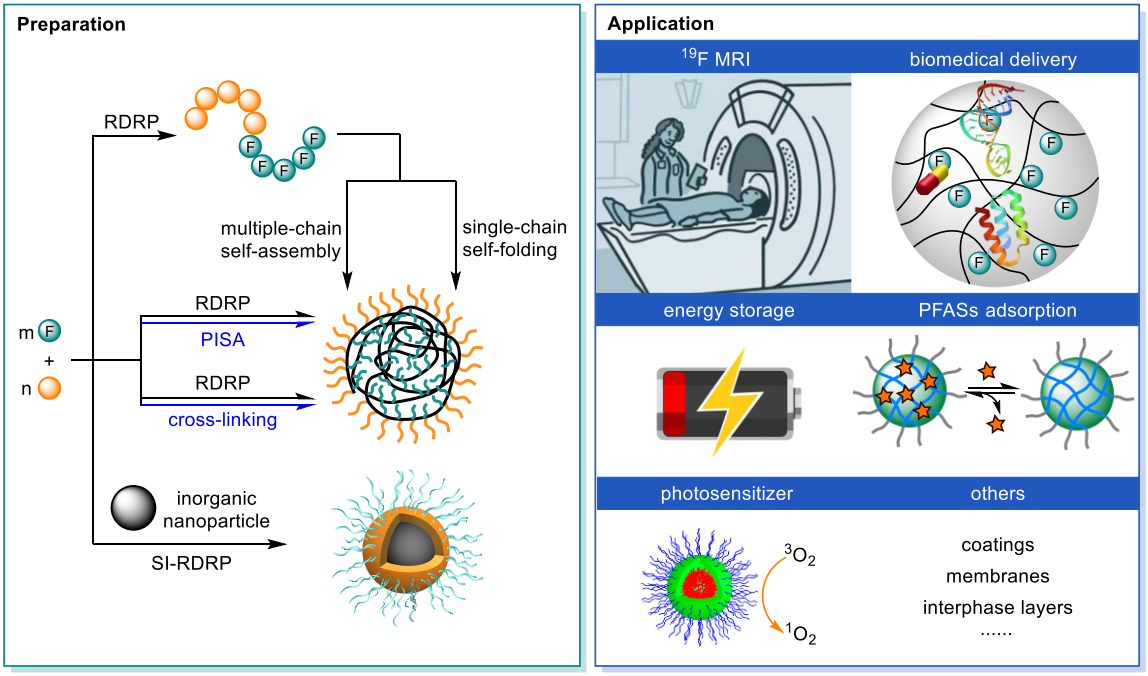

Scheme 1. Schematic illustration for the preparation of FPNPs based on RDRPs and applications in diverse directions. Reproduced with permission from ref [42]. Copyright 2020 American Chemical Society. Reproduced with permission from ref [43]. Copyright 2019 American Chemical Society.

Up to now, a number of reviews have summarized synthetic methods, techniques, as well as applications of PNPs,[1-6] and discussed the synthesis, properties of main-chain and side-chain fluoropolymers.[21, 22, 26, 28] Researchers have also systematically summarized methods and mechanisms of RDRPs.[27, 30-33] In recent years, increasing examples have disclosed attractive features of well-defined nanoparticles and fluoropolymers for high-tech purposes. This present review aims at highlighting advances of RDRPs employed to fabricate FPNPs, and the application studies of those customized FPNPs.

2. PREPARATION OF NANOPARTICLES WITH FLUOROPOLYMERS PREFORMED VIA RDRPS

2.1 Self-Assembly of Multiple Fluoropolymer Chains

Self-assembly has been developed as a powerful strategy for the fabrication of particles with ordered patterns.[44, 45] Organic and inorganic compounds, polymers could be utilized as sub-units for self-assembly. Amphiphilic block copolymers can associate into nanostructures as driven by the dynamic interfacial equilibrium between solvated and solvophobic segments.[46] Traditionally, the preparation of self-assembled PNPs generally includes three steps: 1) synthesis and purification of block copolymers; 2) dissolving copolymers in suitable solvents; 3) microphase separation in a diluted solution as driven by solvophobicity of one of the blocks in copolymers.[47] However, this strategy often provides PNPs of low concentrations (<1% w/w) in solvents. Benefited from RDRPs and other controlled/living polymerizations, tailor-designed block copolymers of predetermined block sequences, functional groups, block ratios, or hierarchical topologies (e.g., block on hyperbranched) could be prepared with easily accessible starting materials, furnishing great opportunities to establish a variety of morphologies.[48]

Due to the fluorophobic effect,[49, 50] highly crystalline fluoropolymers are normally neither miscible with water nor with most organic solvents. Consequently, copolymers with fluorinated segments have a strong tendency toward self-assembly when dispersed in solvents, and exhibit low critical concentrations. The unique fluorophobic property has enabled the preparation of FPNPs with both fluorophilic, lipophilic and hydrophilic segments,[51, 52] which expands the potentials of nanomaterials. However, poly(VDF) and copolymers of VDF are soluble in polar solvents,[53] limiting the preparation of nanoparticles in related solvents. Next, we will discuss the preparation of FPNPs by using fluoropolymers prepared with different RDRPs as bellows.

2.1.1 Fluoropolymers Synthesized via ATRP

The advancements of ATRP have allowed the construction of complex polymers using readily available activated alkyl halides as initiators and metal complexes as catalysts under thermal conditions.[34] The copper-catalyzed activation/deactivation equilibrium facilitates achieving good structural fidelity via simple reliable systems. As influenced by the monomer scope, fluorinated (meth)acrylates and styrene (St) derivates are most commonly employed to afford FPNPs based on ATRP.[54, 55] For example, DeSimone,[56] Matyjaszewski,[57] Boutevin,[58] Haddleton[59] and co-workers demonstrated the controlled synthesis of fluorinated poly(meth)acrylates with alkyl bromides and copper catalysts since the seminal works of ATRP.[60]

In 2001, the Wooley's group[61] reported the synthesis of poly(4-fluorostyrene)-*b*-poly(methyl acrylate) (poly(FSt)-*b*-poly(MA)) via a two-step Cu-catalyzed ATRP initiated from (1-bromoethyl)benzene using a pentamethyldiethylenetriamine ligand (Figure 1). After hydrolysis of the poly(methyl acrylate) (poly(MA)) segment into poly(acrylic acid) (poly(AA)), micelles were formed with the obtained amphiphilic diblock copolymers in aqueous mixtures, which were further stabilized by intra-micellar covalent cross-linking of poly(AA) blocks to generate shell-crosslinked FPNPs. The nanostructures of obtained samples were visualized by both atomic force microscopy (AFM) and transmission electron microscopy (TEM), providing multimodal size distributions, as well as clusters of both small and large shell-crosslinked FPNPs.

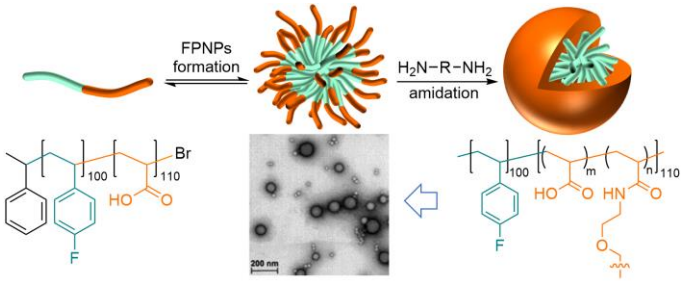

Figure 1. Schematic illustration for the formation of cross-linked FPNPs with poly(FSt)-*b*-poly(AA).[61] Reproduced with permission from ref [61]. Copyright 2001 John Wiley & Sons, Inc.

Besides diblock copolymers, amphiphilic ABA triblock copolymers were prepared based on Cu-catalyzed chain-extension polymerization from telechelic poly(ethylene oxide) (PEO) macroinitiator with two alkyl bromide terminals to afford FPNPs.[62] Huang and co-workers[63] demonstrated the synthesis of amphiphilic ABC triblock copolymers composed of hydrophilic PEO and poly(methacrylic acid) (poly(MAA)) segments, and hydrophobic poly(*p*-(2-(4-biphenyl) perfluorocyclobutoxy)phenyl methacrylate) sequence via Cu-catalyzed two-step chain-extensions from a PEO-based macroinitiator, which provided nanoscale micelles that can encapsulate hydrophilic (e.g., rhodamine) and hydrophobic (e.g., pyrene) molecules in neutral aqueous solution. Tsapis and co-workers[64] reported the synthesis of ABC triblock copolymers composed of PEO, polylactide and poly(heptadecafluorodecyl methacrylate) (poly(17FDMA)) segments based on the combination of ring-opening polymerization and ATRP starting from PEO macroinitiator. The amphiphilic triblock copolymers formed nanocapsules (mean hydrodynamic diameter (D_h) ≈ 110-140 nm) via an emulsion evaporation process, allowing the encapsulation of ultrasound contrast agents (UCAs) of perfluorooctyl bromide.

Howdle et al.[65] employed perfluoropolyether (PFPE) as the CO_2-philic portion, and prepared PFPE-*b*-poly(methyl methacrylate) (PFPE-*b*-poly(MMA)) diblock copolymers via ATRP in supercritical carbon dioxide ($scCO_2$). Because fluoropolymers possess good solubility in $scCO_2$, the fluorinated macroinitiator showed a dramatic impact on the dispersion polymerization of MMA, affording excellent yields (up to 97%) of spherical particles with mean particle diameter (D_n) down to 1.4 μm.[66] Although this method provided highly uniform sizes, fluorinated particles of smaller sizes could not be achieved. Later, Dong and co-workers[67] prepared poly(styrene-*r*-acrylonitrile)-*b*-poly(tetrahydroperfluorooctyl methacrylate) (poly(St-*r*-AN)-*b*-poly(13FOMA)) via ATRP, which was employed as a stabilizer in the dispersion copolymerization of acrylonitrile and vinyl acetate in $scCO_2$, affording spherical PNPs of D_n = 110-210 nm, particle size distribution (*PSD*) = 1.04-1.13.

Topologically controlled polymers have been synthesized as building blocks for FPNPs. Wooley and co-workers[68] developed self-condensing vinyl polymerization based on Cu-catalyzed ATRP of 4-chloromethyl styrene, lauryl acrylate and tris(4′-(2″-bromoisobutyryloxy)phenyl)ethane to yield hyperbranched star-like core capped with alkyl halide terminals (Figure 2). Subsequent chain-extension polymerization allowed the grafting of 2,2,2-trifluoroethyl methacrylate (TFEMA) and *tert*-butyl acrylate (tBA) from the star-like macroinitiator via ATRP. The amphiphilic, hyperbranched star-like copolymers gave fluorinated micelles (D_h = 20-30 nm by dynamic light

scattering (DLS)) that could be useful as nanoscopic magnetic resonance imaging (MRI) agents. Using alkyl bromides capped polyamidoamine dendrimers as a macroinitiator, the Ito group[69] demonstrated chain-extension polymerization using tetrafluoropropyl methacrylate and TFEMA as monomers via ATRP. Sizes (D_h) of FPNPs were controlled by molar mass of hyperbranched polymers in a range of 3-25 nm.

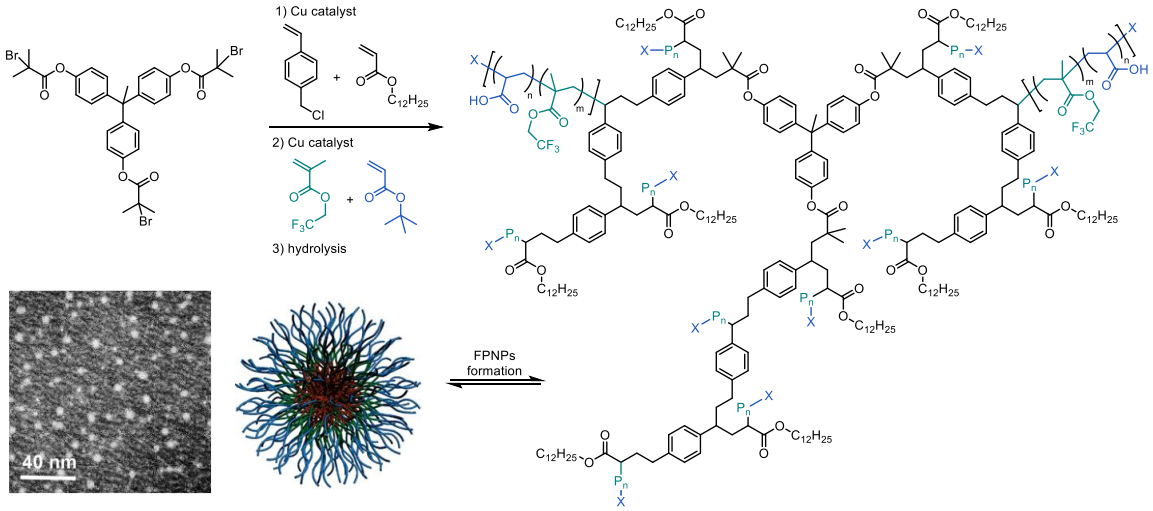

Figure 2. Schematic illustration for the preparation of FPNPs with branched polymers prepared via ATRP.[68] Reproduced with permission from ref [68]. Copyright 2008 American Chemical Society.

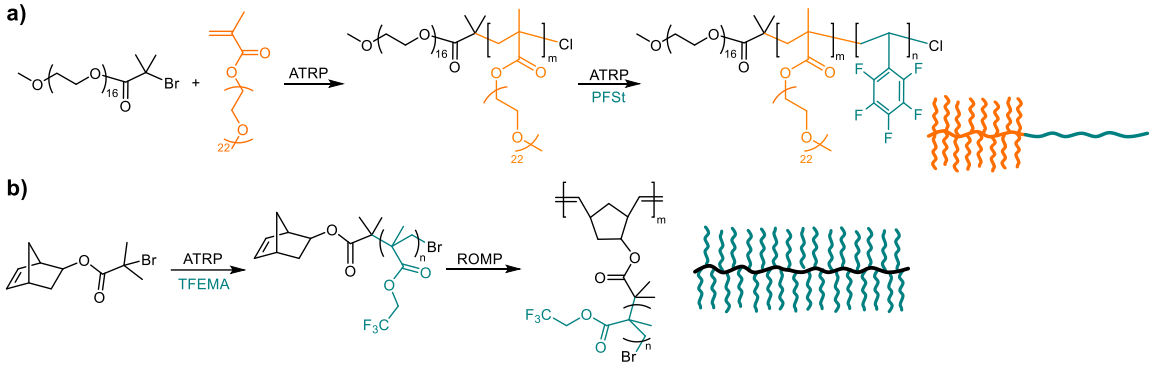

Scheme 2. Synthesis of brush copolymers based on ATRP. a) Synthesis via a two-step ATRP.[70] b) Synthesis via a sequence of ATRP/ROMP transformation.[71]

Fluorinated brush copolymers could also generate FPNPs via solution self-assembly. Davis and co-workers[70] synthesized brush-like amphiphilic diblock copolymers with poly[poly(ethylene glycol)methyl ether methacrylate] (poly(PEGMA)) and poly(pentafluorostyrene) (poly(PFSt)) segments via two-step ATRP (Scheme 2a). The micellar structure comprised of fluorinated core and hydrophilic branches as coronas, with D_h in a range of 54-112 nm as measured by the DLS instrument. Due to the lower critical solution temperature (LCST) of poly(ethylene glycol) (PEG)

brushes, an increase in a temperature leads coronas to dehydrate and shrink, resulting in temperature-dependent hydrodynamic radius of FPNPs. With the combination of Cu-catalyzed ATRP from alkyl bromide functionalized norbornene and Ru-catalyzed ring-opening metathesis polymerization, Hong and co-workers[71] prepared fluorinated bottlebrush polymers (Scheme 2b). These exhibited near spherical particles with the largest diameter of about 25 nm analyzed by TEM, suggesting a partially coiled backbone.

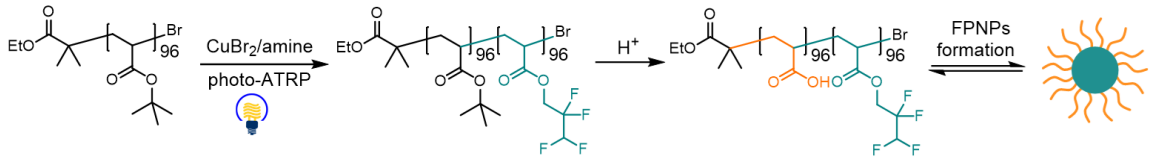

Scheme 3. Preparation of FPNPs via self-assembly of block copolymer synthesized via photo-ATRP/hydrolysis.[66]

Beyond ATRP conducted under thermal conditions, developments of photo-mediated RDRPs have broadened avenues of synthesizing FPNPs under mild conditions. In 2017, the Hawker group[66] reported the development of photo-mediated ATRP of fluorinated (meth)acrylates using $CuBr_2$ catalyst and tris(2-aminoethyl amine) ligand in 2-trifluoromethyl-2-propanol solvent under UV light irradiation (360 nm). This method enables the on-demand access of side-chain fluorinated polymers ($Đ \approx 1.1$) with tunable concentrations of fluorine atoms. High level of chain-growth control allows the facile generation of diblock copolymers of a broad monomer scope. For example, authors prepared poly(*tert*-butyl acrylate)-*b*-poly(trifluoroethyl acrylate) (poly(tBA)-*b*-poly(TFEA)) via the photo-mediated ATRP. The copolymer was hydrolyzed to poly(AA)-*b*-poly(TFEA) that forms micelles of $D_h \approx 30$ nm and a zeta potential of -26 mV in aqueous solution (Scheme 3).

2.1.2 Fluoropolymers Synthesized via RAFT Polymerization

RAFT polymerizations employ sulfur-based compounds (e.g., trithiocarbonates, dithioesters, dithiocarbamates, xanthates) as CTAs (or RAFT agents) in the presence of radical initiators (azobisisobutyronitrile = AIBN, peroxides), and have been normally conducted under thermal conditions.[36, 72, 73] While radicals yielded from initiators could react with CTAs and generate carbon-centered radical intermediates stabilized by sulfur atoms, such intermediates undergo carbon-sulfur bond cleavage to give propagating radicals. The propagating chains could perform degenerative chain transfer with other CTAs to implement dynamic chain-growth control.[74] A number of groups, such as the Lacroix-Desmazes,[75] Théato,[76] Ishihara,[77] Terashima[78] groups, have disclosed the use of RAFT polymerization in preparing fluoropolymers. Although the vast majority of examples are focused on fluorinated (meth)acrylates and styrene derivatives, recent developments have revealed that RAFT agents are able to facilitate the controlled synthesis of main-chain fluoropolymers with gaseous fluoroalkenes.[79-86]

In 2006, Jerome and co-workers[87] prepared diblock copolymers of heptadecafluorodecyl acrylate (17FDA) and 2-hydroxyethyl acrylate (HEA) using a trithiocarbonate compound via a two-step RAFT polymerization. As measured by TEM, the amphiphilic copolymers formed spherical

micelles with an average diameter of 50 to 100 nm. Increasing the concentration for 2-hydroxyethyl acrylate caused the precipitation of poly(17FDA) macroinitiator, resulting in copolymers of limited molar masses.

In 2010, He and co-workers[88] applied two-step RAFT polymerizations to yield diblock copolymers of hexafluorobutyl methacrylate (6FBMA) and poly(propylene glycol) acrylate (PPGA) as monomers with dithiobenzoate agent. Although the poly(PPGA) block merely provides moderate hydrophilic property, the poly(6FBMA)-*b*-poly(PPGA) copolymer self-assembled in aqueous solution, resulting in the accumulation of 40-50 micelles into one aggregate (diameter ≈ 50-60 nm), where micelles were loosely packed as observed by TEM. The Singha group[89] prepared diblock copolymers with PEGMA and heptafluorobutyl acrylate (7FBA) as repeating units. The copolymers formed spherical micelles consisting of fluorinated blocks as cores and hydrophilic blocks as flexible coronas with an average diameter of about 140 nm as measured by TEM. When MMA was used instead of PEGMA, morphologies of block copolymers changed from lamellar to spherical micelles as influenced by the volume ratio of tetrahydrofuran/methyl ethyl ketone solvents.[90] Diblock copolymers were also prepared with poly(methacrylic acid) (poly(MAA)) as the first block and poly(TFEMA)-*co*-poly(hexafluorobutyl acrylate) (poly(TFEMA)-*co*-poly(6FBA)) as the second block via RAFT emulsion polymerization under aqueous conditions, providing core-shell FPNPs with D_h ≈ 56-93 nm by DLS measurement.[91] Authors proposed that the incorporation of less fluorinated TFEMA to copolymerize with 6FBA could improve the overall conversion of fluorinated monomers.

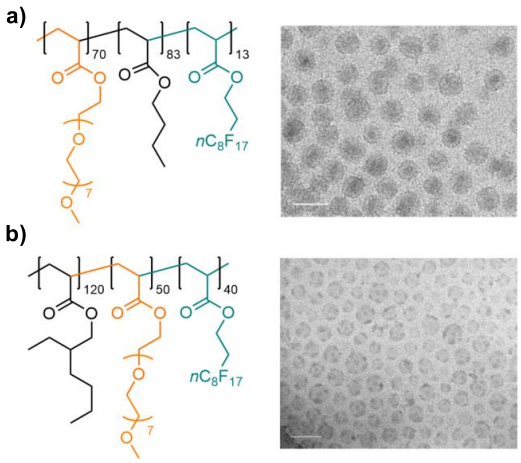

Figure 3. Cryo-TEM micrographs of micellar aggregates prepared with triblock copolymers of a) hydrophilic-lipophilic-fluorophilic sequence, b) lipophilic-hydrophilic-fluorophilic sequence.[92] Reproduced with permission from ref [92]. Copyright 2010 American Chemical Society.

In 2010, Laschewsky and co-workers[92] prepared ABC linear triblock copolymers composed of hydrophilic (poly(PEO-based acrylate)), lipophilic (poly(2-ethylhexyl acrylate) poly(EHA)), poly(*n*-butyl acrylate) poly(nBA)) and fluorophilic (poly(17FDA)) segments with trithiocarbonate agent via successive three-step RAFT polymerizations. As characterized by cryogenic TEM (cryo-TEM), those “triphilic” copolymers underwent local phase separation and afforded various interesting

ultrastructures (Figure 3). Notably, authors revealed that sequences of the triblock copolymers have a clear impact on micelle morphologies. For instance, the hydrophilic-lipophilic-fluorophilic sequence formed multicompartment morphology with core-shell-corona ultrastructure (Figure 3a), the lipophilic-hydrophilic-fluorophilic sequence yielded “patched double micelle” ultrastructure (Figure 3b). Later, the same team[93] used the same synthetic strategy for the preparation of triblock copolymers of PEO-based acrylate, benzyl acrylate and 7FBA, affording diverse structures as visualized by cryo-TEM, such as core-shell-corona ultrastructures, spherical and bispherical micelles, “soccer ball” morphologies and others. The coexistence of both hydrocarbon and fluorocarbon domains side by side might provide opportunities for the selective/independent adsorb and release of different chemicals, mimicking biologically related delivery of various substances.

Instead of successive RDRPs of three different monomers, Huang et al.[94] designed a novel tri-functional monomer of *N*-3-(difluoromethylthio)propyl-*N*-(3-(isopropylamino)-3-oxopropyl)acrylamide (DFTP-NIPAM-AM), and applied it to synthesize amphiphilic homopolymers via RAFT polymerization (Scheme 4). The poly(DFTP-NIPAM-AM) homopolymer could successfully self-assemble into spherical micelles (D_h = 197 nm by DLS) with hydrophobic cores in aqueous media.

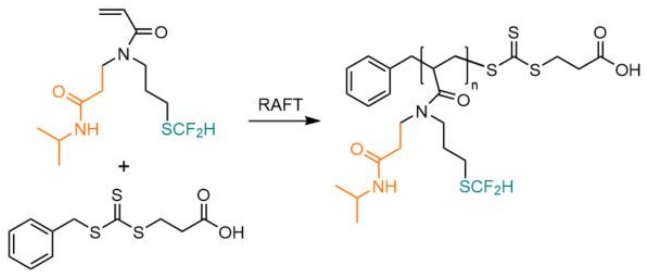

Scheme 4. Synthesis of amphiphilic homopolymer via RAFT polymerization.[94]

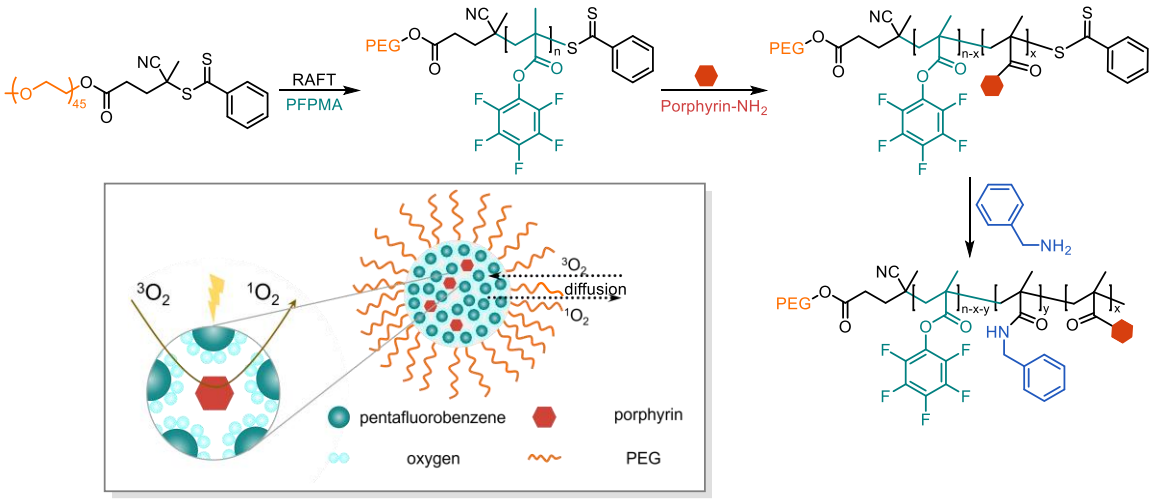

Scheme 5. Synthesis of PEG-based amphiphilic copolymers via RAFT polymerization and post modifications to obtain porphyrin-functionalized FPNPs.[96]

In 2014, Zentel and co-workers[95] reported the synthesis of diblock copolymers via two-step RAFT polymerizations of (pentafluorophenyl methacrylate (PFPMA)) and tri(ethylene glycol)methyl ether methacrylate. With self-assembled aggregates formed by copolymers of different chain lengths, nanogel particles of different diameters (40 and 100 nm) were yielded after adding spermine as a cross-linking agent. Those nanohydrogel materials were further employed to investigate gene knockdown ability.

In 2016, the Huang's group[96] demonstrated the synthesis of PEG-*b*-poly(PFPMA) using dithiobenzoate-capped PEG as a macro-CTA via RAFT polymerization of PFPMA (Scheme 5). Because the pentafluorophenoxy pendants are readily replaceable by amino compounds, the fluorinated micelles ($D_h \approx 17$ nm by DLS) formed with PEG-*b*-poly(PFPMA) were post-modified with tetrakis(4-aminophenyl) porphyrin and benzylamine, providing micelles ($D_h \approx 28$ nm) larger than original ones. An increase in the porphyrin concentration provided enhanced production efficacy of singlet oxygen, which could be useful for photodynamic therapy (section 5.3). When amino substituted Ru-complex was used instead of porphyrin, Ru-based photocatalyst (PC) was embedded into the fluorinate micelles (D_h = 295 nm, by DLS), providing recyclable nanoreactors for visible-light-mediated aerobic oxidation of aryl boronic acids.[97]

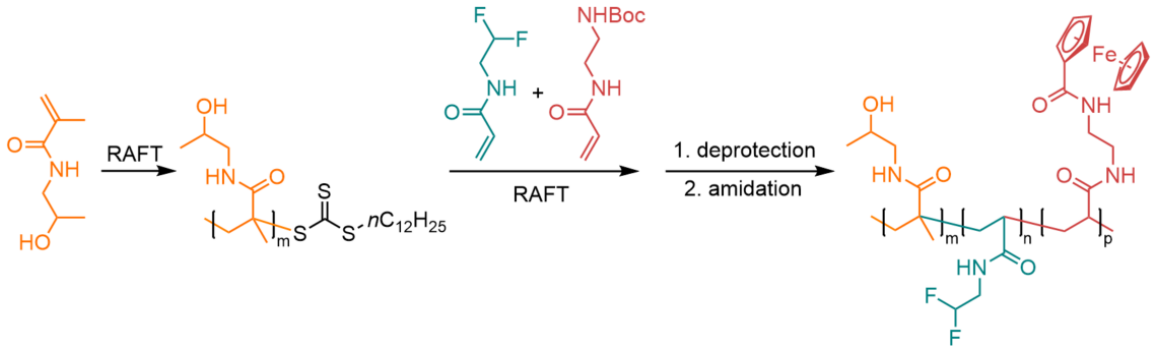

Scheme 6. Synthesis of multi-responsive block copolymers via RAFT polymerization and post-amidation.[98]

In 2021, Hurby and co-workers[98] prepared diblock copolymers with poly(*N*-(2-hydroxypropyl)methacrylamide) (poly(HPMA)) as the hydrophilic block, and poly(*N*-(2,2-difluoroethyl)acrylamide)-*co*-poly(*N*-[2-(ferrocenylcarboxamido)ethyl]acrylamide) (poly(DFEA)-*co*-poly(FcCEA)) as the hydrophobic block (Scheme 6). Regulation of block ratios allowed changing the concentration of ferrocene units, and tuning diameters of FPNPs in a range of 36-133 nm. Thanks to the thermo-responsive property of poly(DFEA) and redox-responsive property of poly(FcCEA), authors investigated the "smart" FPNPs for ^{19}F MRI therapy and diagnostic purposes (section 5.1).

Beyond side-chain fluorinated polymers, the synthesis of main-chain fluoropolymers via RAFT polymerization has also been probed to provide FPNPs. In 2017, Ladmiral and co-workers[79] reported the first synthesis of amphiphilic diblock copolymers of poly(VDF)-*b*-poly(vinyl acetate) (poly(VDF)-*b*-poly(VAc)) through sequential RAFT polymerizations of VDF and VAc (Figure 4) using

a xanthate CTA. Due to the gaseous property of VDF, high-pressure metallic vessels were required to prepare the poly(VDF)-based macroinitiator under thermal and radical conditions. The amphiphilic poly(VDF)-*b*-poly(vinyl alcohol) [poly(VDF)-*b*-poly(VA)] block polymer was formed via hydrolysis of the poly(VAc) block, which self-assembled into spherical micelles of D_h = 147 (by DLS) in water, with the observation of minor particle aggregation.

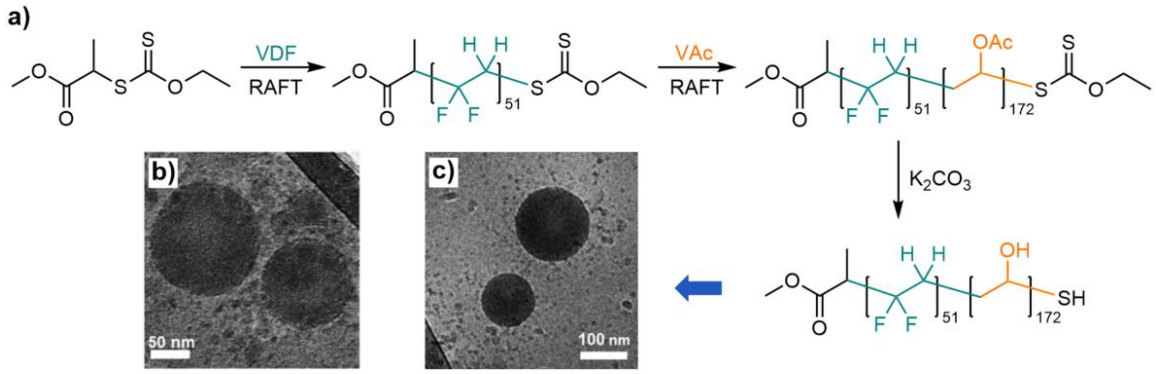

Figure 4. Schematic illustration for a) synthesis of the poly(VDF)-*b*-poly(VA) block copolymer via RAFT polymerizations and hydrolysis, b) and c) cryo-TEM micrographs of self-assembled FPNPs in water.[79] Reproduced with permission from ref [79]. Copyright 2017 Royal Society of Chemistry.

In 2021, D'Agosto, Lansalot et al.[99] disclosed the surfactant-free synthesis of poly(VDF) latexes via RAFT polymerization with xanthate-functionalized PEG as a macro-CTA and potassium persulfate as an initiator (Figure 5). These authors proposed degradative chain transfer onto PEG backbone, providing PEG radicals, followed by coupling reaction with radicals of oligo(VDF).[100] The employment of a very low macro-CTA amount (0.8 wt%) clearly reduced sizes of FPNPs (e.g., 72 nm), in comparison to polymerization using PEG-OH (234 nm). The reliability of this method was evidenced by scale-up polymerization in a 4 L vessel.

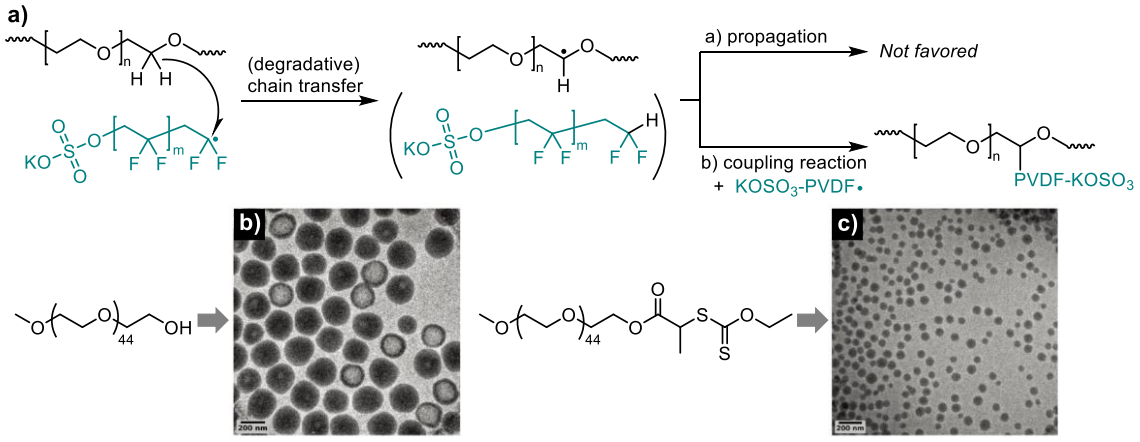

Figure 5. a) Degradative chain transfer onto PEG chains and following reactions. Cryo-TEM micrographs of self-assembled FPNPs prepared in the presence of b) PEG-OH and c) macro-CTA.[99] Reproduced with permission from ref [99]. Copyright 2021 Royal Society of Chemistry.

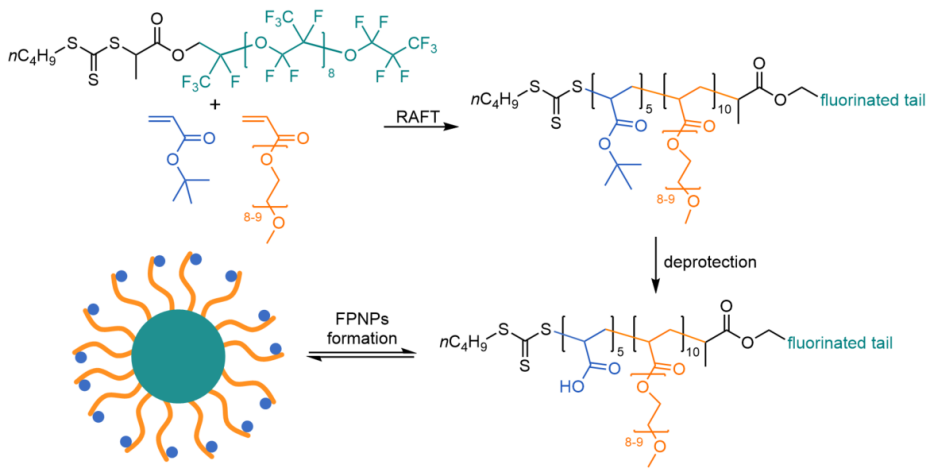

Scheme 7. Synthetic of poly(AA_5-*co*-$OEGA_{10}$)-PFPE FPNPs.[101]

Besides copolymers with fluorinated blocks, polymers with fluorinated tails have also been synthesized via RAFT polymerization from fluorinated CTAs. Monteiro and co-workers[102] reported the employment of a fluorinated xanthate agent to mediate ab initio emulsion polymerization of styrene, which produced PNPs with number-average diameter in a range of 69-81 nm as measured by capillary hydrodynamic fractionation, and low amounts of fluorine. Whittaker and co-workers[101, 103] adopted PFPE-substituted trithiocarbonate CTA in the synthesis of poly(tBA)-*co*-poly(oligo(ethylene glycol) methyl ether acrylate) (poly(tBA)-*co*-poly(OEGA)) with fluorinated tail (Scheme 7), which was further hydrolyzed to fluorinated poly(AA)-*co*-poly(OEGA). Though the hydrophobic PFPE moieties were small, they enabled self-assembling into micelles with fluorinated cores and $D_h \approx 10$ nm (by DLS) in aqueous solution.

Recently, inspired by the combinations of photoredox catalysis and RAFT polymerization,[104-108] Chen and co-workers demonstrated the controlled polymerizations of a variety of fluorinated monomers including semi-fluorinated (meth)acrylates,[109, 110] CTFE[80, 82] and perfluorinated vinyl ethers (PFVEs)[83, 84] with or without comonomers under ambient pressure and at room temperature without using any metal catalyst. Besides homo-polymerization of semi-fluorinated (meth)acrylates, emulsions were observed during the copolymerization,[109, 110] alternating copolymerization, alternating terpolymerization of fluoroalkenes (e.g., CTFE, PFVEs).[80, 82, 83] Although systematic studies regarding the preparation of FPNPs based on such photoredox-mediated RDRP methods have yet to come, the controlled accesses toward main-chain fluoropolymers supply alternative paths to multi-geometry PNPs that could be achieved by complex sequences.[111-113]

2.1.3 Fluoropolymers Synthesized via ITP

ITP is a degenerative chain transfer (DT) polymerization with organic iodocompounds as CTAs.[41] The initiating radicals are generated by the thermal decomposition of conventional initiators. The exchange of iodine from CTA (iodine compound) to the propagating radical results in the formation of a dormant polymer chain. Due to the reversible transfer step, the significantly lowered concentration of free radicals contributes to minimizing undesirable side reactions (irreversible

chain terminations), which is essential to promote chain-growth control during monomer consumption.[28, 114]

VDF is one of the most attractive fluoroalkenes utilized to prepare main-chain fluoropolymers,[115, 116] which are widely explored for applications as coatings, membranes, polymer electrolytes and many more.[117, 118] ITP has been demonstrated as an effective means to furnish customized main-chain fluorinated copolymers of VDF and other fluorinated/non-fluorinated comonomers of block or random sequences.[114, 119-123]

Although ITP is considered as the oldest technique (pioneered in 1979) and a facile approach to generating fluoropolymers, the relatively slow chain transfer increases difficulties in obtaining very narrow molar mass distribution and high chain-end structural fidelity.[115] When many main-chain fluorinated copolymers are formed with CH_2-I, such chain-end groups are not readily reactive for reversible deactivation, which often cause the accumulation of less reactive chains and pose challenges for chain-extension reactions.[124, 125] In addition, polymerizations of gaseous fluoroalkenes require high-pressure metallic vessels and elevated temperatures, which are problematic with conventional reaction techniques and are difficult to be handled by most laboratories. Consequently, when VDF and other gaseous fluoroalkenes are desirable to prepare FPNPs, free-radical emulsion polymerizations are remaining in widespread use, where emulsion ITPs are explored for targets with block sequence or functional composition.[123] A few investigations proposing to provide information about the controlled polymerization behaviors are usually reported as patents,[40, 126] which lack detailed descriptions of the chemical structure, molar masses, polymer dispersity, chain-end fidelity and reaction kinetics.

In 2009, Ameduri and co-workers[116] reported the iodine transfer copolymerization of VDF with α-trifluoromethacrylic acid (TFMA) in an aqueous medium in the presence of 1-perfluorohexyl iodide ($nC_6F_{13}I$) or 1,4-diodoperfluorobutane (IC_4F_8I) as CTAs, which realized a surfactant-free "emulsion" copolymerization without any surfactant (Scheme 8). As characterized by ^1H and ^{19}F nuclear magnetic resonance (NMR), the controllability of the VDF copolymerization was improved by adding a small amount of TFMA. Meanwhile, the presence of TFMA enabled the formation of a stable emulsion and reduction of the particle size by one order of magnitude to smaller than 200 nm as analyzed by light scattering.

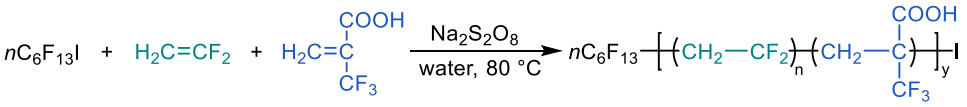

Scheme 8. Iodine transfer copolymerization of VDF and α-trifluoromethacrylic acid.[116]

In 2020, Cheng and co-workers[127] demonstrated the development of photo-controlled iodine-mediated RDRP to obtain main-chain fluorinated alternating copolymers (Scheme 9). In this method, α,ω-diiodoperfluoroalkane and α,ω-nonconjugated diene were utilized as comonomers using Ru-based photocatalyst. Authors proposed that a dynamic equilibrium between the propagating and dormant species was facilitated by the oxygen-iodine interaction in acetone. With the alternating copolymer as a macroinitiator, authors prepared the block copolymer with

poly(PEGMA) as a second block. When this unprecedented block copolymer was dispersed in a pre-mixed solvent of tetrahydrofuran/H_2O, it generated FPNPs of an average diameter of 147 nm as determined by DLS measurement.

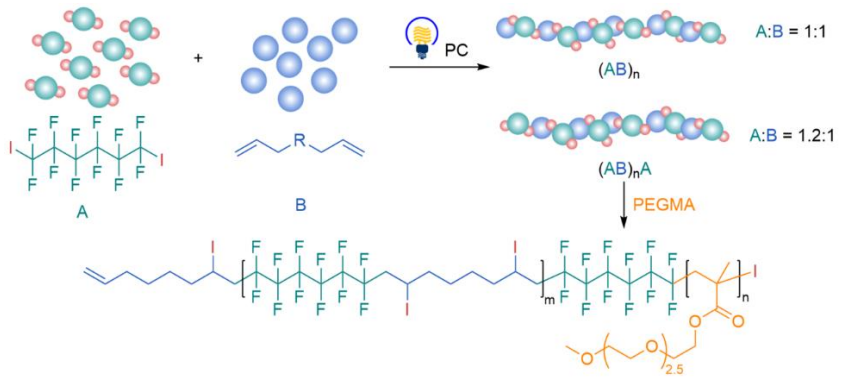

Scheme 9. Synthesis of alternating fluoropolymers via photopolymerization and post modification.[127]

2.1.4 Fluoropolymers Synthesized via NMP

NMP represents another important category of RDRPs, where alkoxyamine compounds have been employed as initiators under thermal conditions.[39] An alkoxyamine undergoes carbon-oxygen bond cleavage, and generates carbon-centered radial and a nitroxide radical. While the carbon-centered radical initiates propagation, the nitroxide radical acts as a persistent radical, which could reversibly terminate propagating species.[128]

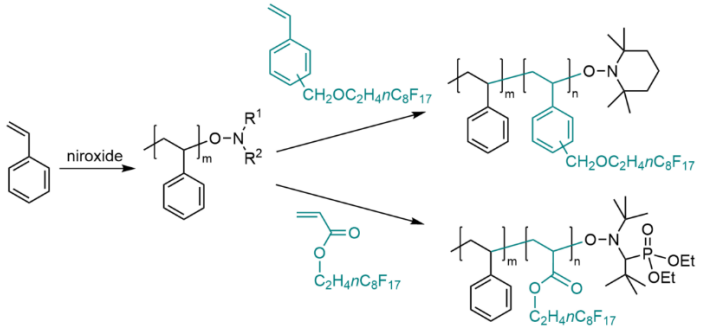

Scheme 10. Synthesis of block copolymers from the poly(St) macro-initiator based on NMP.[129]

In 2004, Lacroix-Desmazes and co-workers[129] reported the synthesis of linear diblock copolymers using poly(St) as a first block, poly(17FDA) or poly(perfluorooctyl-ethylenoxymethylstyrene) (poly(17FDSt)) as a second block via NMP (Scheme 10). Different from preparing FPNPs in water, authors disclosed that both copolymers formed micelles with poly(St) core and fluoropolymer outer shell, a hydrodynamic diameter of about 18 nm in neat $scCO_2$ at moderate pressure.

In addition, NMP has been used to functionalize inorganic nanoparticles with fluoropolymers. For example, poly(pentafluorostyrene) (poly(PFSt)) chains were grafted onto the surface of silica nanoparticles.[130]

2.2 Self-Folding of Single Fluoropolymer Chains

Biomacromolecules in nature always provide inspiration to polymer scientists. The precise arrangement of functional groups and the well-defined three-dimensional architectures of folded single chains enable unique properties and functions for biomacromolecules (e.g., proteins, nucleic acids, enzymes) of both surfaces and interiors.[131] Self-folding of single synthetic polymer chains provides possibilities to obtain small PNPs with tailored functions in the sub 20 nm dimension.[132] Massive efforts have been made to realize intramolecular linking of single polymer chains since 1962.[133] This strategy creates a promising pathway to engineering artificial and smart single-chain polymers that could be attractive for applications of nanoreactors, catalysis, gene/drug delivery, sensors, etc.[131, 134] However, the synthesis of well-defined functional polymers of uniform molar masses and precisely ordered sequence still lies far behind many biomacromolecules.

RDRPs have shown outstanding compatibility with functional groups, and are reliable to tailor sequences and molar masses of polymers. Such synthetic methods have been frequently employed to preform customized polymers for self-folding purposes.[131, 134] The intrachain self-folding has been achieved through covalent bonding, dynamic covalent bonding, and non-covalent interaction.[131, 134] For the non-covalent bonding studies, interactions such as hydrogen bonding, host-guest interaction, hydrophobic interaction, coordination have been probed to generate folded single-chain polymeric nano-objects.[131, 134] The unique properties of fluorine atom (strong electronegativity, fluorophobic effect[49, 50]) expanded possibilities of realizing highly reversible single-chain folding via non-covalent interaction in water and organic solvents.

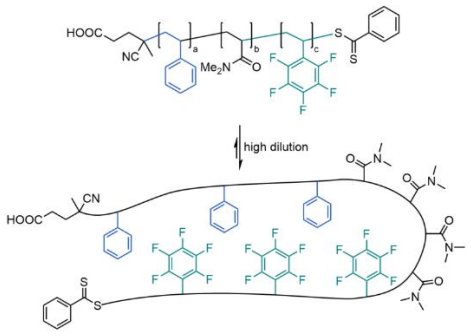

Scheme 11. Schematic illustration of the single-chain folding with poly(St)-*b*-poly(DMA)-*b*-poly(PFSt) prepared by RAFT polymerizations.[135]

In 2014, Weck's group[135] prepared linear ABC triblock copolymers of poly(styrene)-*b*-poly(dimethylacrylamide)-*b*-poly(pentafluorostyrene) (poly(St)-*b*-poly(DMA)-*b*-poly(PFSt)) via sequenced RAFT polymerizations (Scheme 11). The strong electron-deficient property of pentafluorostyrene pendants effectively enhances π-π stacking interaction with phenyl rings at very low concentrations (1 mg/mL) in chloroform, providing FPNPs of average hydrodynamic diameters

down to about 5 nm in chloroform by DLS characterizations, and displaying a very basic level of mimicking for the β-hairpin formation. The quadrupole interactions between poly(St) and poly(PFSt) blocks were evidenced by two-dimensional NMR spectroscopy.

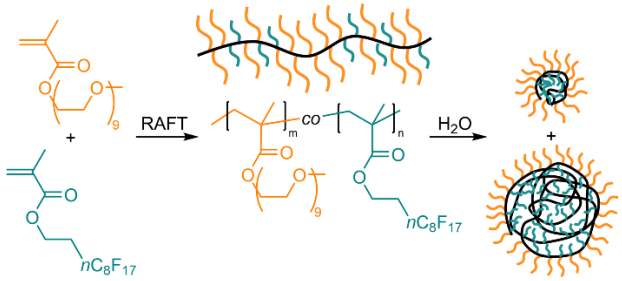

Scheme 12. Synthesis of amphiphilic fluorinated FPNPs via RAFT polymerization and self-assembly in water.[78]

In 2015, Terashima, Maynard and co-workers[78] prepared linear (poly(PEGMA)-*co*-poly(17FDMA)) copolymers via RAFT polymerization from functionalized trithiocarbonates (Scheme 12). Those amphiphilic/fluorous random copolymers are soluble in acetone and water to provide FPNPs of fluorinated cores. While the copolymers exist as unimers in acetone with small diameters of 26-30 nm, they assemble into aggregates with larger diameters of 115-210 nm in water as analyzed by DLS. ^{19}F NMR results suggest that both unimer micelles and larger aggregates possess fluorinated pendants as inner cores and PEG chains as shells. The functional terminal groups from CTAs allow the facile conjugation with biomacromolecules.

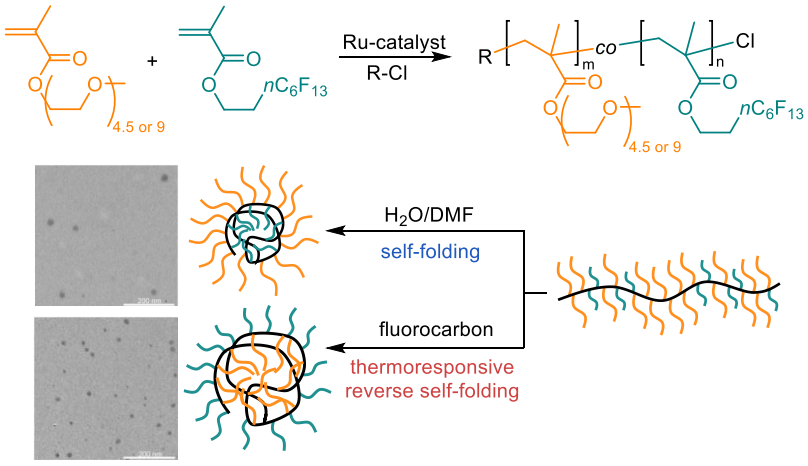

Figure 6. Synthesis and self-folding of amphiphilic fluorinated random copolymers.[136] Reproduced with permission from ref.[136] Copyright 2016 American Chemical Society.

In 2016, Terashima, Sawamoto and co-workers[136] reported multimode self-folding of amphiphilic/fluorous random copolymers synthesized by Ru-catalyzed "living" radical

copolymerization of PEGMA and 13FOMA. Those copolymers possess three segments of distinct properties, fluorophilic fluorinated pendants, hydrophobic backbones, hydrophilic PEG side groups, enabling the variation of folding modes by changing solvents. For example, such copolymers form fluorinated cores in water and DMF, PEG cores in fluorinated solvent (Figure 6). As affected by the location of PEGs and fluorinated pendants, micelles formed in water (38 nm) and fluorinated solvent (16 nm) exhibit different diameters as analyzed by TEM. The reverse self-folding in fluorinated solvent provides thermo-responsive phase separation based on the lower critical solution temperature (LCST) of PEG.

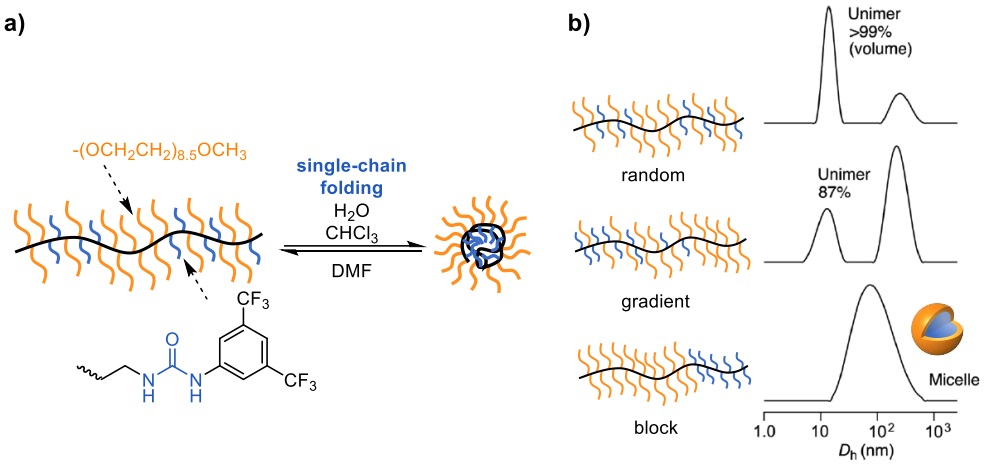

Figure 7. a) Single-chain folding of amphiphilic random copolymers with urea units. b) DLS intensity size distribution of copolymers with different sequences.[137] Reproduced with permission from ref [137]. Copyright 2016 American Chemical Society.

Later, the same group[137] employed a urea-bearing methacrylate substituted by two trifluoromethyl groups instead of 13FOMA with PEGMA (Figure 7). Electron-withdrawing property of trifluoromethyls decreases pKa of urea units and enhances hydrogen bonds for self-folding. Notably, authors disclosed sequences have a clear impact on the self-folding or assembly for copolymers made of the same repeating units. For instance, copolymers of random sequences form spherical unimer micelles ($D_h \approx 16$ nm). Meanwhile, copolymers of gradient (aggregates with $D_h \approx 104$ nm, 87% unimer with $D_h \approx 13$ nm) and block (aggregates with $D_h \approx 250$ nm) sequences tend to provide different extents of aggregation of multiple chains as analyzed by DLS.

Galli, Mennucci and co-workers[138] synthesized random copolymers based on PEGMA and perfluorooctyl acrylate (13FOA) via ATRP. The copolymers afford single-chain nano-assemblies of $D_h \approx 4$ nm, which can reversibly undergo multi-chain aggregation to larger nano-objects of $D_h \approx 390$ nm above LCST of PEGMA segment. Beyond synthetic experiments, the authors conducted molecular dynamics simulations to disclose the formation of self-folded single polymer chains. As exemplified in Figure 8, the single-chain self-folding predicts prolate globular structure in water, where hydrophobic units are buried in the core of the nanostructure. In comparison, a much more open confirmation is given for the same macromolecule in chloroform.

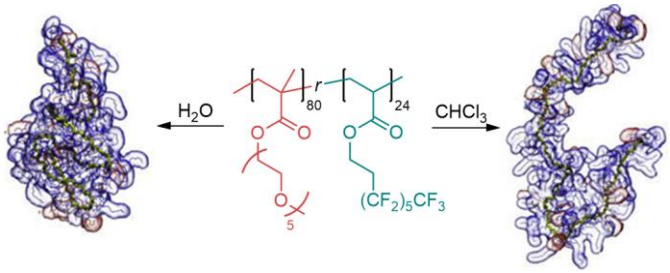

Figure 8. Molecular dynamics simulations for the formation of self-folded single polymer chains in water and chloroform.[138] Reproduced with permission from ref [138]. Copyright 2018 Elsevier Ltd.

3. *IN SITU* SYNTHESIS OF FPNPS VIA RDRPS

Different from solution self-assembly and self-folding, which are post-polymerization techniques that demand multiple steps and provide highly diluted PNPs in solvents, one-step synthesis of PNPs based on RDRP techniques have also been developed. Polymerization induced self-assemble (PISA) and covalent cross-linking based on RDRPs have allowed the direct preparation of FPNPs. Due to solubility issue of fluorinated monomers, such synthetic operations have been conducted in organic solvents via surfactant-free emulsion polymerization, or in water using hydrophilic macro-CTAs/initiators as stabilizers via emulsion polymerization.

3.1 PISA Mediated by RDRPs

PISA allows *in situ* preparation of self-assembled PNPs via chain-extensions from preformed solvophilic polymers (e.g., macro-CTAs, macroinitiators), where solvophobic blocks have been generated under dispersion or emulsion polymerizations as mediated by RDRPs.[139-141] In contrast to traditional self-assembly and self-folding operations, PISA transformations have been achieved under relatively concentrated conditions (e.g., 10-50 wt%) with varied solvent systems, such as water, alcohol, ethylene glycol, etc.[45, 47, 141-148] Although a number of excellent reviews have demonstrated the importance of PISA techniques from perspectives of RDRP methods,[45, 47, 142, 143] polymerization techniques,[141, 144] mechanisms,[139-141] and others,[145-148] it still lack of summary for the preparation of FPNPs based on PISA processes.

Currently, the vast majority of PISA examples for the FPNPs synthesis are based on RAFT polymerization under thermal conditions. Recently, examples demonstrate that photo-mediated RDRPs (e.g., photoinduced electron/energy transfer (PET)-RAFT polymerization[149, 150]), ATRP and cobalt-mediated RDRP could also be adopted for PISA. Semi-fluorinated (meth)acrylates and acrylamides, PFSt have been shown as useful fluorinated monomers for RDRP-based PISA processes. Analogous to PISA of non-fluorinated block copolymers, monomer concentration, degrees of polymerization (DPs) for different blocks and other parameters can implement impacts on morphologies of FPNPs, leading to fluorinated nano-objects of diverse morphologies including spheres, worms, vesicles and many more, as exemplified below.

3.1.1 PISA Mediated by RAFT Polymerization

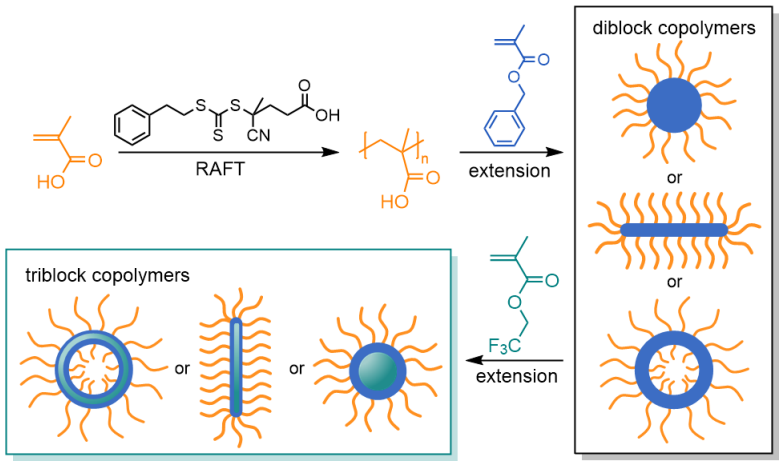

Scheme 13. Synthesis of diblock and triblock copolymers via RAFT polymerization and formation of FPNPs of different morphologies (e.g, sphere, worms, vesicles).[151]

In 2014, Armes and co-workers[152] established the preparation of FPNPs via PISA mediated by RAFT polymerization, using poly(MAA) and poly(DMA) as macro-CTAs and 2,2,2-trifuoroethylmethacrylate (TFEMA) for chain-extension under thermal conditions. Authors disclosed pseudo-living kinetics for chain-extensions under both solution (THF solvent) and dispersion (ethanol solvent) polymerization conditions as monitored by UV-visible adsorption spectroscopy, and obtained FPNPs of low particle size dispersity (e.g., *PSD* = 0.041, D_h = 70 nm) at 20 wt% solids in ethanol. Authors revealed that the dispersion polymerization retained higher fractions of original trithiocarbonate terminals during chain-extensions, when compared to the solution polymerization (above 73-75% *vs* 55-66%). ^{19}F NMR characterizations indicate that the dispersion polymerization progresses through monomer-swollen micelles formed with block copolymers. In the same year, the same group[151] further adopted diblock copolymers of poly(MAA)-*b*-poly(benzyl methacrylate) (poly(MAA)-*b*-poly(BzMA)) with trithiocarbonate terminals as macro-CTAs in the RAFT-mediated PISA in ethanol (Scheme 13). As the TFEMA conversion gradually increases, the morphologies of FPNPs evolve from spheres to worms and finally vesicles as evidenced by TEM.

When highly hydrophilic poly(glycerol monomethacrylate), poly(GMA), capped with dithiobenzoate as a macro-CTA for chain-extension was adopted by Armes and co-workers, the PISA approach allowed the preparation of FPNPs with poly(TFEMA) cores via aqueous emulsion RAFT polymerization.[153] DPs of both poly(GMA) and poly(TFEMA) showed an apparent impact on the particle size, facilitating diameter regulation (20 to 250 nm by TEM) by optimizing the length of two blocks (Figure 9). This method presents a useful pathway to yield FPNPs of low *PSD* (typically < 0.10) at 20 wt% solid contents in water. Later, Czajka and Armes[154] reported the employment of time-resolved small-angle X-ray scattering (SAXS) in aqueous emulsion polymerization of TFEMA using a persulfate initiator, and disclosed that TFEMA was more favorable than styrene for the purpose of *in situ* SAXS, due to the greater X-ray scattering contrast as compared to water.

Although this contribution is not for the formation of FPNPs based on RDRPs, the temporal characterization technique could be further used to provide useful insights into the mechanism of PISA process with fluorinated (meth)acrylates.

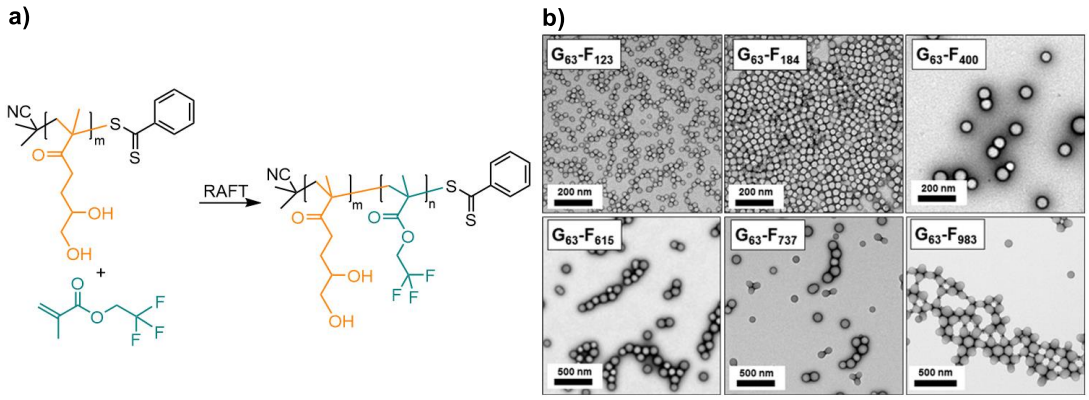

Figure 9. a) Chain-extension from macro-CTA via RAFT polymerization. b) TEM images of poly(GMA)-*b*-poly(TFEMA) block copolymers formed during the PISA process, where G and F represent GMA and TFEMA units, respectively.[153] Reproduced with permission from ref [153]. Copyright 2016 American Chemical Society.

In 2017, Yuan and co-workers[155] demonstrated RAFT-mediated PISA of a family of ABC triblock copolymers using poly(2-dimethylaminoethyl methacrylate)-*b*-poly(benzyl methacrylate) (poly(DMEMA)-*b*-poly(BzMA)) as seeds in ethanol (Scheme 14). Taking advantage of the liquid-crystalline property of poly(17FDMA),[156] when poly(DMEMA)-*b*-poly(BzMA) micelles were used as macro-CTAs, chain-extensions generated poly(DMEMA)-*b*-poly(BzMA)-*b*-poly(17FDMA) assemblies with morphology evolution in a sequence of spheroid, sphere-segregated sphere, phase-segregated spheroid and cylinder, as influenced by the continuously increased DPs of the poly(17FDMA) mesogen. In comparison, when vesicles of poly(DMEMA)-*b*-poly(BzMA) seeds were employed, the triblock copolymer vesicles were modified into raspberry-like particles, micelles, cylinders or larger spheres depending on the chain lengths of poly(BzMA) and poly(17FDMA) blocks. The liquid-crystalline alignment of poly(17FDMA) plays an important role in complicating the multicompartment nanostructures. In the same year, the Yuan's group[157] expanded the investigations of using poly(DMEMA)-*b*-poly(BzMA) of different morphologies including micelles, worm-like micelles, vesicles as seeds in the RAFT-mediated PISA systems. Although 13FOMA with fewer fluorine atoms was used instead of 17FDMA to form the third block, which should decrease the liquid-crystalline property of fluorinated segment, the strong incompatibility between poly(DMEMA)-*b*-poly(BzMA) and poly(13FOMA) effectively enriched the formation of abundant compartmentalized nanostructures, including core-shell-corona, patched, ribbon-shell, raspberry-like micelles and others.

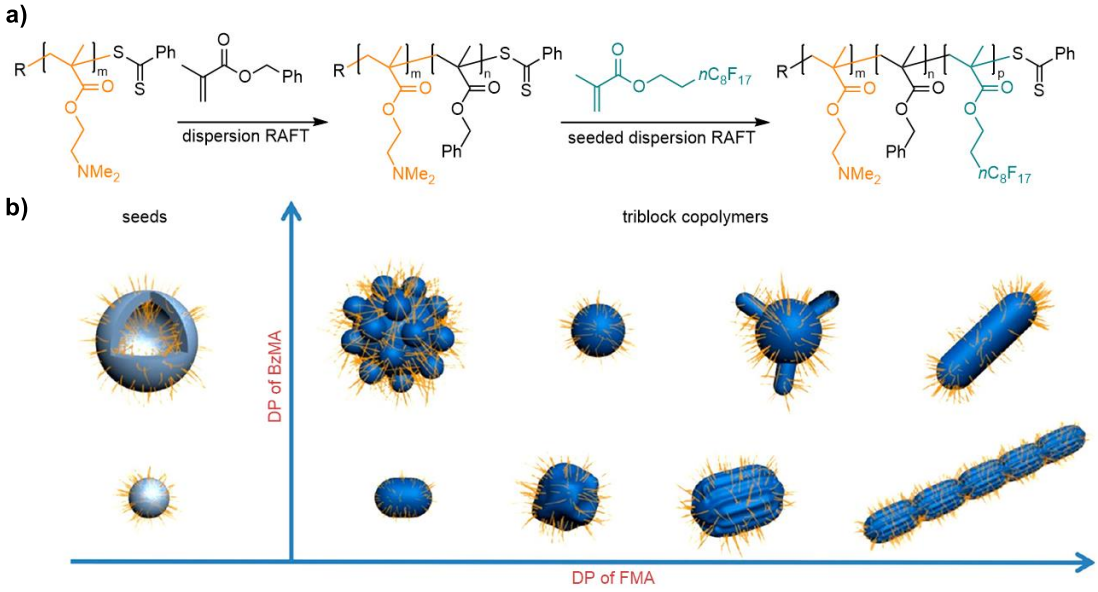

Scheme 14. a) Synthesis of poly(DMEMA)-*b*-poly(BzMA)-*b*-poly(17FDMA) triblock copolymers via dispersion RAFT polymerization. b) Morphology evolution of FPNPs during the PISA process.[155] Reproduced with permission from ref [155]. Copyright 2017 American Chemical Society.

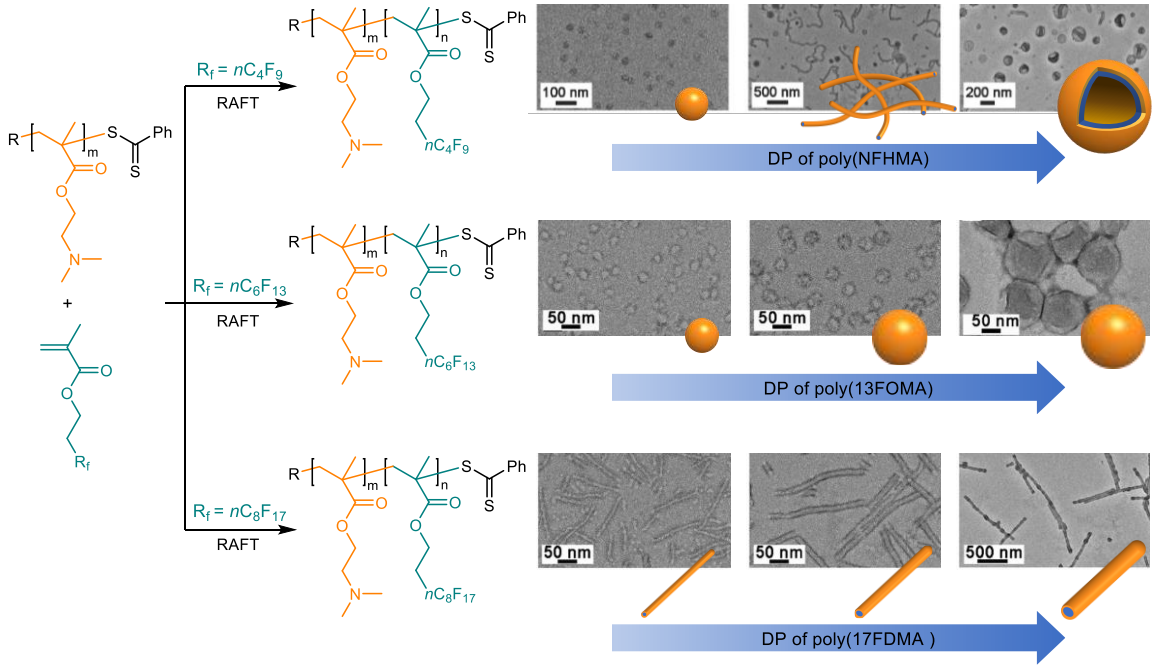

Figure 10. Synthesis of diblock copolymers by chain-extension via RAFT dispersion polymerization and PISA into FPNPs with different morphologies.[159] Reproduced with permission from ref [159]. Copyright 2018 WILEY.

Subsequently, Yuan and co-workers[158] employed mixtures of BzMA and 17FDMA to generate random copolymers as the second blocks in chain-extensions from poly(DMEMA) macro-CTA. Different from compartmentalized nanostructures observed from poly(DMEMA)-*b*-poly(BzMA)-*b*-poly(13FOMA) triblock copolymers,[155, 157] the diblock terpolymers tend to generate large compound micelles and vesicles, nanoporous spheres, etc. Interestingly, when nonafluorohexyl methacrylate (9FHMA), 13FOMA or 17FDMA were used, respectively, in the chain-extension from poly(DMEMA) macro-CTA, dramatically different morphologies were generated (Figure 10).[159] Indeed, dispersion polymerizations with 9FHMA provided spherical and worm-like micelles, and vesicles, transformations with 13FOMA afforded only spheres of different sizes, whereas PISA with 17FDMA formed liquid-crystalline cylindrical micelles of different diameters, as their morphologies or sizes varied along with DPs of fluorinated blocks, as confirmed by TEM. The influence of DPs on particle sizes/morphologies was also observed in chain-extension from poly(AA) in water, using poly(7FBA) as the second blocks via RAFT PISA.[160, 161]

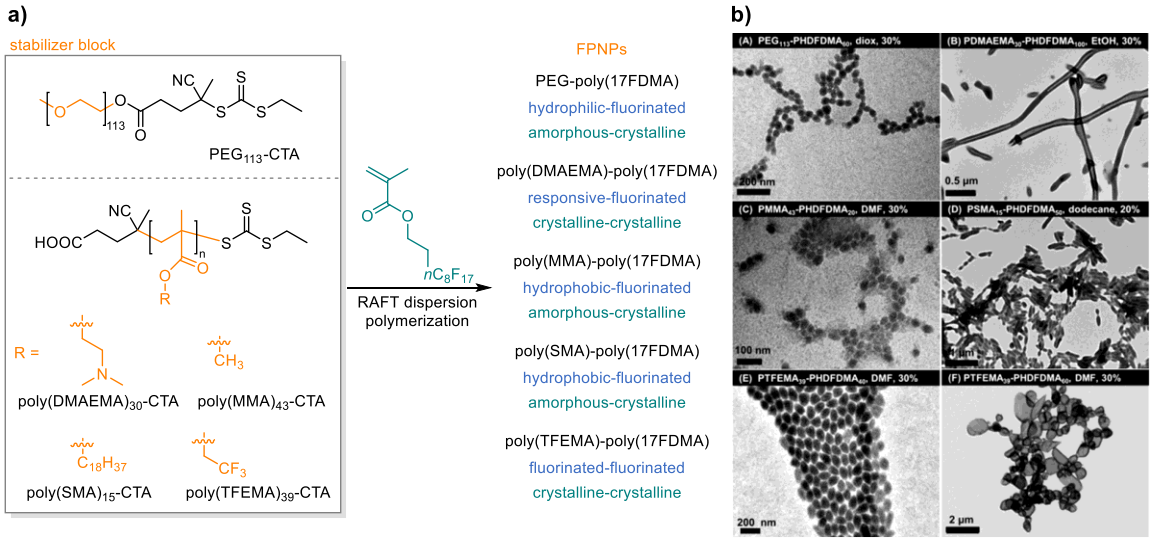

Figure 11. a) Synthesis of block copolymer via a RAFT dispersion PISA process. b) Representative TEM micrographs of FPNPs of different morphologies.[162] Reproduced with permission from ref [162]. Copyright 2018 American Chemical Society.

In 2018, An and co-workers[162] demonstrated the synthesis of diblock copolymers using poly(17FDMA) as the second block by chain-extension from a variety of macro-CTAs under thermal conditions, yielding FPNPs of fusiform, vesicle, rod-like, tube-like morphologies via PISA process (Figure 11). Although poly(17FDMA) possesses very low solubility in most solvents, and could cause precipitation during chain-growth, this robust dispersion polymerization enables direct access to diblock copolymers with poly(17FDMA) segments at high concentrations and with quantitative 17FDMA conversions. Obtained FPNPs show excellent dispersibility in many organic solvents, such as acetone, acetonitrile, ethyl acetate, dioxane, dimethyl sulfoxide (DMSO), dimethylformamide, dichloromethane, toluene, etc., which could expand their applicable scope.

Moreover, by selecting different macro-CTAs as the first blocks, this approach successfully merges two blocks of distinctive properties. For example, hydrophilic/crystalline PEG and fluorophilic/crystalline poly(17FDMA) are combined in PEG-*b*-poly(17FDMA); hydrophobic/amorphous poly(MMA) and poly(17FDMA) are combined in poly(MMA)-*b*-poly(17FDMA). The broad attainable scope of amphiphilic block copolymers is promising as novel Pickering emulsifiers.

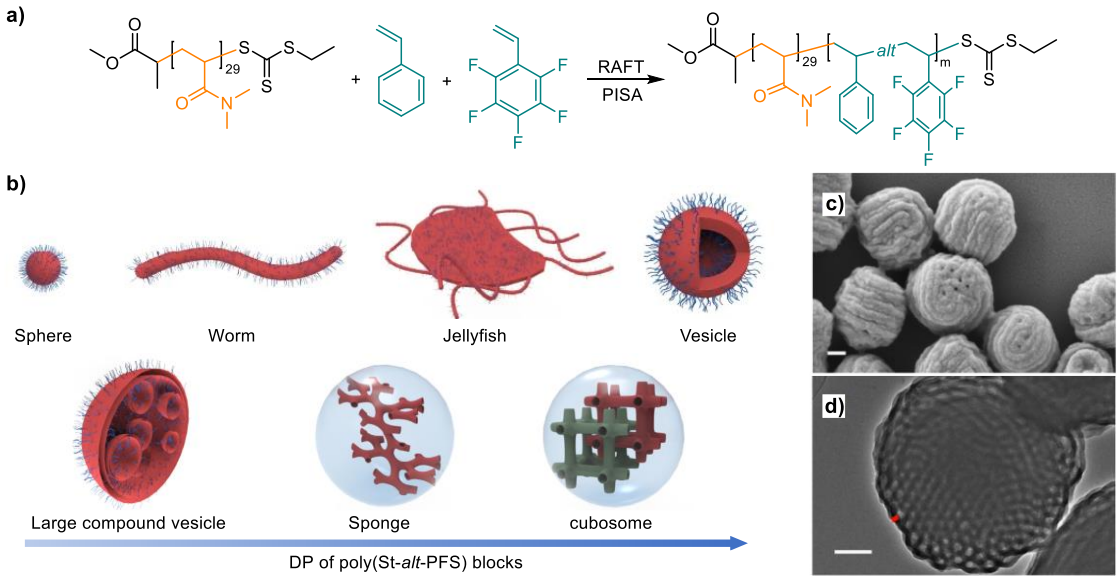

Figure 12. a) Synthesis of poly(DMA)-*b*-poly(St-*alt*-PFSt) block copolymers via RAFT dispersion PISA process. b) Schematic illustration of morphological evaluation of FPNPs. c) and d) Representative SEM and TEM micrographs of cubosomes (scale bar = 200 nm).[163] Reproduced with permission from ref [163]. Copyright 2019 Nature Publishing Group.

PNPs of ordered inverse morphologies are challenging to be obtained due to the complicated formation mechanism and elusive reaction parameters. In 2019, Wu and An[163] disclosed the scalable synthesis of amphiphilic block copolymers comprising poly(DMA) as the first block and alternating copolymers based on styrene and PFSt as the second blocks (Figure 12). The electron-donor and acceptor interaction between St and PFSt plays a vital role in affording the alternating sequence. During chain-extensions from poly(DMA) macro-CTA via dispersion RAFT polymerization, the resulting poly(DMA)-*b*-poly(St-*alt*-PFSt) copolymers yield FPNPs evolving in a sequence of spherical, worm-like, jellyfish-like, vesicle, large compound vesicle, sponge-like and cubosome morphologies.[163, 164] In sharp contrast to typical spherical PNPs with relatively smooth surfaces, high-resolution TEM and SAXs analyses validate the highly ordered internal patterns with solvophobic and solvophilic channels for cubosome FPNPs. Authors reveal that while relatively short stabilizer blocks from macro-CTAs and high solid contents (>30 wt%) can promote the morphological transformation to ordered inverse cubosome mesophases, a minimal amount of cosolvent that is miscible with the growing chains (e.g., toluene), can function as a plasticizer at high monomer conversions and facilitate the final morphological transition.

The pentylfluorophenyl pendants of PFSt repeating units provide chances to post-modify FPNPs without clear impact on their spherical, worm-like morphologies via nucleophilic substitution by thiol compounds, and such morphologies could be strengthened by cross-linking with dithiol compounds.[165]

Whittaker and co-workers[166] demonstrated that chain-extensions with styrene derivatives from fluorinated macro-CTAs could provide morphology evolution from spheres to worm-like nanoparticles, and ultimately vesicles via PISA mediated by RAFT dispersion polymerization in alcoholic solvent. The strategy of chain-extension from fluorinated macro-CTAs has also allowed the facile preparation of spherical FPNPs of low *PSD* with poly(MMA) cores (CO_2-phobic) and fluorinated shells (CO_2-philic) via PISA process under $scCO_2$ conditions.[167] The employment of fluorinated copolymers of poly(DMEMA)-*co*-poly(TFEMA) as macro-CTAs was also investigated in RAFT-mediated PISA in ethanol, yielding helical nanowires using poly(13FOMA) as the second block.[168]

3.1.2 PISA Mediated by Photopolymerization

Motivated by the well-established merits of photo-mediated RDRPs, such as low-cost and environmentally sustainable visible light, spatiotemporal control, as well as mild reaction conditions, PISA techniques based on photo-mediated RDRPs (photo PISA) have received increasing interests as summarized by Boyer and co-workers.[104, 142] Although photo-PISA has only provided limited types of morphologies as compared to thermal-initiated RAFT PISA until now,[169-171] it remains an alternative means for the preparation of FPNPs, which could be potentially useful for the facile and *in situ* encapsulation of temperature-sensitive moieties (e.g., proteins, genes).

In 2019, O'Reilly and co-workers[172] demonstrated the fabrication of FPNPs with PEG-based macro-CTA via chain-extension with PFPMA in DMSO under 405 nm light irradiation. The photo PISA process exhibits two-stage reaction kinetics as observed in many PISA systems conducted under thermal conditions. Although a variety of DPs for poly(PFPMA) were examined, authors only obtained uniform spheres of textured surfaces ($D_h \approx$ 320-400 nm, *PSD* < 0.14 by DLS), which are easily modifiable by reaction with amino compounds.

In 2020, Chen and co-workers[173] reported a macro-CTA differentiation strategy, which enables the controlled synthesis of ultra-high-molecular-weight (UHMW, $M_n > 10^6$ Da) polymers using fluorinated (meth)acrylates (e.g., 9FHMA, nonafluorohexyl acrylate (9FHA), dodecafluoroheptyl methacrylate (12FHMA)) and acrylamides (e.g., nonafluorohexyl methacrylamide) in chain-extensions under visible-light irradiation conditions. In comparison to conventional RDRPs, where all CTAs are supposed to be consumed in chain-growth, the macro-CTA differentiation strategy involves a more complex polymerization process as disclosed by kinetic investigation[173, 174] and machine-learning assistance.[175] The chain-growth of ultra-long solvophobic fluorinated blocks onto non-fluorinated solvophilic macro-CTA (e.g., poly(DMA), poly(MMA)) generates spherical FPNPs ($D_h \approx$ 80-280 nm by DLS) of low *PSD* (<0.14) and with up to 50 wt% solid contents in DMSO. However, when this reaction was conducted at elevated temperature (e.g., 70 ºC) with AIBN initiator via RAFT polymerization, all macro-CTAs were consumed to provide polymers of regular molar masses, without the detection of macro-CTA differentiation, revealing that the mild reaction conditions should be crucial to afford UHMWs in this system.

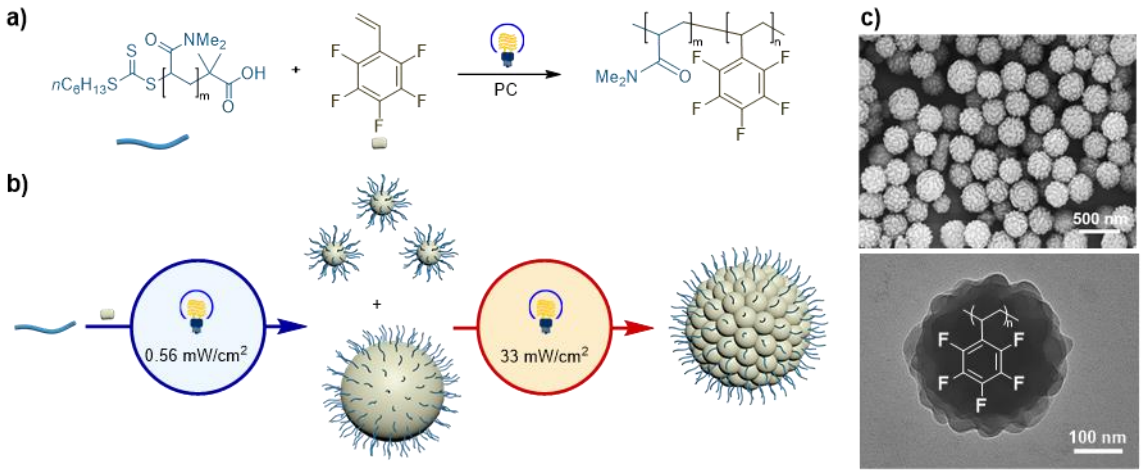

Figure 13. a) and b) Synthesis and schematic illustrations of raspberry-like FPNPs via a tandem photo-mediated polymerization. c) SEM and TEM micrographs of raspberry-like FPNPs.[176] Reproduced with permission from ref 175. Copyright 2020 Royal Society of Chemistry.

Later, the Chen group[176] established a tandem light-irradiation approach using the same wavelength but two light intensities (weak light, 0.56 W/cm^2; strong light, 33 W/cm^2), successively, through photo PISA (Figure 13), which enables nonsynchronous growth of raspberry-like FPNPs of uniform diameters (D_h ≈ 210-370 nm by DLS) and low *PSD* in DMSO. This method affords raspberry-like FPNPs at quantitative yields by chain-extensions from solvophilic macro-CTAs (e.g., poly(DMA), PEG) using PFSt to form the solvophobic block, where chain lengths of macro-CTAs and poly(PFSt) could be used to tune particle sizes without losing the raspberry-like morphology. During the photo PISA process, two populations of molar masses were observed throughout the entire transformation by size-exclusion chromatography (SEC) instrument, suggesting the presence of macro-CTA differentiation under mild reaction conditions.[173-175] TEM results support the presence and fusion of small and large FPNPs under weak-light irradiation during the photo PISA. Inspired by the role of the minimal amount of co-solvent in PISA,[163] authors proposed that the remaining PFSt under weak-light irradiation could act as plasticizers to enhance the mobility of fluoropolymers in FPNPs and promote fusion, while the strong-light irradiation at the late-stage of the photo PISA could accelerate the complete consumption of PFSt and contribute to the maintenance of the surface roughness. Thanks to the unique properties of PFSt units, the raspberry-like FPNPs could be easily post-modified via chemical or physical interactions, without a clear impact on the morphology. Cross-linking via nucleophilic aromatic substitution with dithiol compounds clearly improves the thermal stability of FPNPs for over 30 ºC.

Furthermore, photo PISA approach facilitates the fabrication of FPNPs under long-wavelength light irradiation.[177] Cao and co-workers[178] employed fluorophenyl bacteriochlorin as a near-infrared PC to prepare FPNPs, providing fluorinated micelles of poly(PEGMA)-*b*-poly(12FHMA) (D_h = 279 nm), poly(PEGMA)-*b*-poly(12FHMA) (D_h = 185 nm) via PET-RAFT polymerization under 740 nm light irradiation.

3.1.3 PISA Mediated by ATRP and Other Reactions

PISA mediated by ATRP was pioneered by the Pan[179] and Armes[180, 181] groups, which are probably the earliest examples of employing RDRPs in PISA systems. Those examples shed light on the possibilities of synthesizing micelles at improved concentrations via *in situ* growing solvophobic chains onto solvophilic macroinitiators using copper catalysts under thermal conditions. However, regarding the preparation of FPNPs, only very limited examples have been reported based on ATRP-mediated PISA. Wang and co-workers prepared poly[oligo(ethylene glycol) methyl ether methacrylate], poly(OEOMA), capped with bromide as a macroinitiator/stabilizer, employed 13FOMA and GMA as comonomers in Cu-catalyzed ATRP. Authors found that a lower dosage of GMA yielded spherical FPNPs of larger diameters, while a smaller 13FOMA amount produced smaller spherical FPNPs and short worms.[182]

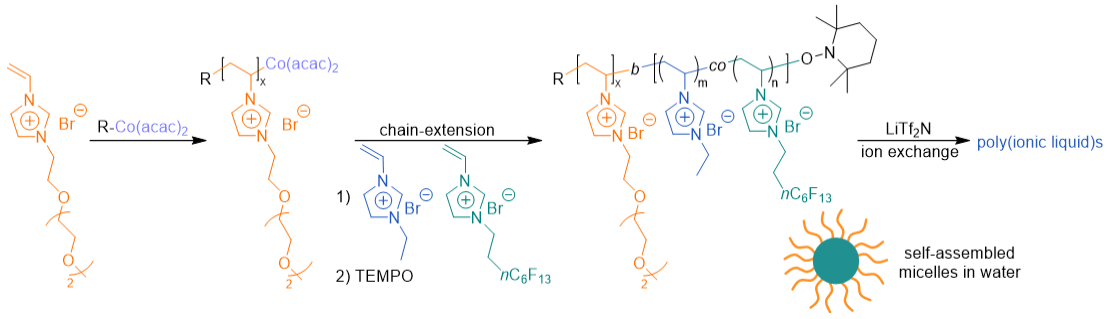

Scheme 15. Synthesis of poly(ionic liquid)s via sequenced cobalt-mediated PISA of various *N*-vinyl-3-alkyl-imidazolium comonomers.[183]

In 2017, the Detrembleur group[183] reported the development of cobalt-mediated RDRP PISA in water, which has allowed the synthesis of poly(ionic liquid)s based on the combination of three *N*-vinyl-3-alkyl-imidazolium derivatives as comonomers (Scheme 15). In this method, poly(*N*-vinyl-3-triethylene glycol-imidazolium bromide) polymers capped with cobalt terminals are used as solvophilic macroinitiators in the chain-extension through the cobalt-mediated copolymerization of *N*-vinyl-3-ethyl-imidazolium bromide and *N*-vinyl-3-perfluorooctyl-imidazolium bromide in water, yielding FPNPs of D_h = 48-144 nm with *PSD* = 0.11-0.19 as analyzed by DLS. Subsequent anion (Br^-) exchange with bis(trifluoromethylsulfonyl) imide anion affords poly(ionic liquid)s that could be interesting for polymer electrolyte purpose. In the same year, this group[184] reported cobalt-mediated chain-extension copolymerization of perfluorohexylethylene and VAc from poly(VAc) with cobalt chain-end. For block copolymers before and after hydrolysis, both samples exhibit two populations of FPNPs in terms of diameters as analyzed by DLS and TEM, where the larger particles ($D_h \approx 400$ nm) could be caused by aggregation during sample preparation.

3.2 Covalent Cross-Linking during RDRPs

Covalent cross-linking of polymers is an important strategy to provide PNPs of strengthened stability toward chemicals, pH variation, elevated temperature, etc. Covalently cross-linked polymer networks have been successively constructed through post-polymerization modifications of PNPs

obtained via solution self-assembly, self-folding and PISA strategies as mentioned in previous sections. Alternatively, the cross-linked networks can also be formed during chain-growth in RDRPs by adding monomer and cross-linker (e.g., divinyl compounds), simultaneously. Related examples based on such a strategy will be highlighted in this section.

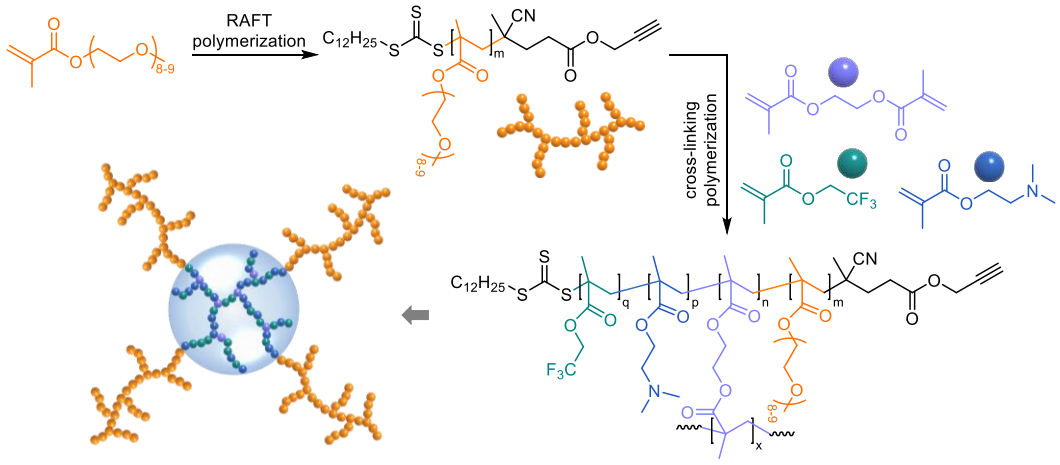

Scheme 16. Schematic illustration for the synthesis of cross-linked FPNPs based on RAFT polymerization.[185]

The Whittaker group[185] demonstrated the synthesis of spherical FPNPs with cross-linked fluorinated cores and hydrophilic arms by chain-extension random copolymerization (RAFT mechanism) of TFEA and DMEMA repeating units onto poly(PEGMA) macro-CTAs (Scheme 16). To afford polymer networks, ethylene glycol dimethacrylate (EDGMA) was employed as a cross-linker, and was added during copolymerization. While dimethyl amine groups on poly(DMEMA) segments provide FPNPs with pH-responsive properties (diameter = 20-25 nm at pH 6, diameter ≈ 10 nm at pH 9 observed by cryo-TEM), poly(PEGMA) arms supply biocompatible and hydrophilic shells in water. One year later, the same team[186] reported that when bis(2-methacryloyl)oxyethyl disulfide was used instead of EDGMA during the formation of covalently cross-linked cores based from RAFT polymerization, it provides degradable function toward reducing agents (e.g., tris(2-carboxyethyl)phosphine hydrochloride, L-glutathione), attributing to the oxidative property of disulfide group. Later, this team[187] also designed poly(OEGA) with trithiocarbonate end-groups and PFPE tails as macro-CTAs to yield hyperbranched FPNPs with cross-linked cores via RAFT copolymerization of EDGMA and OEGA. The customized preparations of those FPNPs provide promising and effective tools for ^{19}F MRI purposes (section 5.1).

Terashima et al.[188] disclosed the use of alkyl chloride functionalized PEG as a macroinitiator in the Ru-catalyzed controlled radical copolymerizations of EDGMA and 13FOMA (Scheme 17). When DMEMA or [2-(methacryloyloxy)ethyl]-trimethylammonium chloride was employed as a comonomer in addition to EDGMA and 13FOMA, dual functionalized PNPs with hydrodynamic diameters of D_h = 48-74 (by DLS) were successfully afforded, providing high concentrations of fluorine atoms in the cross-linked cores. The presence of fluorine and amine, or fluorine and

ammonium salt in FPNPs effectively facilitates cooperative recognition of per- and polyfluorinated alkyl substances (PFASs, section 5.5) based on dual interactions (e.g., fluorophilic/acid-base interaction, fluorophilic/ionic interaction). Alternatively, the PEG-based macroinitiator could be replaced by poly(MMA) capped with alkyl chloride in the Ru-catalyzed RDRP, which has further allowed the preparation of FPNPs in organic solvents and with a variety of fluorinated methacrylates bearing 9 to 17 fluorine atoms in each monomer.[189, 190]

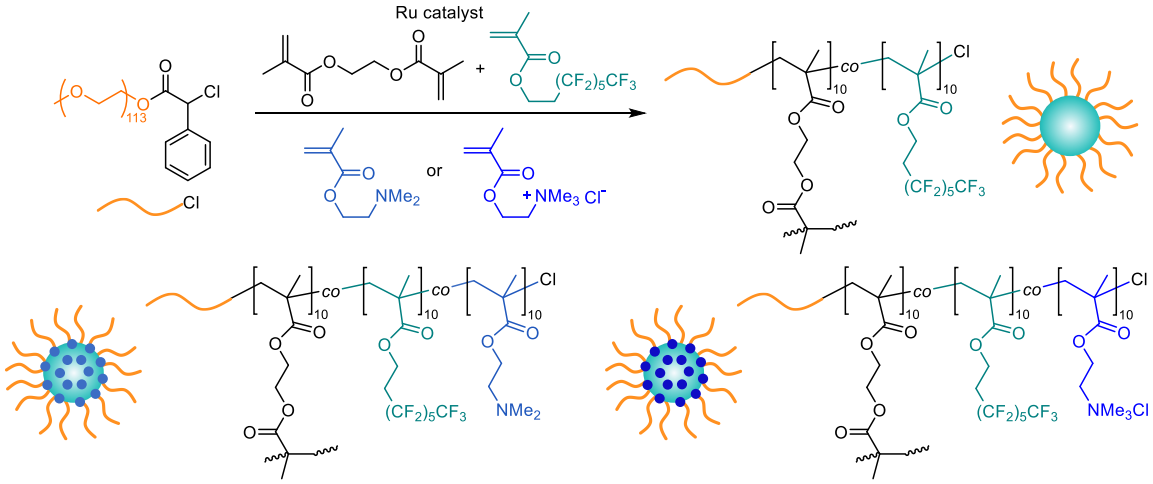

Scheme 17. Schematic illustration for the synthesis of functional cross-linked FPNPs based on Ru-catalyzed polymerization.[188]

Chen and co-workers[42] developed photoredox-mediated RAFT polymerization of nonafluorohexyl methacrylamide or perfluorooctyl methacrylamide using ethylenedimethacrylamide as a cross-linker, phenothiazine derivative as a photocatalyst, PEG substituted trithiocarbonate as a CTA, under visible-light irradiation in ethanol. This method not only provides cross-linked FPNPs of high fluorine concentrations in cores and narrow particle size dispersity (e.g., *PSD* = 0.140, D_h = 25 nm by DLS), but also avoids metal-contamination concerns by using organic photocatalyst and improves chemical stability by introducing methacrylamide-based fluorinated monomers. The observations of remaining macro-CTA and the high-molar-mass fluoropolymers (up to about 10^6 Da) are in accord with findings in their previous works.[173-175] Taking advantage of the remaining macro-CTA and PC in a solvent, as well as trithiocarbonate functionalized FPNPs, when the reaction mixture was treated with additional acrylamide, ethylenedimethacrylamide and water under light irradiation, FPNPs-embedded hydrogels were produced at quantitative yields, which was further examined for PFASs adsorption (section 5.5).

4. GRAFTING FROM INORGANIC NANOPARTICLES VIA RDRPS

Inorganic-polymeric core-shell nanohybrids have served as robust platforms to provide high-performance nanostructured materials.[191-193] The large surface energy of nanoparticles inevitably causes the formation of aggregates in the polymer matrix, which exhibit many negative impacts on

the behaviors of nanocomposites, particularly, when high loadings of nanoparticles are demanded.[194] To solve problems, preparations of core-shell nanohybrids via SI-RDRPs,[191] for instance, SI-ATRP and SI-RAFT polymerization,[195] have attracted great interests by merging with the "grafting from" strategy. In this strategy, because initiation and propagation of polymers are performed from the inorganic surface,[196] the polymeric shell layers are firmly attached to the inorganic nanoparticles via covalent bonds, which can efficiently avoid nanoparticle aggregation and increase the compatibility between polymers and inorganic nanoparticles.[197, 198]

4.1 Grafting from Inorganic Nanoparticles via ATRP

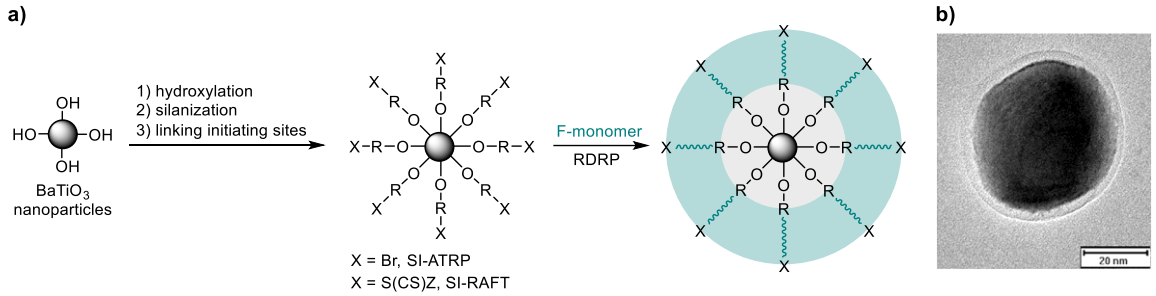

Figure 14. a) Preparation of fluoropolymer@$BaTiO_3$ via SI-RDRPs. b) TEM micrograph.[199] Reproduced with permission from ref [199]. Copyright 2013 Elsevier.

Takahara and co-workers[200, 201] developed SI-ATRP of (meth)acrylates using different surfaces and particles as substrates. The use of fluoroalcohol solvents allows controlled chain-growth of ionic monomers with copper catalysts. In 2013, Ma, Yang and co-workers[199] reported the preparation of nanocomposites poly(13FOMA)@$BaTiO_3$ based on SI-ATRP (Figure 14a), yielding hybrid FPNPs of 30-50 nm inorganic cores and about 5 nm polymeric shells (Figure 14b). The synthetic process includes two stages: (i) the modification of $BaTiO_3$ nanoparticle surface via a sequence of hydroxylation, silylation and amidation to yield $BaTiO_3$ nanoparticles linked with alkyl bromide as initiating sites; (ii) the synthesis of core-shell structured poly(13FOMA)@$BaTiO_3$ nanoparticles through grafting from modified $BaTiO_3$ surface. Different ratios of $BaTiO_3$/13FOMA were utilized to probe the influence on dielectric properties. The results demonstrated that increasing the $BaTiO_3$ content is favorable to achieve a high dielectric constant (up to 7.4 at 100 kHz at room temperature) and reducing dielectric loss, which is of interest to high energy storage devices (section 5.4).

In 2014, He's group[202] prepared fluorinated diblock copolymers grafted onto silica particles via SI-ATRP of MMA and 12FHMA. Nanohybrids of SiO_2-*g*-poly(MMA)-*b*-poly(12FHMA) were synthesized with 25-30 nm spherical core-shell nanoparticles from 10-25 nm silica particles as observed by TEM. In comparison to poly(MMA)-*b*-poly(12FHMA) diblock copolymers obtained by ATRP, the diblock copolymer shells grafted from silica nanoparticles are favorable to increasing the surface roughness of films, which can promote the hydrophobic and oleophobic properties.

4.2 Grafting from Inorganic Nanoparticles via RAFT Polymerization

In 2018, Zhang, Luo and co-workers[203] demonstrated the synthesis of novel rigid liquid-crystalline fluoropolymers of poly[2,5-bis[(4-trifluoromethoxyphenyl)oxycarbonyl]styrene], poly(TFMPCS). It enables the preparation of a series of core-shell structured poly(TFMPCS)@$BaTiO_3$ via SI-RAFT with different thicknesses of interfacial layers. The shell thickness could be regulated by modulating the degree of polymerization of TFMPCS. The introduction of poly(TFMPCS) shell layer onto $BaTiO_3$ surface improved the affinity with poly(VDF-TrFE-CTFE) as a matrix. The poly(TFMPCS)@$BaTiO_3$/poly(VDF-TrFE-CTFE) nanohybrid films were fabricated via solution blending. The dielectric behavior and energy storage capacity were probed to explore the potentials for energy storage purpose (section 5.4).

In 2019, Ameduri's group[204] reported the fabrication of inorganic-polymeric core-shell particles using VDF for the first time, yielding PVDF-*g*-$BaTiO_3$ nanohybrids via SI-RAFT of VDF from surface-functionalized $BaTiO_3$ nanoparticles (Figure 14a). The ceramic nanoparticles were surface-modified to connect with xanthate groups as CTAs, which ensured the grafting of PVDF from the modified $BaTiO_3$ surface. Decreasing the $BaTiO_3$ concentration from 20 wt% to 5 wt% led to the thickness of polymer shell varying from 2.2 nm to 5.1 nm. Authors demonstrated that high $BaTiO_3$ loading tends to improve the thermal stability of the nanomaterials and reduce their crystallinity rate.

5. APPLICATIONS

Since the last century, FPNPs have been broadly applied for coatings, paintings, additives, membranes and other purposes in construction, automobile, aerospace, chemical industries and so on.[7-9] Advancements in RDRPs have brought FPNPs with customized functionalities, fluorine densities, morphologies, sizes, solubilities, mechanical strength and other desirable properties, which have allowed their increasing investigations for high-tech applications. This section will highlight the emerging applications of FPNPs afforded based on RDRPs in recent years, which include ^{19}F MRI, biomedical delivery, energy storage, PFASs adsorption, photosensitizer and others.

5.1 Magnetic Resonance Imaging

MRI is one of the most useful clinical imaging techniques, attributed to the noninvasive property and high versatility that facilitates in-situ investigations of physiological, anatomical information.[205-207] ^{19}F MRI allows unambiguous detection of fluorine signals with negligible background influence from the human body, and ^{19}F nucleus possesses 100% natural abundance with satisfactory resonance frequency (versus about 94% of ^{1}H nucleus) and magnetic resonance sensitivity (versus about 83% of ^{1}H nucleus).[208, 209] The strong C-F bonds provide outstanding bio-inertness for fluorocarbons. As a result, ^{19}F MRI has been developed as a powerful and visualizable technique which provides independent and complementary information for biological and clinical imaging applications.[210, 211] Various fluorine-containing imaging agents have been designed, including small molecules, macromolecules and FPNPs, as well as paramagnetic metal-based substances.[212] Among them, FPNPs are able to provide high fluorine density, tunable circulation time, stimulus responsiveness, and therefore have received considerable attention. This section highlights examples of applying FPNPs in ^{19}F MRI investigations.

$$I \approx N(F)\exp\left(\frac{-\mathrm{TE}}{T_2}\right)\left[1-2\exp\left(\frac{-\left(\mathrm{TR}-\frac{\mathrm{TE}}{2}\right)}{T_1}\right)+\exp\left(\frac{-\mathrm{TE}}{T_1}\right)\right]$$

Equation 1

In MRI, imaging intensity (I) depends on various parameters as N(F) represents the ^{19}F atoms that are detectable by NMR, TR is pulse sequence repetition time, and TE is echo delay time (Equation 1) .[213] To afford high imaging intensity in ^{19}F MRI, high spin-spin relaxation time (T_2) and low spin-lattice relaxation time (T_1) are favorable according to this equation, where an increase of T_2 causes enhanced signal-to-noise ratio, and a decrease of T_1 declines scan time. The relaxation time of T_2 parameter is dictated by dipolar coupling of the ^{19}F nuclei with nearby ^{19}F/^{1}H nuclei. Therefore, T_2 can be influenced by the spatial distribution of ^{19}F/^{1}H and their relative mobility.[185, 213]

Fluorine contents can cause different extents of influences on T_1 and T_2, as demonstrated by FPNPs obtained via solution self-assembly, PISA and covalent cross-linking processes.[166, 185, 186] For nano-objects of spherical, worm-like and vesicle morphologies, T_1 and T_2 remain constant, indicating no dependence of relaxation time on morphology, and implying that architectures and dynamics of hydrophilic shells of FPNPs are not detectably altered for those nano-objects.[166] In comparison, using Chinese Hamster Ovarian (CHO) cells as an example, authors illustrated that morphology exhibited an apparent impact on cell uptake,[166] where worm-like FPNPs showed the highest uptake, and those FPNPs exhibited little or no cytotoxicity.

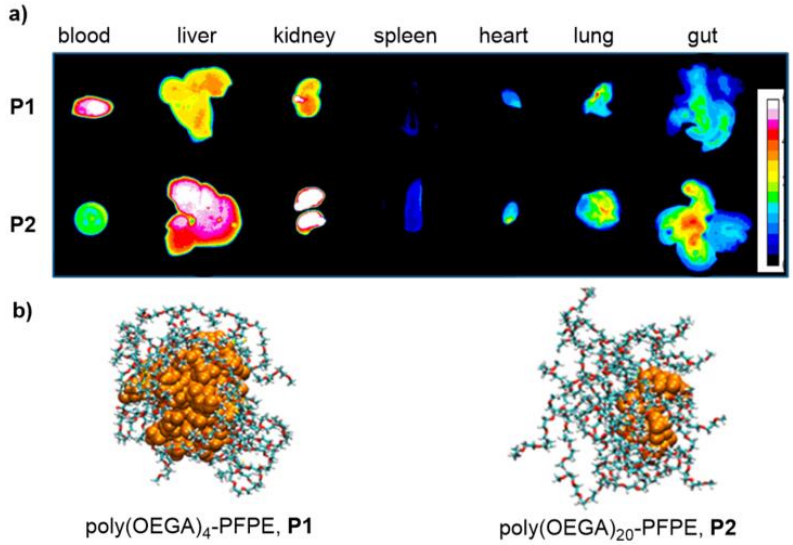

Figure 15. a) *Ex vivo* fluorescence images of organs for biodistribution of PFPE-*b*-poly(OEGA) copolymers. b) Simulated conformation of assemblies with **P1** and **P2** in solution.[214] Reproduced with permission from ref [214]. Copyright 2017 American Chemical Society.

Aggregation states of FPNPs also show considerable impacts on ^{19}F MRI applications. FPNPs formed by PFPE-*b*-poly(OEGA) copolymers have been explored as ^{19}F MRI agents with high

fluorine contents up to about 30 wt%, providing T_2 ≈ 80 ms and T_1 ≈ 400 ms in a biological environment (Figure 15).[214] In a series of PFPE-*b*-poly(OEGA) copolymers, shorter poly(OEGA) blocks (**P1**) give small aggregates of multiple chains (D_h ≈ 8.1 nm), and longer poly(OEGA) blocks (**P2**) lead to single-chain folding (D_h ≈ 8.3 nm).[214] The two types of FPNPs exhibit different *in vivo* biodistribution, where the self-folded FPNPs give higher uptake in kidneys, liver and lungs, suggesting better recognition and clearance in organs. When the poly(OEGA) segments in diblock copolymers are replaced by poly(oligo(2-oxazoline)acrylate)s, the self-assembled FPNPs are thermo-responsive.[215] While the formation of smaller aggregates gives higher ^{19}F MRI signal intensity below the LCST, larger FPNPs are formed above the LCST (338 K), which leads to a decline in the ^{19}F MRI intensity. Hruby and co-workers[216] found that block copolymers with longer thermo-responsive blocks show better labeling behavior. Decomposition of core cross-linked FPNPs leads to structural change to linear polymers, resulting in intensified ^{19}F MRI signals.[217]

Using cross-linked FPNPs with amine-functionalized cores, Whittaker et al.[185, 186] developed pH-responsive contrast agents for ^{19}F MRI. When the environmental solution is acidic, the poly(DMEMA) segments embedded in cores are prone to expand to the swollen state, attributing to electrostatic repulsion between positively charged ammonium groups, and leading to improved mobility of fluorinated pendants with prolonged T_2 up to about 40 ms at pH <6.5.[185] In comparison, T_2 is significantly reduced (<10 ms) under basic conditions. A similar hypothesis for the explanation of reduced relaxation time has also been demonstrated by others, where cross-linking strategy has been probed to preserve the morphology of assemblies.[218] Since tumor tissues are normally acidic, the pH-responsive T_2 relaxation time of amine-functionalized FPNPs potentially provides a selective ^{19}F MRI technique for tumor diagnosis. The concept of pH-responsive ^{19}F MRI agents has been successfully expanded by conjugating FPNPs onto inorganic substrates (e.g., manganese-based layered double hydroxides), which have allowed *in vivo* detection of breast cancer tissues via intravenous injection.[101]

Exotic responsive functions are added into FPNPs via customized selection of non-fluorinated comonomers. For instance, Hruby and co-workers[98] incorporated small amounts of *N*-[2-(ferrocenylcarboxamido)ethyl]acrylamide (FcCEA) into FPNPs. At the reduced state of ferrocene (Fe(II)), the FPNPs are hydrophobic and diamagnetic, but they changed to hydrophilic, paramagnetic and dissembled polymers upon oxidation to Fe(III). This chemical responsive property could potentially allow drug delivery under reactive oxygen species-responsive environments.[219]

Innovations based on fluorinated monomers are often good options to develop novel ^{19}F MRI agents. For instance, Couturaud et al.[220] developed bifunctional fluorinated acrylate with both trifluoromethyl and adamantane units to enable the host-guest interaction between adamantane and *β*-cyclodextrin in copolymers. The supramolecular complexation effectively poses impacts on the relaxation properties and ^{19}F MRI intensity, presenting an interesting example of exploring supramolecular FPNPs as novel contrasting agents. Kong, Wang et al.[221] designed 2-((2,4-dinitro-*N*-(trifluoropropyl)-phenyl)sulfonamido)ethyl methacrylate, and applied it to prepare biothiol-responsive FPNPs via RAFT copolymerization with PEGMA, which provide T_2 up to about 300 ms and allow effectively intracellular and intra-tumoral imaging of glutathione. Using nonafluoro-*tert*-

butoxyethyl acrylate (a monomer of highly densified and chemically equivalent fluorine atoms) to copolymerize with poly(ethylene glycol)methyl ether acrylate via RAFT polymerization, Leibfarth's team[222] prepared FPNPs (D_h = 4.3-17 nm by DLS) as oxygen sensitive ^{19}F MRI contrasting agents. Those materials permit quantifying solution oxygenation at clinically relevant magnetic field strengths with an outstanding signal-to-noise ratio. Notably, a machine-learning-assisted continuous-flow polymerization technique has been further established to promote the comprehensive optimization of the fluorinated contrasting agents,[223] enabling the discovery of more than 10 ^{19}F MRI agents that surpass state-of-the-art materials in an automated pathway.

Beyond poly(OEGA), other hydrophilic monomers, including 2-(methylsulfinyl)ethyl acrylate (MSEA),[224] have been employed to copolymerize with TFEA via RAFT polymerization. FPNPs of poly(OEGA)-*co*-poly(TFEA) and poly(MSEA)-*co*-poly(TFEA) prepared under similar conditions are systematically examined.[224] While the former particles give D_h = 2.7-8.3 nm, T_1 = 423-459 ms, T_2 = 28-139 ms in a ^{19}F content range of 6.0-18.5%, the latter ones offer D_h = 2.1-7.2 nm, T_1 = 444-641 ms and T_2 = 22-330 ms in a ^{19}F content range of 5.8-19.3%, suggesting comparable properties, even improved parameters can be achieved by optimizing the chemical structure of hydrophilic repeating units.

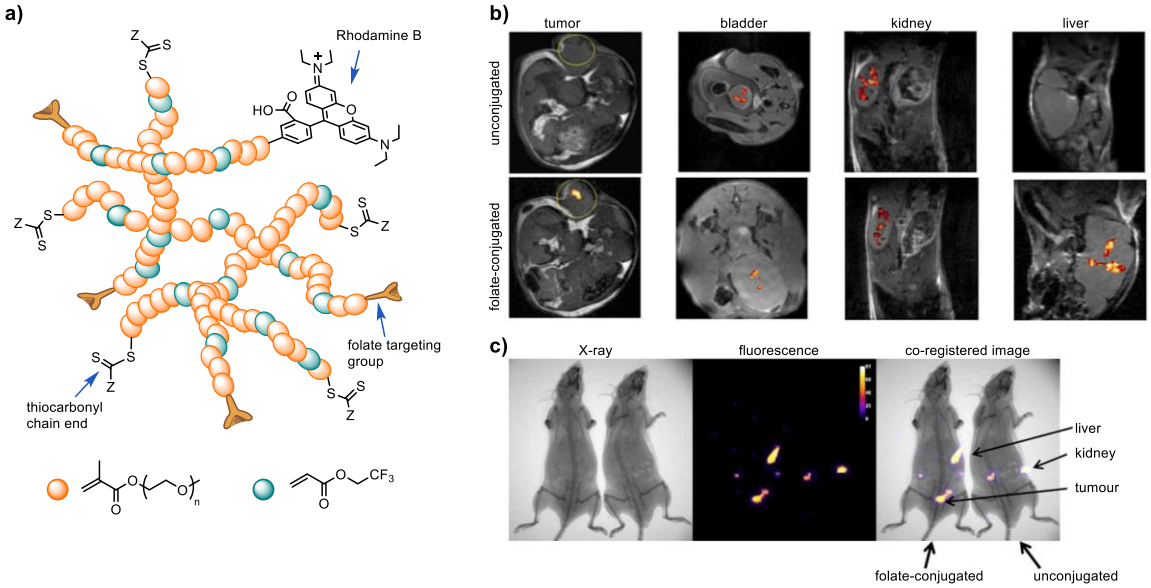

Figure 16. a) Schematic illustration of multi-functional hyper-branched polymers. b) MRI images of organs with unconjugated and folate-conjugated polymers. c) Fluorescence images of mice after injecting unconjugated and folate-conjugated polymers.[225] Reproduced with permission from ref [225]. Copyright 2014 American Chemical Society.

To allow multimodal imaging, different functional groups are connected onto FPNPs. Thurecht and co-workers[225] demonstrated the first combination of ^{19}F MRI and fluorescence imaging in FPNPs. Because FPNPs are synthesized based on RAFT chemistry, terminal groups introduced from CTAs enable facile connections of folic acid (folate targeting ligand for FOLRα receptor[226]) and/or Rhodamine B (fluorescent marker) onto polymer chain-ends (Figure 16a) via copper-

catalyzed “click” reactions between azides and alkynes. Since good segmental mobility in both serum and intracellular fluid is important, regulation of particle sizes allows exerting control over biodistribution and pharmacokinetics of FPNPs, affording fast clearance (< 2 h) with particle radius of less than 8 nm and prolonged circulation time with particle radius of above 11 nm. Both MRI and fluorescence images (Figures 16b and 16c) display the existence of folate-conjugated and unconjugated FPNPs in organs. While ^{19}F MRI supplies high-resolution analysis results that allow analyzing the distribution of FPNPs in diverse organs, fluorescence characterizations give entire images of mice for tracking purposes. The presence of folate-targeted samples in the bladder and kidney suggests the good mobility of FPNPs. This work provides versatile FPNPs that can merge multiple imaging modalities in a single system without compromising their distinct advantages, which can potentially promote *in vivo* detection of various diseases. In addition, based on rational combinations of compatible functional groups in different RDRPs, the alkyne- or azide-functionalized FPNPs provide a useful platform to integrate with different functions, such as near infrared fluorescent dyes, therapeutic agents, bringing additional functions beyond ^{19}F MRI.[227-229]

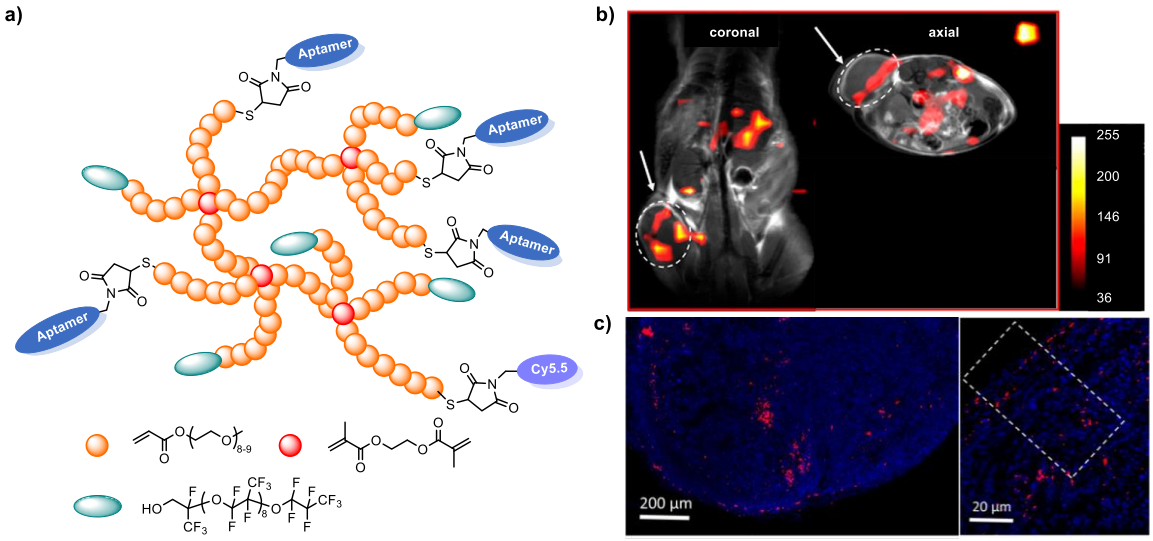

Figure 17. a) Schematic illustration of aptamer-conjugated hyperbranched PFPE FPNPs. b) Coronal and axial MRI images of a mouse loaded with HBPFPE-apt particles. c) Fluorescence micrograph of tumor section with HBPFPE-apt particles.[187, 230] Reproduced with permission from ref [187]. Copyright 2018 American Chemical Society.

Post-polymerization modification of trithiocarbonate terminals yields PFPE-based hyperbranched FPNPs with unprotected thiol groups, which have been employed as covalent linkers to connect with fluorescence dye (Cy5.5) and peptide aptamer (targeting ligand) via thiol-maleimide “click” chemistry (Figure 17a).[187] The dye and aptamer-conjugated hyperbranched PFPE (HBPFPE-apt) particles are examined as a novel multifunctional contrast agent for *in vivo* detection of breast cancer cells using both fluorescence and ^{19}F MRI techniques. The HBPFPE-apt agent not only provides outstanding ^{19}F MRI signals in the tumor region, but also furnishes

higher uptake into cells, faster transport across cellular barriers, faster clearance from the body, presenting an excellent candidate for ^{19}F MRI detection of diseases *in vivo* (Figures 17b and 17c).[230] The outstanding penetration into tumors implies that such PFPE-based particles could be potentially useful for both diagnosis and treatment of diseases. Moreover, the thiol groups on FPNPs are versatile functional groups to connect with other functional molecules to facilitate multiple imaging purposes.[231]

5.2 Biomedical Delivery

In past decades, a variety of substances such as nanomaterials, polymers and lipids have been explored as candidates for biomedical delivery.[26, 232] However, problems including biocompatibility, transfer efficiency, carrying ability and others have hindered practical applications of many candidates. To address such difficulties, rationally designed FPNPs of tunable water solubility have been disclosed as promising materials for biomedical delivery (e.g., gene, protein and drug delivery), providing fruitful results as summarized in several excellent reviews.[26, 232-235] Although most studies are based on FPNPs prepared via conventional organic reactions, for example, modifications of macromolecules with fluorinated small-molecular agents (e.g., perfluorinated anhydride, perfluorinated carboxylic acid, perfluorinated acyl chloride, etc.) via amidation, esterification and others,[26, 232-235] RDRPs present an alternative pathway that allows customized access to FPNPs with readily available starting materials. In this section, advantages of fluoropolymers in related applications will be discussed, and studies of gene, protein and drug deliveries with FPNPs prepared based on RDRPs will be highlighted.

5.2.1 Gene Delivery

The utilization of genes as therapeutic agents to recover defective production of proteins, regulate gene expression holds great potentials for the treatment of both heritable and acquired diseases.[235] However, the lack of effective carriers has largely restricted the usage of genetic therapeutics. A successful gene carrier should provide protection to genes, avoid detection/clearance, prevent undesirable interactions with non-target proteins/cells, selectively release genes after overcoming various barriers, meanwhile, maintain non-toxicity during the whole process. In addition, nucleic acids are normally negatively charged. Lots of developments have used cationic polymers as carriers to form nanoscale complexes with genes, namely, polyplexes, via electrostatic interactions.[235-237] Because of the abundant presence of salts, serum proteins and other polyanions in the physiological environment, lots of polyplexes with genes are lack of enough stability, leading to the usage of higher amounts of cationic carrying materials, which could simultaneously bring risks of destroying cell membranes, causing inflammation, etc.[238]

To address such problems, researchers have developed fluorinated polymeric carriers.[239] Thanks to the strong hydrophobic and fluorophilic properties, fluorinated segments connected on the cationic polymers could stabilize polyplexes in physiological environments at low critical concentrations, defending them from destabilized by serum proteins and other negatively charged biomacromolecules.[239-243] At the same time, while fluoropolymers have shown bio-inert and anti-fouling properties, fluorinated polyplexes have exhibited improved serum tolerance without decreasing transfection efficiency.[244-248] To deliver nucleic acids such as DNA, siRNA, miRNA, etc., synthetic modifications of polyamidoamine, poly(ethylenimine), poly(propylenimine), poly(amino

ester), polypeptides and many other dendrimers with fluorinated agents have been developed to produce cationic fluorinated carriers.

To expand the fluoropolymer scope for the transduction of nucleic acids, Zentel and co-workers[249] prepared poly(PFPMA)-*b*-poly(PEGMA) copolymers via RAFT polymerization, which were cross-linked via post-modifications with diamine to give nanohydrogel particles of different diameters. These authors demonstrated that fluorinated cationic particles of smaller sizes could avoid acidic compartments via endolysosomal uptake avenues, possibly benefiting the exclusive siRNA knockdown.[95]

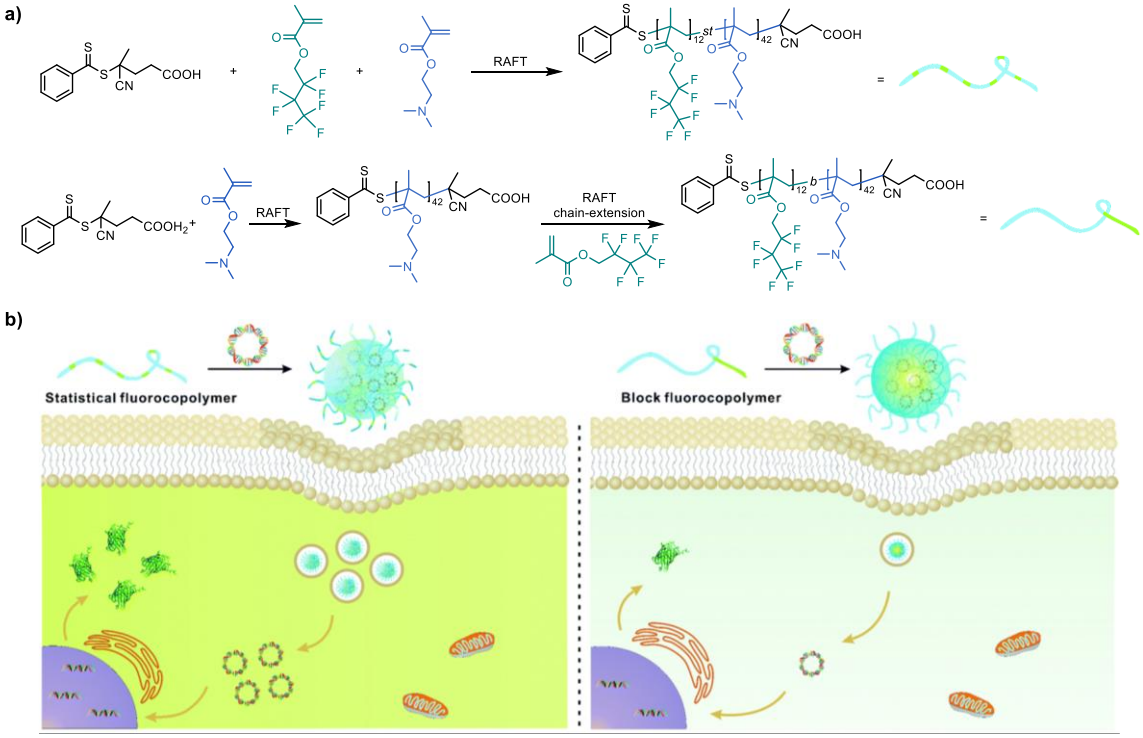

Scheme 18. a) Synthesis of statistical and block fluorinated copolymers via RAFT polymerization. b) Mechanisms of copolymers of two sequences in gene delivery.[250] Reproduced with permission from ref [250]. Copyright 2018 Royal Society of Chemistry.

Cheng and co-workers[250] prepared copolymers of both statistical and block sequences using DMEMA and heptafluorobutyl methacrylate (7FBMA) as a comonomer pair through RAFT polymerization (Scheme 18a). When the transfection efficiencies were examined, the statistical copolymer afforded clearly higher performance in gene delivery, probably owing to the better DNA uptake by transfected cells (Scheme 18b). In comparison to non-fluorinated counterparts, fluorinated poly(DMEMA)-*st*-poly(7FBMA) exhibited much superior gene delivering efficiency, better serum compatibility and lower cytotoxicity, shedding light on the design of fluorinated gene carriers based on RDRPs. Ge and co-workers[251] illustrated the employment of RAFT polymerization and thiolactone chemistry in combinatorial methodology to construct a library of

multifunctional polymers for pDNA delivery. The fluorinated copolymers displayed higher gene transfection efficiency and lower cytotoxicity than that of non-fluorinated counterparts.

Since intracellular gene delivery should interact with several liquid-solid interfaces including membranes of cell, endosomal and nuclear, investigations on the dynamics of polymer kinetics on the related interfaces are important for the design of polymer carriers.[235-237] Higgins, Iyer and co-workers[252] prepared linear random copolymers via ATRP and post-functionalized copolymers with azide side groups. Poly(amidoamine) dendrons were grafted onto the linear backbone via click reaction between azide and alkyne functional groups, followed by post-modification of poly(amidoamine) with perfluorinated anhydride. This protocol allows the regulation of molar masses, charge density on the dendronized linear polymeric topology. As assisted by high-speed AFM, authors systematically probed polymer dynamics (velocity, displacement, diffusion) under physiologically related conditions, and demonstrated that the interaction strength and diffusion performance with fluorinated polyplexes are relevant to the transfection potential.

5.2.2 Protein Delivery

Proteins are capable of acting precisely on targets and regulate biological processes with outstanding selectivity and potency, providing protein-based therapeutics with high specificity and low adverse effects as compared to small-molecule drugs.[253-255] Despite the merits, protein-based therapeutics encounter significant obstacles posed by *in vitro* and *in vivo* instability. The rational design of suitable carriers, which can shield proteins from enzymatic degradation and prolong retention of proteins without introducing cytotoxicity, is a painful task due to the intrinsic characteristics of proteins, such as indeterminate charge properties depending on the isoelectric point and environmental pH value.[256] The limited negative charges on proteins are the major barrier to mimicking gene delivery, which adopts cationic polymers as carriers. Unstable protein-carrier complexes will disassemble in the presence of salts, polyanions and phospholipids in corresponding bio-environmental conditions.[257-260] To address these issues, two approaches have been developed, including a) fabrication of protein-polymer conjugates via dynamic covalent linkages, b) improving binding affinity between polymeric carriers and proteins via synthesis of well-defined functional polymers or chemical modifications of proteins.[255]

While current protein drugs are frequently restricted to extracellular targets due to the limited membrane permeability of proteins,[261] intracellular protein delivery has drawn considerable attention in recent years. For this purpose, fluorinated polymers and oligomers are promising candidates as delivery carriers for proteins, particularly for intracellular protein delivery.[260] The hydrophobic and lipophobic properties endow fluoropolymers with high efficiency of transporting across cell membranes, because hydrophobicity facilitates membrane association, and lipophobicity prevents blending with phospholipids on cellar membranes.[26] The restricted fusion of amphiphilic fluoropolymers with phospholipids can effectively avoid destroying cellar membranes, supplying polymeric carriers of low cytotoxicity. Furthermore, amphiphilic fluoropolymers with fluorinated segments exhibit minimal protein denaturation owing to the fluorophilic characteristic, which induces little influence on the secondary structure of proteins.[260, 262] Until now, most examples of generating such fluoropolymers have been based on post-synthetic modifications of non-

fluorinated substrates with fluorinated small molecules as mentioned above.[26] Fluoropolymers accessed via RDRPs are explored as convenient and useful candidates to study protein deliveries.

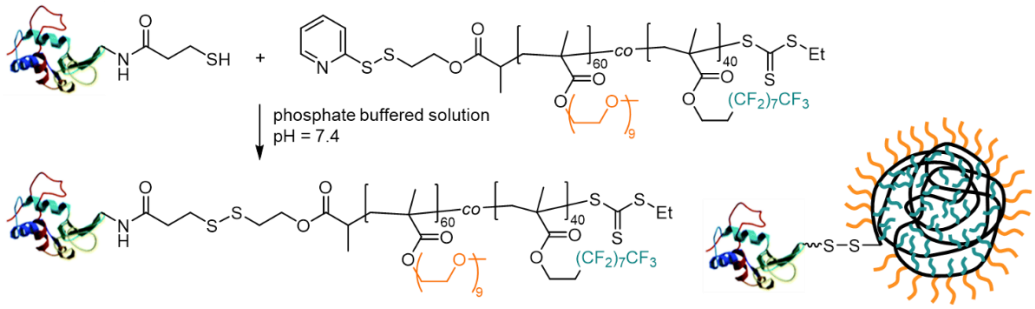

Scheme 19. Generation of the protein-FPNP conjugate via a cleavable disulfide linkage.[78] Reproduced with permission from ref [78]. Copyright 2015 Royal Society of Chemistry.

When FPNPs are employed as protein delivery carriers, many efforts are focusing on the formation of protein-polymer conjugates. For example, Sawamoto and co-workers[78] synthesized random copolymers bearing PEG chains and fluorinated pendants via RAFT copolymerization of PEGMA and 17FDMA (Scheme 19). The aggregates of amphiphilic and fluorinated random polymers carrying pyridyl disulfide terminals were successfully conjugated with thiolated lysozymes via cleavable disulfide linkages. These conjugates are considered as feasible carriers for hypoxic tumor therapy.

Whittaker and co-workers[263] developed water-soluble fluoropolymers with high fluorine contents of up to 25 wt% with *N*-(2-((2,2,2-trifluoroethyl)sulfinyl)ethyl)acrylamide (FSAM) as a monomer. Using bovine serum albumin as a model therapeutic protein, authors prepared protein-fluoropolymer conjugates via a grafting-from method mediated by PET-RAFT polymerization to demonstrate the therapeutic potential with improved pharmacokinetic profiles and in vivo tracking through ^{19}F MRI, which is based on the weak interaction with cellular contents and fluorine atoms. Pharmacokinetic studies revealed that protein-fluoropolymer conjugates effectively extended the circulation time of bovine serum albumin in the bloodstream. The conjugates exhibit outstanding imaging sensitivity, and supply an effective method to examine tissue biodistribution and rates of clearance. At the same time, the capability of direct imaging, negating additional attachment of imaging moieties further underline the advantages of fluoropolymers for protein conjugation and delivery.

5.2.3 Drug Delivery

Although chemotherapy provides an essential approach for cancer treatment, problems in drug delivery, such as poor water solubility and physiological barriers, decrease the efficacy.[264, 265] Meanwhile, normal cells are prone to be influenced by free drugs, causing toxicity to patients. Suitable drug delivery systems, especially with nanoparticles as carriers, are promising to overcome these issues. The drug-nanoparticle combined systems are able of reaching increased drug solubility, providing protection for drugs from quick clearance, allowing sustained drug release

and minimizing side effects.[265-267] Typical nanocarriers include PNPs, inorganic nanoparticles and liposomes. Among them, PNPs are able to furnish good tunability for the drug release process based on their remarkable structural versatility.[268] To this end, fluoropolymers display desirable attributes in several aspects, including 1) excellent self-assembly and self-folding behaviors that can enhance the stability of complexes, 2) good integration of drug carrying and *in vivo* imaging that can combine diverse functions within a uniform system, 3) improved endocytic efficiency that can optimize therapeutic efficacy.[26, 269, 270]

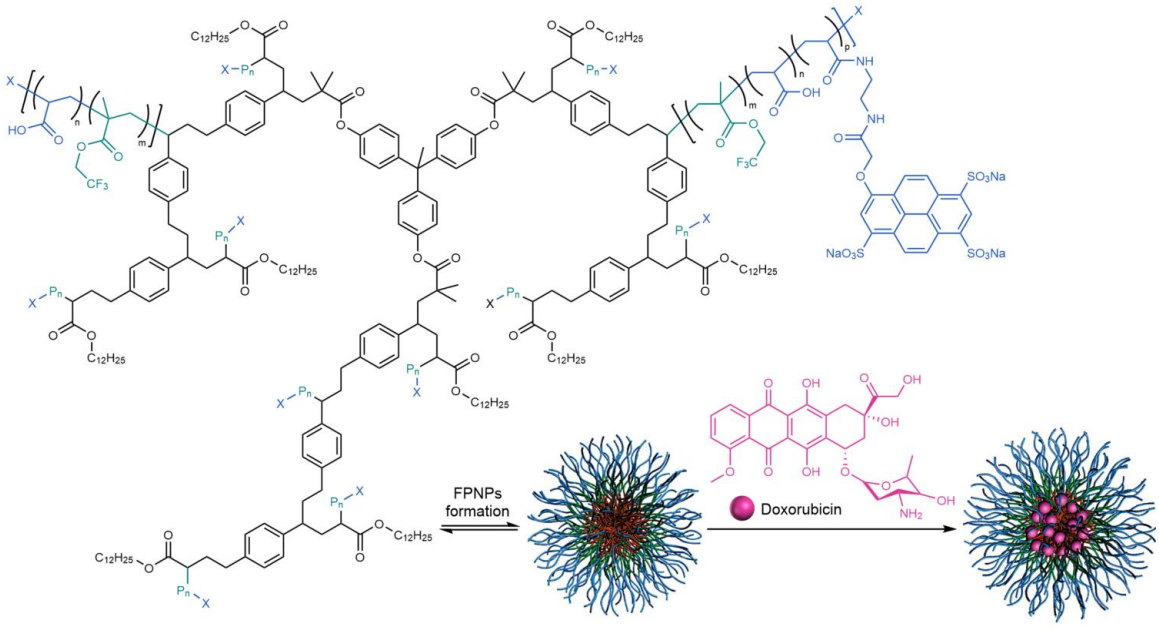

Scheme 20. Chemical Structures for the star-block copolymers and the loading of Doxorubicin (DOX) into FPNPs.[271] Reproduced with permission from ref [271]. Copyright 2008 American Chemical Society.

The Wooley group [68, 271] prepared star-block copolymers with a hydrophobic hyperbranched core and amphiphilic fluorinated arms by merging ATRP and self-condensing vinyl (co)polymerization, which were designed as drug delivery nanostructures and labeled with cascade blue as a fluorophore. The multi-functional fluorinated micelles were loaded with Doxorubicin (DOX) to probe their behaviors of treating U87-MG-EGFRvIII-CBR cancer cells (Scheme 20). The DOX-loaded nanostructures show cell cytotoxicity as influenced by the polymeric composition in the nanoparticles, providing cell viability comparable to that of free DOX. ^{19}F MRI demonstrated that a partial degradation of the fluorinated segments enhanced the extent of release. The multi-functional micelles could be interesting for *in vivo* labeling, imaging, as well as therapeutic delivery.

Tao and co-workers[272] combined enzymatic transacylation and RAFT polymerization to prepare well-defined copolymers bearing different functions, which contain fluorine, PEG, benzaldehyde and azido groups (Figure 18). The enzymatic transacylation between TFEMA and

functional alcohols *in situ* generates functional monomers during polymerization in a one-pot fashion. In the versatile copolymer platform, the PEG pendants improve water solubility and biocompatibility, the fluorinated segments are used as contrast agents in ^{19}F MRI, glucose moiety specifically binding to lectin is introduced as a targeting group via a copper-catalyzed click reaction, aldehyde groups are adopted to yield the polymer-DOX complex via the pH-sensitive imine formation. After self-assembly of the amphiphilic polymer-DOX complexes in aqueous solution, acidic microenvironments of tumors could accelerate the release of DOX due to the pH responsive property of imine bonds. Cellar experiments indicate that the fluoropolymer-DOX complex possesses lower toxicity to cells than that of native DOX, while maintaining analogous cytotoxicity against cancer cells, highlighting the applicable potential of multi-functional fluoropolymer drug carriers.

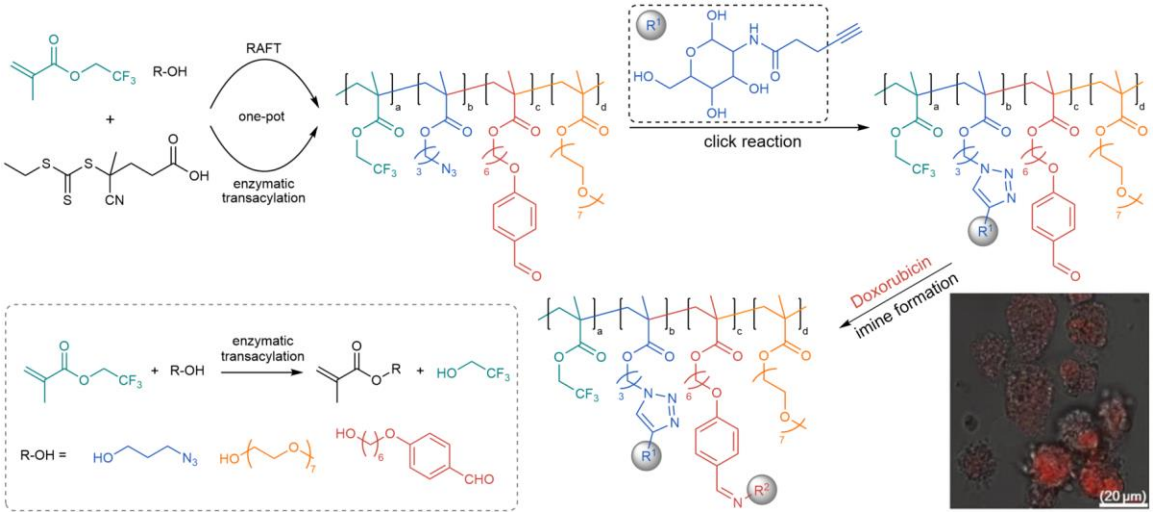

Figure 18. One-pot synthesis via combining RAFT and enzymatic transacylation and post-modification toward multi-functional copolymers. The inset is a representative confocal laser scanning microscopy image of HeLa cells treated with fluoropolymer-DOX complexes.[272] Reproduced with permission from ref [272]. Copyright 2016 Royal Society of Chemistry.

Zhang et al[269]. investigated the influence of fluorine on transporting behaviors with a series of poly(OEGA)-*b*-PFPE copolymers prepared via RAFT chain-extension from PFPE-functionalized macro-CTA (Figures 19a and 19b). The different fluorine contents in copolymers affect the aggregation behavior in water, where copolymers of lower fluorine content tend to form unimers, but copolymers of higher fluorine content form multiple-chain aggregates. Consistent with molecular dynamics simulations, unimers provide a larger exposure of the fluorinated segments to the cell membrane, resulting in higher cellular uptake, deeper tumor penetration, and improved therapeutic result as compared to aggregates that show less PFPE exposed to the cell surface. This work discloses that the aggregation property of fluoropolymers is critical for internalization, transportation in living cells, shedding new light on the fabrication of robust delivery agents.

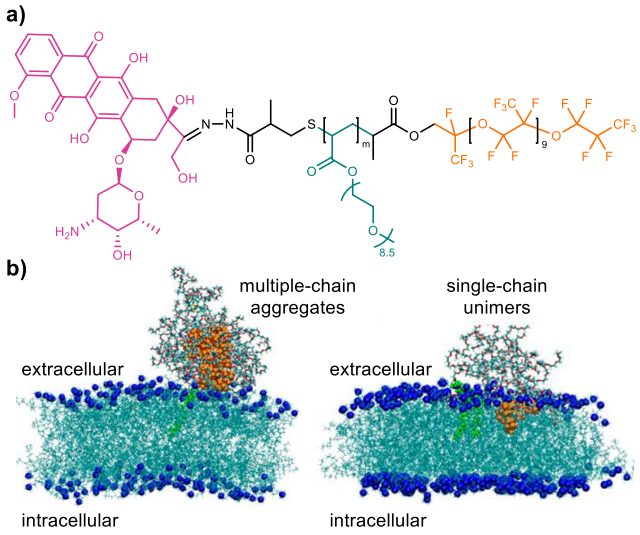

Figure 19. a) Chemical structure of DOX-loaded fluoropolymers. b) Molecular dynamics simulations that represent penetration of multiple-chain aggregates and single-chain unimers.[269] Reproduced with permission from ref [269]. Copyright 2020 American Chemical Society.

5.3 Photosensitizer

Photodynamic therapy (PDT) is a non-invasive and practical treatment for cancers and non-malignant diseases.[273] Photosensitizers (PSs) employed in PDT can be activated by visible-light irradiation, enabling energy transfer to ground-state oxygen ($^3O_2$) to generate singlet oxygen ($^1O_2$). The photo-excited oxygen can destruct tumor cells via apoptosis and/or necrosis, affect tumor vasculature that can induce tumor hypoxia and starvation.[274] In comparison to conventional therapies, PDT displays many merits relevant to its minimized invasive nature, dual specificity depending on both PSs accumulation and light delivery at the lesion location, as well as the capability of repeating treatment without initiating resistance.[275, 276] However, the therapeutic efficacy of PDT is limited by the solubility of PSs and the availability of oxygen within tissues.

Owing to the hydrophobic property, many PSs are prone to aggregate in aqueous solutions, thus causing insufficient tumor uptake and quenching photosensitivity, severely. Although a variety of delivery systems, especially nanoparticles, have been developed to improve the water solubility of PSs, PS-located cores become the major hindrance to oxygen diffusion. At the same time, the PDT process is oxygen-dependent. Photosensitization will not occur in anoxic areas of tissues. While the pathophysiological property of hypoxia has been observed in many solid tumors, hypoxia also arises from PDT-induced oxygen consumption and vascular damage.[96, 277]

Fluorocarbons exhibit good oxygen affinity,[233, 234] which can solubilize much more oxygen than their hydrocarbon counterparts.[278] Based on the unique properties of fluorocarbon and merits of RDRPs, customized FPNPs are promising to combine desirable properties including good water solubility and efficient oxygen supply, relieving issues caused by the hypoxia microenvironment in tumor sites.

To investigate the influence of the content of fluorine on PDT, Huang and co-workers[96] synthesized spherical nanoparticles with different ratios of PFPMA to porphyrin within the core

(Scheme 5). Authors indicated that the increase of PFPMA content resulted in a greater amount of reactive oxygen species production, and caused improvement of PDT efficacy, because the fluorinated segments improve the solubility and diffusivity of oxygen. It was hypothesized that fixing porphyrins onto the polymer network is beneficial to reduce its aggregation and self-quenching of the photo-excited species.[279] This work offers a versatile platform to obtain photosensitizer delivery carriers, potentiating PDT in various disease treatments.

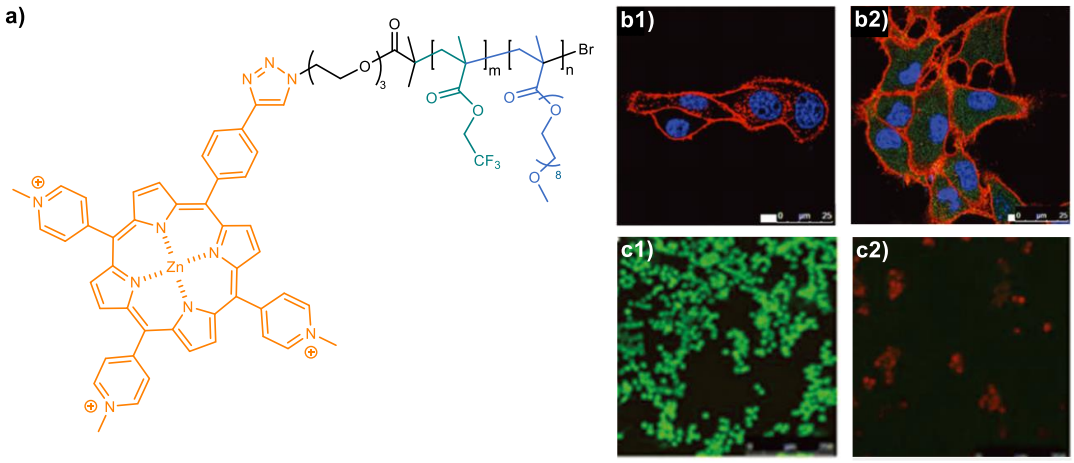

Figure 20. a) Chemical structure of the fluoropolymer-PS conjugate (zinc porphyrin-copolymer). b1) and b2) Confocal micrographs, where b1) is B16F10 cell-only control and b2) is B16F10 cells incubated with zinc porphyrin-copolymer. c1) and c2) Representative live/dead images of B16F10 cells incubated with zinc porphyrin-copolymer, where c1) and c2) represents cells kept in dark and light, respectively.[280] Reproduced with permission from ref [280]. Copyright 2017 Royal Society of Chemistry.

Pokorski and co-workers[280] revealed that the utility of fluoropolymer-PS conjugates could emerge as a possible remedy for skin cancer. Zinc porphyrin was covalently conjugated to statistical copolymers of TFEMA and OEGMEMA via post-modification using click reaction,[280] forming water-dispersible micellar FPNPs. The ability of FPNPs to be internalized and effectual for PDT was demonstrated by in vitro experiments in different cell lines, inducing cell death in two skin cancer models of squamous cell carcinoma and melanoma (Figures 20a-20c). Though the incorporation of zinc porphyrin slightly decreased the potency, FPNPs displayed a rising in oxygen delivery and enhanced singlet oxygen production, allowing an enhanced potential to monitor the disease state by ^{19}F MRI.

Given the acidic and hypoxia environment of tumors, Zhang and co-workers[43] prepared pH-responsive and oxygen self-supplying therapeutic FPNPs through self-assembly of poly(PEGMA)-*b*-poly(DEAEMA-*co*-GMA) block copolymers conjugated with tetrafluorophenyl substituted porphyrins (Scheme 21). The hydrophilic shell of poly(PEGMA) induced improved solubility and biocompatibility for FPNPs, resulting in a partial reduction in non-specific cellular uptake or protein adsorption during the accumulation of FPNPs to tumor sites. The fluorinated porphyrins in cores

promote both oxygen load and transport that alleviate the oxygen shortage in solid tumors. pH-responsive DEAEMA undergoes protonation in acidic tumor environments, which improves cellular internalization on account of the activation by positive surface charge. In addition, the FPNPs could be disassembled at a lower pH in the cells, reducing the quenching effect caused by PSs aggregation, and thus allowing a necessary photosensitivity. Therefore, the PDT efficacy against solid tumors was clearly improved by developing oxygen self-supplying and pH-sensitive FPNPs, which could be effectively taken up and broken to release oxygen at the lesion locations.

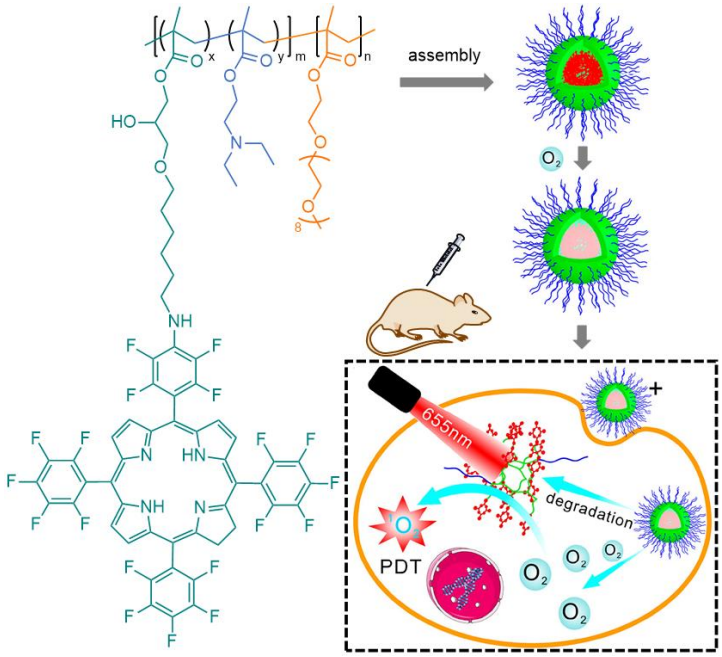

Scheme 21. Schematic illustration for the acidic pH-responsiveness and oxygen transport of FPNPs.[43] Reproduced with permission from ref [43]. Copyright 2019 American Chemical Society.

5.4 Energy Storage

Dielectric materials with high dielectric constant and sufficient electric breakdown strength have drawn widespread interest owing to their broad potential applications in energy storage devices.[195, 281, 282] Energy density (U_e), a parameter for characterizing the storage capacity of dielectric materials, is defined as Equation 2 for nonlinear dielectric materials:[203, 282-284]

$$U_e = \int E \, \mathrm{d}D \qquad \text{Equation 2}$$

where E represents the applied electric field, D represents the electric displacement. When it comes to linear dielectric materials, the energy density can be determined with Equation 3,

$$U_e = \frac{1}{2}\varepsilon_r \varepsilon_0 E_b^2 \qquad \text{Equation 3}$$

Where ε_r, ε_0 and E_b are the relative dielectric constant, vacuum dielectric constant and breakdown strength, respectively.[203] According to Equation 3, U_e can be enhanced by increasing the dielectric constant ε_r or/and E_b of the dielectric materials.[282]

High dielectric constants can be achieved with ceramic materials, particularly with $BaTiO_3$. However, the relatively low electric breakdown strength and processing difficulties of inorganic materials hinder their usage in many electronic devices.[195, 285] In this regard, high electric breakdown strength can be achieved by merging with polymers, which meanwhile possess advantages of low dielectric loss, easy processing and low cost.[204, 284, 286] However, even for ferroelectric fluorinated polymers (e.g., PVDF and VDF copolymers), which exhibit the highest dielectric constants (ε ~10 at 1 kHz) among numerous polymers,[115, 124, 287, 288] their blends with ceramic materials often afford poor performance as limited by processing techniques. The high surface energy and large specific surface area of ceramic nanoparticles cause aggregation in the polymer matrix, giving rise to electron conduction with considerable dielectric loss, poor breakdown strength and other deteriorated electrical properties. To achieve homogeneous nanoparticle dispersion, surface modification of ceramic nanoparticles based on "grafting from" strategy (section 4) has been shown as powerful tools.[195, 289]

Based on the low surface energy of fluoropolymers, Ma, Yang and co-workers[199] prepared poly(13FOMA)@$BaTiO_3$ nanocomposites via SI-ATRP reaction (Figure 14). The intrinsic nature of C-F bonds is beneficial to decrease the polarization of materials. Authors revealed that poly(13FOMA)@$BaTiO_3$ nanohybrids not only increased the dielectric constant, which is almost three times poly(13FOMA), but also significantly reduced the dielectric loss.

When employing SI-RAFT polymerization, this technique avoids metal-contamination concerns in polymer synthesis process, which is favorable to preventing high leakage currents under high electric fields.[289] In 2018, Zhang, Luo and co-workers[203] fabricated core-shell structured PTFMPCS@$BaTiO_3$ via SI-RAFT (Figure 14), and blended these nanohybrids with poly(VDF-TrFE-CTFE) matrix. This work demonstrates that the shell thickness affects the dielectric constant, breakdown strength and energy density. When the shell thickness was approximately 11 nm in nanocomposites containing 5 vol% $BaTiO_3$, the energy density was up to 16.18 J cm^{-3}, providing useful information for further engineering of high-energy-density dielectric material.

With PVDF@$BaTiO_3$ made via SI-RAFT polymerization,[204] Raihane et al.[289] reported that the core-shell FPNPs provide enhanced dielectric permittivity of about 50% higher than the prediction of the nanocomposite based on the Maxwell Garnett dielectric model, suggesting the promising PVDF/$BaTiO_3$ interface achieved by "grafting from" polymerization.

5.5 Per- and Polyfluoroalkyl Substances Adsorption

PFASs represent a family of synthetic chemicals that are broadly used as surfactants, water and oil repellents, fire retardants in industrial and consumer products (>200 applications) for many decades.[290-292] In recent years, researchers found that PFASs show high persistence in the environment (e.g., different water sources including lakes, rivers, underground water as well as inland seas and oceans) and a tendency to bio-accumulate.[293] Rodent and human studies have identified adverse effects associated with PFAS exposure.[294] Many national, regional regulatory agencies and organizations have already restricted the use of several PFASs, especially,

perfluorooctanoic acid (PFOA), perfluorooctanesulfonic acid (PFOS) and perfluorononanoic acid (PFNA).

In contrast to low-molar-mass PFASs which are water-soluble, mobile, persistent, bioaccumulative and toxic, fluoropolymers are safe, bioinert, non-toxic, non-bioaccumulative and insoluble in water.[290, 295] In addition, approximately 96% of fluoropolymers fulfill the "Polymer of Low Concern" (PLC) criteria[296, 297] defined by Organization for Economic Cooperation and Development (OECD). Year 2023 is crucial for the issue and recently the five authorities and the European Chemicals Agency (ECHA) has supplied a proposal of restriction of all PFASs, [298] though fluoropolymers have not found any alternatives.

A variety of porous sorbents such as carbon-based materials, ion exchange resins have been investigated to remove PFASs.[299, 300] However, such sorbents show limited selectivity and low affinity for PFASs in the presence of background inorganic/organic substances. Moreover, for most sorbents, the adsorption behaviors of PFASs are dramatically affected by pH levels of environmental conditions, as well as substances of several orders of magnitude higher concentrations than PFASs in natural water sources.[301-303] Therefore, selective PFASs separation under environmentally relevant and complex conditions remains highly challenging.[304]

Motivated by the fluorophilicity effect, FPNPs have emerged as an attractive candidate for PFASs adsorption. Because FPNPs are highly resistant to non-fluorinated ions, molecules existing in environmental conditions, FPNPs could exhibit selective affinity to PFASs. The Sawamoto group[188, 305] prepared star polymers with fluorinated nanogel cores and hydrophilic PEG arms via ruthenium-catalyzed RDRP (Scheme 17), which have enabled efficient and selective adsorption of PFASs into the fluorinated cores. For instance, when above ten thousand fluorine atoms are contained in each core, the fluorinated nano-gel (e.g., D_h = 38-74 nm by DLS) removes PFOA from 10 ppm to ppb level. The versatile RDRP path also facilitates the preparation of difunctional nanogels with fluorinated cores and amino groups (or ammonium groups), which are capable of cooperatively recognizing PFOA (or its ammonium salt) as confirmed by ^{19}F NMR studies. The adsorbed PFASs could be reversibly released upon treatment with organic solvents.

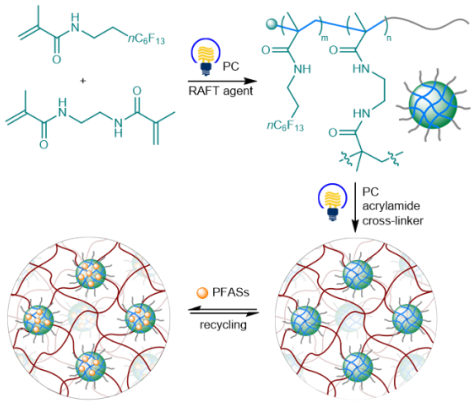

Scheme 22. Schematic illustration for the synthesis of FPNP-embedded hydrogel and investigation on PFASs adsorption.[42] Reproduced with permission from ref [42]. Copyright 2020 American Chemical Society.

Later, Chen and co-workers[42] investigated PFASs adsorption with an FPNP-embedded hydrogel, which was prepared by tandem photo-mediated RDRP (Scheme 22). The FPNPs exhibit outstanding adsorption performance to a wide range of PFASs, including cationic, anionic, neutral and zwitterionic compounds. The strong and selective affinity toward fluorocarbons allows clearance of PFASs at high to environmentally relevant concentrations in water without being dramatically affected by acidic/basic conditions and background ions. Additionally, the FPNP-embedded hydrogel exhibited good mechanical strength, which is favorable to facilitating separation, regeneration and recycling of hydrogel.

Beyond FPNPs, researchers also developed other fluorinated sorbents as outstanding host molecules for PFASs guests. For example, cross-linked fluoropolymer gels[301, 306] β-cyclodextrin-based polymers,[307] granular activated carbon[308] are demonstrated as highly efficient polymeric materials to capture neutral and/or anionic PFASs. The “smart” performance of those fluoropolymers further highlights that the fluorophilicity effect could be utilized as a fundamental principle to promote PFASs adsorption toward a sustainable society.

5.6 Others

Apart from above-mentioned applications in the fields of MRI agents, biomedical carriers, energy storage and PFASs removal, FPNPs have also gained considerable interests in other applications. Because we only found a few studies for each direction that benefits from FPNPs prepared via RDRPs, related examples are introduced below.

Thanks to the hydro-oleophobicity and extremely low surface energies of fluoropolymers, especially those bearing a perfluorinated side chain, nano-structural fluorinated coatings provide an important foundation for the design of superhydrophobic surfaces (water contact angle (WCA) above 150° and water droplet roll-off angle (RoA) below 10°), which are capable of self-cleaning, anti-fouling and anti-bacterial.[26, 309] Superhydrophobic surfaces are normally prepared through the integration of surface roughness and low surface energy materials. However, surface roughness reduces transparency owing to increased light scattering, which causes hindrance to the fabrication of transparent superhydrophobic coatings.[310] For this problem, Detrembleur and co-workers[311] prepared amphiphilic fluorinated block copolymers of 17FDMA, which form FPNPs via a PISA process. After a thermal treatment to promote chain movement and film reorganization, the fluorinated blocks migrated from the core of FPNPs to the film-air interface, providing hydrophobic coatings. When blending FPNPs with silica nanoparticles to improve surface roughness, superhydrophobic coatings (WCA = 153 °, RoA < 2 °) with high transparency were successfully formed.

PNPs formed by block copolymers are important stabilizers for the formation of Pickering emulsions, which are surfactant-free, kinetically stabilized dispersions of two immiscible liquids.[312] Motivated by environmental reasons, Pickering emulsions have attracted many interests to mitigate the adoption of surfactants and organic solvents, and found applications across different industrial processes.[312] An and co-workers[162] synthesized FPNPs of diverse surface wetting properties based on RAFT polymerization, and explored their behaviors as Pickering stabilizers for solvents of a broad range of polarity. Pickering emulsions of both oil-in-water and oil-in-oil systems were prepared using commonly used toluene, DMF, DMSO as organic solvents, showcasing the

versatility and robustness of the fluoropolymers. Notably, in many examples, block copolymers are cross-linked to prevent the break of emulsions, and a large number of surfactants are required to form high internal phase emulsions. In sharp contrast, this system avoids complicated synthesis and enables the emulsion formation with up to 80% of the internal phase.

While ultrasound is broadly applied as a clinical imaging technique,[313] it is still limited by the lack of robust contrast agents to improve the distinction among different tissues.[314] The fast diffusion of gas encapsulated in conventional ultrasound contrast agents lead to short circulation time. To provide stable nanosized ultrasound contrast agents, Tsapis and co-workers[64] prepared triblock copolymers of PEG-polylactide-poly(17FDMA). In comparison to PEG-polylactide nano-carriers, the FPNPs provide a 2-fold increase in the encapsulation efficiency for perfluorooctyl bromide. The FPNPs afford a higher *in vitro* ultrasound signal than that of PEG-polylactide nano-carriers, and exhibit insignificant *in vitro* cytotoxicity.

6. CONCLUSION AND FUTURE PERSPECTIVES

FPNPs that merge properties of fluoropolymers and polymeric nanoparticles, are of great interests for a broad range of applications. While conventional paths toward FPNPs are limited to free radical polymerizations, researchers have made enormous efforts to synthesize well-defined fluoropolymers based on RDRPs, which have promoted the fabrication of FPNPs with controlled chemical compositions, versatile functional substituents, tunable sizes and diversified/complicated morphologies. Those synthetic avenues can be classified into several groups, including 1) self-assembly or self-folding of purified fluorinated copolymers into multi-chain aggregates or single-chain unimers in solvents, 2) direction formation of FPNPs through PISA or cross-linking during controlled radical chain-growth, 3) grafting from inorganic nanoparticles to yield covalently bonded FPNPs with inorganic cores. Inspired by those synthetic advancements, extensive studies toward applications have been carried out worldwide. The unique physical, chemical and biological properties of fluorine, as well as the ultra-low size, high specific surface area and other attributes of PNPs have enabled FPNPs as high-performance ^{19}F MRI agents, biomedical nano-carriers and PDT photosensitizers toward healthy problems, robust and selective sorbents for PFASs related to environmental issues, dielectric nanohybrids toward energy storage goals, superhydrophobic coatings and emulsifiers in laboratorial and industrial applications. Although investigations of FPNPs synthesis based RDRPs and their applications are growing into a booming stage, many challenges remain to be addressed.

First of all, although RDRPs allow facile preparation of fluoropolymers, most examples are limited to side-chain fluorinated polymers with semi-fluorinated, (meth)acrylates, styrene derivatives as repeating units. Consequently, the synthesis and applications of FPNPs mainly focus on such polymeric structures. To polymerize gaseous fluoroalkenes (e.g., TFE, VDF, CTFE),[7-12, 115] which are largely manufactured in industries, conventional techniques highly rely on high-pressure metallic autoclaves. Although ITP that is the oldest and RAFT polymerization are promising to afford main-chain fluoropolymers of complicated compositions and structures, the high-pressure operations at elevated temperatures and limited controllability could be challenging to realize on-

demand access to fluoropolymers, particularly for non-experts in polymer synthesis. To address such issues, novel synthetic methodologies and techniques have yet to be developed. Recently, the development of photoredox-mediated RDRPs provides new opportunities to accomplish controlled polymerizations of fluoroalkenes, enabling tailoring main-chain fluoropolymers at ambient conditions with common Schlenk glassware and synthesizing many unprecedented sequences with a broad scope of comonomers, though the scaling-up ability has yet to be promoted.[80-83] Meanwhile, continuous-flow polymerizations have been shown as a striking technique to promote polymerization without losing control over chain-growth, and are useful to facilitate manipulation of gaseous and low-boiling-point monomers via precise in-line regulation and computer-aided programmable operation.[315, 316] We anticipate that those novel synthetic approaches and platforms will be quite interesting to promote the bottom-up engineering of novel FPNPs with fluoropolymers of a broader monomer scope, larger sequence and topological scopes.

Second, despite morphologies playing an important role in influencing the properties of FPNPs, it has been rarely possible to access diverse morphologies with each strategy, and complicated nanostructures are quite limited. In order to obtain diversified morphological FPNPs, various strategies have been explored through the integration of solvophilic and solvophobic segments along the macromolecular backbone based on RDRPs, where each strategy presents different scopes of morphologies. For example, with the PISA strategy, nano-objects including spheres, worms, cylinders, vesicles, raspberry-like particles, sponge-like particles, even cubosomes, have been produced via thermal or photo-induced chain-extension polymerization from solvophilic macro-initiators/CTAs. In comparison, with the single-chain folding and cross-linking polymerization strategies, spherical FPNPs are normally afforded, where more complicated morphologies are hardly observed so far. It is still difficult to provide comparable scopes of FPNPs with different strategies. Because many applications highly depend on size, stability, concentration of FPNPs, which are synthetic characteristics of different methods, it will be useful to expand the FPNPs scope for each avenue. Moreover, emerging studies have disclosed that multicomponent PNPs could be achieved by complex sequences.[111, 112, 163] However, fluoropolymers with complex sequences and suitable solvophilicity/solvophobicity are extremely limited so far. It is highly desirable to further expand the scope of such fluoropolymers and explore their aggregation behaviors, which is important to elucidate the in-depth relationship between microstructures and properties.

Last but not least, compared to the vast applications of fluoropolymers in a broad range of areas, investigations with tailor-made FPNPs are still at the early stage. For example, well-defined fluoropolymers have been demonstrated as promising materials for solid polymer electrolytes[317, 318] and protective coatings on electrodes[319] for the next-generation lithium batteries thanks to their electrochemical stability,[29] high-performance coatings for microelectronic purposes due to their thermal and chemical inertness,[320, 321] functional membranes for water purification and energy applications,[322, 323] and others. In comparison, tailor-made FPNPs, especially for nanoparticles with morphologies other than spheres, have been rarely investigated toward such cutting-edge areas. It will be interesting and fruitful to rational design FPNPs and expand their applications based on the outstanding behaviors demonstrated by well-defined fluoropolymers. However, it is difficult, even inaccessible for most scientists to handle both polymerization methods for FPNPs fabrication

and various analyzing/characterizing techniques (e.g., tools in biomedical, energy, environmental studies) for applications. Therefore, systematic developments toward practical applications will highly rely on cooperation between different laboratories.

AUTHOR INFORMATION

Corresponding Author

*[a]Email: chenmao@fudan.edu.cn

*[b]Email: bruno.ameduri@enscm.fr

Notes

The authors declare no competing financial interest.

ACKNOWLEDGEMENTS

This research was financially supported by the Science and Technology Commission of Shanghai Municipality and the Shanghai Pilot Program for Basic Research Fudan University 21TQ1400100 (no. 21TQ007), the NSFC (no. 22171051) and the State Key Laboratory of Molecular Engineering of Polymers.BA thanks CNRS and the French Fluorine Network (GIS).

REFERENCES

(1) Ramos J.; Forcada, J.; Hidalgo-Alvarez, R., Cationic Polymer Nanoparticles and Nanogels: From Synthesis to Biotechnological Applications. *Chem. Rev.* **2014,** *114*, 367-428.

(2) Lu X.-Y.; Wu, D.-C.; Li, Z.-J.; Chen, G.-Q., Chpater 7 - Polymer Nanoparticles. In *Prog. Mol. Biol. Transl. Sci.*, Villaverde, A., Ed. Academic Press: 2011; Vol. 104, pp 299-323.

(3) Adhikari C., Polymer nanoparticles-preparations, applications and future insights: a concise review. *Polym.-Plast. Tech. Mat.* **2021,** *60*, 1996-2024.

(4) Li K.; Liu, B., Polymer-encapsulated organic nanoparticles for fluorescence and photoacoustic imaging. *Chem. Soc. Rev.* **2014,** *43*, 6570-6597.

(5) Rao J. P.; Geckeler, K. E., Polymer nanoparticles: Preparation techniques and size-control parameters. *Prog. Polym. Sci.* **2011,** *36*, 887-913.

(6) Mavila S.; Eivgi, O.; Berkovich, I.; Lemcoff, N. G., Intramolecular Cross-Linking Methodologies for the Synthesis of Polymer Nanoparticles. *Chem. Rev.* **2016,** *116*, 878-961.

(7) Ebnesajjad S., *Introduction to Fluoropolymers: Materials, Technology, and Applications*. Elsevier: Waltham, 2013.

(8) Scheirs J., *Modern Fluoropolymers: High Performance Polymers for Diverse Applications*. Wiley: New York, 1997.

(9) Améduri B.; Sawada, H., *Fluorinated Polymers, Volume 2: Applications*. RSC: Cambridge: 2017.

(10) Améduri B.; Fomin, S., *Fascinating Fluoropolymers and Their Applications*. Elsevier: Cambridge, 2020.
(11) Smith D. W.; Iacono, S. T.; Iyer, S. S., *Handbook of Fluoropolymer Science and Technology*. Wiley: New Jersey, 2014.
(12) Hougham G.; Cassidy, P. E.; Johns, K.; Davidson, J., *Fluoropolymers: Synthesis and Applications*. Plenum: New York, 1999.
(13) Hollamby M. J.; Eastoe, J.; Mutch, K. J.; Rogers, S.; Heenan, R. K., Fluorinated microemulsions as reaction media for fluorous nanoparticles. *Soft Matter* **2010,** *6*, 971-976.
(14) Ma W.; Lopez, G.; Ameduri, B.; Takahara, A., Fluoropolymer Nanoparticles Prepared Using Trifluoropropene Telomer Based Fluorosurfactants. *Langmuir* **2020,** *36*, 1754-1760.
(15) Fan D.; Li, Z. X.; Ye, H. H.; Yuan, J., Study on Emulsion Polymerization of Fluorinated Acrylate and its Application. *Adv. Mat. Res.* **2012,** *518-523*, 619-622.
(16) Yamauchi M.; Hirono, T.; Kedama, S. I.; Matsuo, M., Fluoropolymer emulsions. *Eur. Coat. J.* **1996**, 124-128.
(17) Nenov S.; Hoffmann, M. S.; Steffen, W.; Klapper, M.; Müllen, K., Fluorous miniemulsions: A powerful tool to control morphology in metallocene-catalyzed propene polymerization. *J. Polym. Sci., Part A: Polym. Chem.* **2009,** *47*, 1724-1730.
(18) Suwa T.; Watanabe, T.; Seguchi, T.; Okamoto, J.; Machi, S., Emulsifier-free emulsion polymerization of tetrafluoroethylene by radiation. II. Effects of reaction conditions on polymer particle size and number. *J. Polym. Sci.: Polym. Chem. Ed.* **1979,** *17*, 111-127.
(19) Xu S.; Liu, W., Synthesis and surface characterization of an amphiphilic fluorinated copolymer via emulsifier-free emulsion polymerization of RAFT. *J. Fluorine Chem.* **2008,** *129*, 125-130.
(20) Kim C. U.; Lee, J. M.; K. Ihm, S., Emulsion polymerization of tetrafluoroethylene: effects of reaction conditions on particle formation. *J. Fluorine Chem.* **1999,** *96*, 11-21.
(21) Boschet F.; Ameduri, B., (Co)polymers of chlorotrifluoroethylene: synthesis, properties, and applications. *Chem. Rev.* **2014,** *114*, 927-980.
(22) Puts G. J.; Crouse, P.; Ameduri, B. M., Polytetrafluoroethylene: Synthesis and Characterization of the Original Extreme Polymer. *Chem. Rev.* **2019,** *119*, 1763-1805.
(23) Banerjee S.; Schmidt, J.; Talmon, Y.; Hori, H.; Asai, T.; Ameduri, B., A degradable fluorinated surfactant for emulsion polymerization of vinylidene fluoride. *Chem. Commun.* **2018,** *54*, 11399-11402.
(24) Landfester K.; Rothe, R.; Antonietti, M., Convenient Synthesis of Fluorinated Latexes and Core-Shell Structures by Miniemulsion Polymerization. *Macromolecules* **2002,** *35*, 1658-1662.
(25) Brandl F.; Thünemann, A. F.; Beuermann, S., Poly(meth)acrylate-PVDF core–shell particles from emulsion polymerization: preferential formation of the PVDF β crystal phase. *Polym. Chem.* **2018,** *9*, 5359-5369.
(26) Lv J.; Cheng, Y., Fluoropolymers in biomedical applications: state-of-the-art and future perspectives. *Chem. Soc. Rev.* **2021,** *50*, 5435-5467.
(27) Corrigan N.; Jung, K.; Moad, G.; Hawker, C. J.; Matyjaszewski, K.; Boyer, C., Reversible-deactivation radical polymerization (Controlled/living radical polymerization): From discovery to materials design and applications. *Prog. Polym. Sci.* **2020,** *111*, 101311.

(28) Mohammad S. A.; Shingdilwar, S.; Banerjee, S.; Ameduri, B., Macromolecular engineering approach for the preparation of new architectures from fluorinated olefins and their applications. *Prog. Polym. Sci.* **2020,** *106*, 101255.
(29) Lopez J.; Mackanic, D. G.; Cui, Y.; Bao, Z., Designing polymers for advanced battery chemistries. *Nat. Rev. Mater.* **2019,** *4*, 312-330.
(30) Braunecker W. A.; Matyjaszewski, K., Controlled/living radical polymerization: Features, developments, and perspectives. *Prog. Polym. Sci.* **2007,** *32*, 93-146.
(31) Jenkins A. D.; Jones, R. G.; Moad, G., Terminology for reversible-deactivation radical polymerization previously called "controlled" radical or "living" radical polymerization (IUPAC Recommendations 2010). *Pure Appl. Chem.* **2010,** *82*, 483-491.
(32) Truong N. P.; Jones, G. R.; Bradford, K. G. E.; Konkolewicz, D.; Anastasaki, A., A comparison of RAFT and ATRP methods for controlled radical polymerization. *Nat. Rev. Chem.* **2021,** *5*, 859-869.
(33) Parkatzidis K.; Wang, H. S.; Truong, N. P.; Anastasaki, A., Recent Developments and Future Challenges in Controlled Radical Polymerization: A 2020 Update. *Chem* **2020,** *6*, 1575-1588.
(34) Matyjaszewski K.; Xia, J., Atom Transfer Radical Polymerization. *Chem. Rev.* **2001,** *101*, 2921-2990.
(35) Matyjaszewski K.; Tsarevsky, N. V., Macromolecular engineering by atom transfer radical polymerization. *J. Am. Chem. Soc.* **2014,** *136*, 6513-6533.
(36) Moad G.; Rizzardo, E.; Thang, S. H., Toward Living Radical Polymerization. *Acc. Chem. Res.* **2008,** *41*, 1133-1142.
(37) Chiefari J.; Chong, Y. K.; Ercole, F.; Krstina, J.; Jeffery, J.; Le, T. P. T.; Mayadunne, R. T. A.; Meijs, G. F.; Moad, C. L.; Moad, G.; Rizzardo, E.; Thang, S. H., Living Free-Radical Polymerization by Reversible Addition−Fragmentation Chain Transfer: The RAFT Process. *Macromolecules* **1998,** *31*, 5559-5562.
(38) Perrier S.; Takolpuckdee, P., Macromolecular design via reversible addition–fragmentation chain transfer (RAFT)/xanthates (MADIX) polymerization. *J. Polym. Sci.: Polym. Chem. Ed.* **2005,** *43*, 5347-5393.
(39) Hawker C. J.; Bosman, A. W.; Harth, E., New Polymer Synthesis by Nitroxide Mediated Living Radical Polymerizations. *Chem. Rev.* **2001,** *101*, 3661-3688.
(40) Oka M.; Tatemoto, M., Vinylidene Fluoride-Hexafluoropropylene Copolymer having Terminal Iodines. In *Contemporary Topics in Polymer Science: Volume 4*, Bailey, W. J.; Tsuruta, T., Eds. Springer New York: Boston, MA, 1984; pp 763-777.
(41) David G.; Boyer, C.; Tonnar, J.; Ameduri, B.; Lacroix-Desmazes, P.; Boutevin, B., Use of Iodocompounds in Radical Polymerization. *Chem. Rev.* **2006,** *106*, 3936-3962.
(42) Quan Q.; Wen, H.; Han, S.; Wang, Z.; Shao, Z.; Chen, M., Fluorous-Core Nanoparticle-Embedded Hydrogel Synthesized via Tandem Photo-Controlled Radical Polymerization: Facilitating the Separation of Perfluorinated Alkyl Substances from Water. *ACS Appl. Mater. Interfaces* **2020,** *12*, 24319-24327.
(43) Liu Z.; Xue, Y.; Wu, M.; Yang, G.; Lan, M.; Zhang, W., Sensitization of Hypoxic Tumor to Photodynamic Therapy via Oxygen Self-Supply of Fluorinated Photosensitizers.

Biomacromolecules **2019,** *20*, 4563-4573.
(44) Xu Q.; Li, S.; Yu, C.; Zhou, Y., Self-assembly of Amphiphilic Alternating Copolymers. *Chem. Eur. J.* **2019,** *25*, 4255-4264.
(45) Derry M. J.; Fielding, L. A.; Armes, S. P., Polymerization-induced self-assembly of block copolymer nanoparticles via RAFT non-aqueous dispersion polymerization. *Prog. Polym. Sci.* **2016,** *52*, 1-18.
(46) Hayward R. C.; Pochan, D. J., Tailored Assemblies of Block Copolymers in Solution: It Is All about the Process. *Macromolecules* **2010,** *43*, 3577-3584.
(47) D'Agosto F.; Rieger, J.; Lansalot, M., RAFT-Mediated Polymerization-Induced Self-Assembly. *Angew. Chem. Int. Ed.* **2020,** *59*, 8368-8392.
(48) Hirao A.; Sugiyama, K.; Yokoyama, H., Precise synthesis and surface structures of architectural per- and semifluorinated polymers with well-defined structures. *Prog. Polym. Sci.* **2007,** *32*, 1393-1438.
(49) Marsh Z. M.; Blom, D. A.; Stefik, M., Tunable Fluorophobic Effect Determines Nanoparticle Dispersion in Homopolymers and Block Polymers. *Adv. Mater. Interfaces* **2020,** *7*, 1901691.
(50) Percec V.; Johansson, G.; Ungar, G.; Zhou, J., Fluorophobic Effect Induces the Self-Assembly of Semifluorinated Tapered Monodendrons Containing Crown Ethers into Supramolecular Columnar Dendrimers Which Exhibit a Homeotropic Hexagonal Columnar Liquid Crystalline Phase. *J. Am. Chem. Soc.* **1996,** *118*, 9855-9866.
(51) Lodge T. P.; Rasdal, A.; Li, Z.; Hillmyer, M. A., Simultaneous, Segregated Storage of Two Agents in a Multicompartment Micelle. *J. Am. Chem. Soc.* **2005,** *127*, 17608-17609.
(52) Li Z.; Kesselman, E.; Talmon, Y.; Hillmyer, M. A.; Lodge, T. P., Multicompartment Micelles from ABC Miktoarm Stars in Water. *Science* **2004,** *306*, 98-101.
(53) Marshall J. E.; Zhenova, A.; Roberts, S.; Petchey, T.; Zhu, P.; Dancer, C. E. J.; McElroy, C. R.; Kendrick, E.; Goodship, V., On the Solubility and Stability of Polyvinylidene Fluoride. *Polymers* **2021,** *13*, 1354.
(54) Gong H.; Gu, Y.; Chen, M., Controlled/Living Radical Polymerization of Semifluorinated (Meth)acrylates. *Synlett* **2018,** *29*, 1543-1551.
(55) Yao W.; Li, Y.; Huang, X., Fluorinated poly(meth)acrylate: Synthesis and properties. *Polymer* **2014,** *55*, 6197-6211.
(56) Betts D.; Johnson, T.; LeRoux, D.; DeSimone, J. M., New materials by controlled radical polymerization: controlled radical polymerization methods for the synthesis of nonionic surfactants for CO2. *ACS Symp. Ser.* **1998,** *685*.
(57) Xia J.; Johnson, T.; Gaynor, S. G.; Matyjaszewski, K.; DeSimone, J., Atom Transfer Radical Polymerization in Supercritical Carbon Dioxide. *Macromolecules* **1999,** *32*, 4802-4805.
(58) Otazaghine B.; Boutevin, B.; Lacroix-Desmazes, P., Controlled radical polymerization of n-butyl α-Fluoroacrylate. 1. Use of atom transfer radical polymerization as the polymerization method. *Macromolecules* **2002,** *35*, 7634-7641.
(59) Perrier S.; Jackson, S. G.; Haddleton, D. M.; Améduri, B.; Boutevin, B., Preparation of Fluorinated Copolymers by Copper-Mediated Living Radical Polymerization. *Macromolecules* **2003,** *36*, 9042-9049.

(60) Wang J.-S.; Matyjaszewski, K., Controlled/"living" radical polymerization. atom transfer radical polymerization in the presence of transition-metal complexes. *J. Am. Chem. Soc.* **1995,** *117*, 5614-5615.
(61) Becker M. L.; Remsen, E. E.; Wooley, K. L., Diblock copolymers, micelles, and shell-crosslinked nanoparticles containing poly(4-fluorostyrene): Tools for detailed analyses of nanostructured materials. *J. Polym. Sci., Part A: Polym. Chem.* **2001,** *39*, 4152-4166.
(62) Hussain H.; Busse, K.; Kressler, J., Poly(ethylene oxide)- and Poly(perfluorohexylethyl methacrylate)-Containing Amphiphilic Block Copolymers: Association Properties in Aqueous Solution. *Macromol. Chem. Phys.* **2003,** *204*, 936-946.
(63) Xu B.; Yao, W.; Li, Y.; Zhang, S.; Huang, X., Perfluorocyclobutyl Aryl Ether-Based ABC Amphiphilic Triblock Copolymer. *Sci. Rep.* **2016,** *6*, 39504.
(64) Houvenagel S.; Moine, L.; Picheth, G.; Dejean, C.; Brûlet, A.; Chennevière, A.; Faugeras, V.; Huang, N.; Couture, O.; Tsapis, N., Comb-Like Fluorophilic-Lipophilic-Hydrophilic Polymers for Nanocapsules as Ultrasound Contrast Agents. *Biomacromolecules* **2018,** *19*, 3244-3256.
(65) Woods H. M.; Nouvel, C.; Licence, P.; Irvine, D. J.; Howdle, S. M., Dispersion Polymerization of Methyl Methacrylate in Supercritical Carbon Dioxide: An Investigation into Stabilizer Anchor Group. *Macromolecules* **2005,** *38*, 3271-3282.
(66) Discekici E. H.; Anastasaki, A.; Kaminker, R.; Willenbacher, J.; Truong, N. P.; Fleischmann, C.; Oschmann, B.; Lunn, D. J.; Read de Alaniz, J.; Davis, T. P.; Bates, C. M.; Hawker, C. J., Light-Mediated Atom Transfer Radical Polymerization of Semi-Fluorinated (Meth)acrylates: Facile Access to Functional Materials. *J. Am. Chem. Soc.* **2017,** *139*, 5939-5945.
(67) Yang Y.; Wang, Z.; Gao, Y.; Liu, T.; Hu, C.; Dong, Q., Synthesis of fluorinated diblock copolymer by ATRP and its application of PAVAc polymerization in ScCO2. *J. Appl. Polym. Sci.* **2006,** *102*, 1146-1151.
(68) Du W.; Nystrom, A. M.; Zhang, L.; Powell, K. T.; Li, Y.; Cheng, C.; Wickline, S. A.; Wooley, K. L., Amphiphilic Hyperbranched Fluoropolymers as Nanoscopic 19F Magnetic Resonance Imaging Agent Assemblies. *Biomacromolecules* **2008,** *9*, 2826-2833.
(69) Ogawa M.; Nitahara, S.; Aoki, H.; Ito, S.; Narazaki, M.; Matsuda, T., Fluorinated Polymer Nanoparticles as a Novel 19F MRI Contrast Agent Prepared by Dendrimer-Initiated Living Radical Polymerization. *Macromol. Chem. Phys.* **2010,** *211*, 1369-1376.
(70) Tan B. H.; Hussain, H.; Liu, Y.; He, C. B.; Davis, T. P., Synthesis and Self-Assembly of Brush-Type Poly[poly(ethylene glycol)methyl ether methacrylate]-block-poly(pentafluorostyrene) Amphiphilic Diblock Copolymers in Aqueous Solution. *Langmuir* **2010,** *26*, 2361-2368.
(71) Xu Y.; Wang, W.; Wang, Y.; Zhu, J.; Uhrig, D.; Lu, X.; Keum, J. K.; Mays, J. W.; Hong, K., Fluorinated bottlebrush polymers based on poly(trifluoroethyl methacrylate): synthesis and characterization. *Polym. Chem.* **2016,** *7*, 680-688.
(72) Hill M. R.; Carmean, R. N.; Sumerlin, B. S., Expanding the Scope of RAFT Polymerization: Recent Advances and New Horizons. *Macromolecules* **2015,** *48*, 5459-5469.
(73) Perrier S., 50th Anniversary Perspective: RAFT Polymerization—A User Guide. *Macromolecules* **2017,** *50*, 7433-7447.
(74) Keddie D. J.; Moad, G.; Rizzardo, E.; Thang, S. H., RAFT Agent Design and Synthesis.

Macromolecules **2012,** *45*, 5321-5342.

(75) Ma Z.; Lacroix-Desmazes, P., Synthesis of hydrophilic/CO2-philic poly(ethylene oxide)-b-poly(1,1,2,2-tetrahydroperfluorodecyl acrylate) block copolymers via controlled/living radical polymerizations and their properties in liquid and supercritical CO2. *J. Polym. Sci., Part A: Polym. Chem.* **2004,** *42*, 2405-2415.

(76) Eberhardt M.; Théato, P., RAFT Polymerization of Pentafluorophenyl Methacrylate: Preparation of Reactive Linear Diblock Copolymers. *Macromol. Rapid Commun.* **2005,** *26*, 1488-1493.

(77) Inoue Y.; Watanabe, J.; Takai, M.; Yusa, S.-I.; Ishihara, K., Synthesis of sequence-controlled copolymers from extremely polar and apolar monomers by living radical polymerization and their phase-separated structures. *J. Polym. Sci., Part A: Polym. Chem.* **2005,** *43*, 6073-6083.

(78) Koda Y.; Terashima, T.; Sawamoto, M.; Maynard, H. D., Amphiphilic/fluorous random copolymers as a new class of non-cytotoxic polymeric materials for protein conjugation. *Polym. Chem.* **2015,** *6*, 240-247.

(79) Guerre M.; Schmidt, J.; Talmon, Y.; Améduri, B.; Ladmiral, V., An amphiphilic poly(vinylidene fluoride)-b-poly(vinyl alcohol) block copolymer: synthesis and self-assembly in water. *Polym. Chem.* **2017,** *8*, 1125-1128.

(80) Chen K.; Zhou, Y.; Han, S.; Liu, Y.; Chen, M., Main-Chain Fluoropolymers with Alternating Sequence Control via Light-Driven Reversible-Deactivation Copolymerization in Batch and Flow. *Angew. Chem. Int. Ed.* **2022,** *61*, e202116135.

(81) Zhao Y.; Chen, Y.; Zhou, H.; Zhou, Y.; Chen, K.; Gu, Y.; Chen, M., Controlled radical copolymerization of fluoroalkenes by using light-driven redox-relay catalysis. *Nat. Synth.* **2023**, doi. 10.1038/s44160-023-00284-9.

(82) Jiang K.; Han, S.; Ma, M.; Zhang, L.; Zhao, Y.; Chen, M., Photoorganocatalyzed Reversible-Deactivation Alternating Copolymerization of Chlorotrifluoroethylene and Vinyl Ethers under Ambient Conditions: Facile Access to Main-Chain Fluorinated Copolymers. *J. Am. Chem. Soc.* **2020,** *142*, 7108-7115.

(83) Quan Q.; Ma, M.; Wang, Z.; Gu, Y.; Chen, M., Visible-Light-Enabled Organocatalyzed Controlled Alternating Terpolymerization of Perfluorinated Vinyl Ethers. *Angew. Chem. Int. Ed.* **2021,** *60*, 20443-20451.

(84) Quan Q. Z.; Zhao, Y. C.; Chen, K. X.; Zhou, H. Y.; Zhou, C. D.; Chen, M., Organocatalyzed Controlled Copolymerization of Perfluorinated Vinyl Ethers and Unconjugated Monomers Driven by Light. *ACS Catal.* **2022,** *12*, 7269-7277.

(85) Girard E.; Marty, J.-D.; Ameduri, B.; Destarac, M., Direct Synthesis of Vinylidene Fluoride-Based Amphiphilic Diblock Copolymers by RAFT/MADIX Polymerization. *ACS Macro Lett.* **2012,** *1*, 270-274.

(86) Bouad V.; Guerre, M.; Totée, C.; Silly, G.; Gimello, O.; Améduri, B.; Tahon, J.-F.; Poli, R.; Barrau, S.; Ladmiral, V., RAFT polymerisation of trifluoroethylene: the importance of understanding reverse additions. *Polym. Chem.* **2021,** *12*, 2271-2281.

(87) Grignard B.; Jérôme, C.; Calberg, C.; Detrembleur, C.; Jérôme, R., Controlled synthesis of carboxylic acid end-capped poly(heptadecafluorodecyl acrylate) and copolymers with 2-

hydroxyethyl acrylate. *J. Polym. Sci., Part A: Polym. Chem.* **2007,** *45*, 1499-1506.
(88) Mya K. Y.; Lin, E. M. J.; Gudipati, C. S.; Gose, H. B. A. S.; He, C., Self-Assembly of Block Copolymer Micelles: Synthesis via Reversible Addition-Fragmentation Chain Transfer Polymerization and Aqueous Solution Properties. *J. Phys. Chem. B* **2010,** *114*, 9128-9134.
(89) Koiry B. P.; Chakrabarty, A.; Singha, N. K., Fluorinated amphiphilic block copolymers via RAFT polymerization and their application as surf-RAFT agent in miniemulsion polymerization. *RSC Adv.* **2015,** *5*, 15461-15468.
(90) Koiry B. P.; Ponnupandian, S.; Choudhury, S.; Singha, N. K., Syntheses and morphologies of fluorinated diblock copolymer prepared via RAFT polymerization. *J. Fluorine Chem.* **2016,** *189*, 51-58.
(91) Jiang Y.; Li, L.; Liu, J.; Wang, R.; Wang, H.; Tian, Q.; Li, X., Hydrophobic films of acrylic emulsion by incorporation of fluorine-based copolymer prepared through the RAFT emulsion copolymerization. *J. Fluorine Chem.* **2016,** *183*, 82-91.
(92) Skrabania K.; Berlepsch, H. v.; Böttcher, C.; Laschewsky, A., Synthesis of Ternary, Hydrophilic-Lipophilic-Fluorophilic Block Copolymers by Consecutive RAFT Polymerizations and Their Self-Assembly into Multicompartment Micelles. *Macromolecules* **2010,** *43*, 271-281.
(93) Marsat J.-N. l.; Heydenreich, M.; Kleinpeter, E.; Berlepsch, H. v.; Böttcher, C.; Laschewsky, A., Self-Assembly into Multicompartment Micelles and Selective Solubilization by Hydrophilic-Lipophilic-Fluorophilic Block Copolymers. *Macromolecules* **2011,** *44*, 2092-2105.
(94) Liu H.; Zhang, S.; Huang, X.; Ding, A.; Lu, G., Construction of well-defined difluoromethylthio-containing amphiphilic homopolymers by RAFT polymerization. *Polym. Chem.* **2020,** *11*, 7542-7550.
(95) Nuhn L.; Tomcin, S.; Miyata, K.; Mailander, V.; Landfester, K.; Kataoka, K.; Zentel, R., Size-dependent knockdown potential of siRNA-loaded cationic nanohydrogel particles. *Biomacromolecules* **2014,** *15*, 4111-21.
(96) Que Y.; Liu, Y.; Tan, W.; Feng, C.; Shi, P.; Li, Y.; Huang, X., Enhancing Photodynamic Therapy Efficacy by Using Fluorinated Nanoplatform. *ACS Macro Lett.* **2016,** *5*, 168-173.
(97) Que Y.; Ruan, J.; Xiao, Y.; Feng, C.; Lu, G.; Huang, X., Fluorinated vesicles embedded with Ru-based catalysts as efficient and recyclable nanoreactors for photo-mediated aerobic oxidation. *Polym. Chem.* **2020,** *11*, 1727-1734.
(98) Kolouchova K.; Groborz, O.; Cernochova, Z.; Skarkova, A.; Brabek, J.; Rosel, D.; Svec, P.; Starcuk, Z.; Slouf, M.; Hruby, M., Thermo- and ROS-Responsive Self-Assembled Polymer Nanoparticle Tracers for 19F MRI Theranostics. *Biomacromolecules* **2021,** *22*, 2325-2337.
(99) Fuentes-Exposito M.; Norsic, S.; Février, T.; Dugas, P.-Y.; Boutti, S.; Devisme, S.; Bonnet, A.; D'Agosto, F.; Lansalot, M., Surfactant-free emulsion polymerization of vinylidene fluoride mediated by RAFT/MADIX reactive poly(ethylene glycol) polymer chains. *Polym. Chem.* **2021,** *12*, 5640-5649.
(100) Devisme S.; Kahn, A.; Fuentes-Exposito, M.; McKenna, T.; D'Agosto, F.; Lansalot, M.; Bonnet, A. Latex synthesis of poly(vinylidene fluoride) without surfactant by emulsion RAFT polymerization. WO2019063445A1, 2019.
(101) Zhang C.; Li, L.; Han, F. Y.; Yu, X.; Tan, X.; Fu, C.; Xu, Z. P.; Whittaker, A. K., Integrating Fluorinated Polymer and Manganese-Layered Double Hydroxide Nanoparticles as pH-activated 19F MRI Agents for Specific and Sensitive Detection of Breast Cancer. *Small* **2019,** *15*, 1902309.

(102) Monteiro M. J.; Adamy, M. M.; Leeuwen, B. J.; van Herk, A. M.; Destarac, M., A "Living" Radical ab Initio Emulsion Polymerization of Styrene Using a Fluorinated Xanthate Agent. *Macromolecules* **2005,** *38*, 1538-1541.
(103) Sawada H., Novel self-assembled molecular aggregates formed by fluoroalkyl end-capped oligomers and their application. *J. Fluorine Chem.* **2003,** *121*, 111-130.
(104) Corrigan N.; Yeow, J.; Judzewitsch, P.; Xu, J.; Boyer, C., Seeing the Light: Advancing Materials Chemistry through Photopolymerization. *Angew. Chem. Int. Ed.* **2019,** *58*, 5170-5189.
(105) Wu C.; Corrigan, N.; Lim, C. H.; Liu, W.; Miyake, G.; Boyer, C., Rational Design of Photocatalysts for Controlled Polymerization: Effect of Structures on Photocatalytic Activities. *Chem. Rev.* **2022,** *122*, 5476-5518.
(106) Corbin D. A.; Miyake, G. M., Photoinduced Organocatalyzed Atom Transfer Radical Polymerization (O-ATRP): Precision Polymer Synthesis Using Organic Photoredox Catalysis. *Chem. Rev.* **2022,** *122*, 1830-1874.
(107) Pan X.; Tasdelen, M. A.; Laun, J.; Junkers, T.; Yagci, Y.; Matyjaszewski, K., Photomediated controlled radical polymerization. *Prog. Polym. Sci.* **2016,** *62*, 73-125.
(108) Chen M.; Zhong, M.; Johnson, J. A., Light-Controlled Radical Polymerization: Mechanisms, Methods, and Applications. *Chem. Rev.* **2016,** *116*, 10167-10211.
(109) Gong H.; Zhao, Y.; Shen, X.; Lin, J.; Chen, M., Organocatalyzed Photo-Controlled Radical Polymerization of Semi-Fluorinated (Meth)acrylates Driven by Visible Light. *Angew. Chem. Int. Ed.* **2018,** *57*, 333-337.
(110) Zhao Y.; Ma, M.; Lin, X.; Chen, M., Photoorganocatalyzed Divergent Reversible-Deactivation Radical Polymerization towards Linear and Branched Fluoropolymers. *Angew. Chem. Int. Ed.* **2020,** *59*, 21470-21474.
(111) Li S.; Xu, Q.; Li, K.; Wang, Y.; Yu, C.; Zhou, Y., Multigeometry Nanoparticles from the Orthogonal Self-Assembly of Block Alternating Copolymers via Simulation. *J. Phys. Chem. B* **2019,** *123*, 8333-8340.
(112) Yin R.; Sahoo, D.; Xu, F.; Huang, W.; Zhou, Y., Scalable preparation of crystalline nanorods through sequential polymerization-induced and crystallization-driven self-assembly of alternating copolymers. *Polym. Chem.* **2020,** *11*, 2312-2317.
(113) Li S.; Xu, Q.; Li, K.; Yu, C.; Zhou, Y., High-χ alternating copolymers for accessing sub-5 nm domains via simulations. *Phys. Chem. Chem. Phys.* **2020,** *22*, 5577-5583.
(114) Asandei A. D., Photomediated Controlled Radical Polymerization and Block Copolymerization of Vinylidene Fluoride. *Chem. Rev.* **2016,** *116*, 2244-2274.
(115) Ameduri B., Copolymers of vinylidene fluoride with functional comonomers and applications therefrom: Recent developments, challenges and future trends. *Prog. Polym. Sci.* **2022,** *133*, 101591.
(116) Boyer C.; Améduri, B., Iodine transfer copolymerization of vinylidene fluoride and α-trifluoromethacrylic acid in emulsion process without any surfactants. *J. Polym. Sci., Part A: Polym. Chem.* **2009,** *47*, 4710-4722.
(117) Guerre M.; Semsarilar, M.; Totée, C.; Silly, G.; Améduri, B.; Ladmiral, V., Self-assembly of poly(vinylidene fluoride)-block-poly(2-(dimethylamino)ethylmethacrylate) block copolymers

prepared by CuAAC click coupling. *Polym. Chem.* **2017,** *8*, 5203-5211.
(118) Banerjee S.; Patil, Y.; Ono, T.; Ameduri, B., Synthesis of ω-Iodo and Telechelic Diiodo Vinylidene Fluoride-Based (Co)polymers by Iodine Transfer Polymerization Initiated by an Innovative Persistent Radical. *Macromolecules* **2017,** *50*, 203-214.
(119) Simpson C. P.; Adebolu, O. I.; Kim, J.-S.; Vasu, V.; Asandei, A. D., Metal and Ligand Effects of Photoactive Transition Metal Carbonyls in the Iodine Degenerative Transfer Controlled Radical Polymerization and Block Copolymerization of Vinylidene Fluoride. *Macromolecules* **2015,** *48*, 6404-6420.
(120) Zhang L.; Zhu, Z.; Azhar, U.; Ma, J.; Zhang, Y.; Zong, C.; Zhang, S., Synthesis of Well-Defined PVDF-Based Amphiphilic Block Copolymer via Iodine Transfer Polymerization for Antifouling Membrane Application. *Ind. Eng. Chem. Res.* **2018,** *57*, 8689-8697.
(121) Boyer C.; Valade, D.; Sauguet, L.; Ameduri, B.; Boutevin, B., Iodine Transfer Polymerization (ITP) of Vinylidene Fluoride (VDF). Influence of the Defect of VDF Chaining on the Control of ITP. *Macromolecules* **2005,** *38*, 10353-10362.
(122) Boyer C.; Ameduri, B.; Hung, M. H., Telechelic Diiodopoly(VDF-co-PMVE) Copolymers by Iodine Transfer Copolymerization of Vinylidene Fluoride (VDF) with Perfluoromethyl Vinyl Ether (PMVE). *Macromolecules* **2010,** *43*, 3652-3663.
(123) Altomare A.; Bozorg, M.; Loos, K., Chapter 2 - PVDF-based multiferroic. In *Fascinating Fluoropolymers and Their Applications*, Ameduri, B.; Fomin, S., Eds. Elsevier: 2020; pp 45-81.
(124) Ameduri B., From Vinylidene Fluoride (VDF) to the Applications of VDF-Containing Polymers and Copolymers: Recent Developments and Future Trends. *Chem. Rev.* **2009,** *109*, 6632-6686.
(125) Zapsas G.; Patil, Y.; Gnanou, Y.; Ameduri, B.; Hadjichristidis, N., Poly(vinylidene fluoride)-based complex macromolecular architectures: From synthesis to properties and applications. *Prog. Polym. Sci.* **2020,** *104*, 101231.
(126) Tatemoto M.; Yutani, Y.; Fujiwara, K. Novel iodine-containing compound, preparation thereof and block copolymer comprising the same. EP272698A2, 1988.
(127) Cheng J.; Tu, K.; He, E.; Wang, J.; Zhang, L.; Cheng, Z.; Zhu, X., Photocontrolled iodine-mediated reversible-deactivation radical polymerization with a semifluorinated alternating copolymer as the macroinitiator. *Polym. Chem.* **2020,** *11*, 7497-7505.
(128) Nicolas J.; Guillaneuf, Y.; Lefay, C.; Bertin, D.; Gigmes, D.; Charleux, B., Nitroxide-mediated polymerization. *Prog. Polym. Sci.* **2013,** *38*, 63-235.
(129) Lacroix-Desmazes P.; Andre, P.; Desimone, J. M.; Ruzette, A.-V.; Boutevin, B., Macromolecular surfactants for supercritical carbon dioxide applications: Synthesis and characterization of fluorinated block copolymers prepared by nitroxide-mediated radical polymerization. *J. Polym. Sci., Part A: Polym. Chem.* **2004,** *42*, 3537-3552.
(130) Yin Q.; Charlot, A.; Portinha, D.; Beyou, E., Nitroxide-mediated polymerization of pentafluorostyrene initiated by PS–DEPN through the surface of APTMS modified fumed silica: towards functional nanohybrids. *RSC Adv.* **2016,** *6*, 58260-58267.
(131) Altintas O.; Barner-Kowollik, C., Single-Chain Folding of Synthetic Polymers: A Critical Update. *Macromol. Rapid Commun.* **2016,** *37*, 29-46.
(132) Chen R.; Berda, E. B., 100th Anniversary of Macromolecular Science Viewpoint: Re-

examining Single-Chain Nanoparticles. *ACS Macro Lett.* **2020,** *9*, 1836-1843.
(133) Kuhn W.; Balmer, G., Crosslinking of single linear macromolecules. *J. Polym. Sci.* **1962,** *57*, 311-319.
(134) Alqarni M. A. M.; Waldron, C.; Yilmaz, G.; Becer, C. R., Synthetic Routes to Single Chain Polymer Nanoparticles (SCNPs): Current Status and Perspectives. *Macromol. Rapid Commun.* **2021,** *42*, 2100035.
(135) Lu J.; Ten Brummelhuis, N.; Weck, M., Intramolecular folding of triblock copolymers via quadrupole interactions between poly(styrene) and poly(pentafluorostyrene) blocks. *Chem. Commun.* **2014,** *50*, 6225-7.
(136) Koda Y.; Terashima, T.; Sawamoto, M., Multimode Self-Folding Polymers via Reversible and Thermoresponsive Self-Assembly of Amphiphilic/Fluorous Random Copolymers. *Macromolecules* **2016,** *49*, 4534-4543.
(137) Matsumoto K.; Terashima, T.; Sugita, T.; Takenaka, M.; Sawamoto, M., Amphiphilic Random Copolymers with Hydrophobic/Hydrogen-Bonding Urea Pendants: Self-Folding Polymers in Aqueous and Organic Media. *Macromolecules* **2016,** *49*, 7917-7927.
(138) Guazzelli E.; Martinelli, E.; Galli, G.; Cupellini, L.; Jurinovich, S.; Mennucci, B., Single-chain self-folding in an amphiphilic copolymer: An integrated experimental and computational study. *Polymer* **2019,** *161*, 33-40.
(139) Sun J.-T.; Hong, C.-Y.; Pan, C.-Y., Formation of the block copolymer aggregates via polymerization-induced self-assembly and reorganization. *Soft Matter* **2012,** *8*, 7753-7767.
(140) Canning S. L.; Smith, G. N.; Armes, S. P., A Critical Appraisal of RAFT-Mediated Polymerization-Induced Self-Assembly. *Macromolecules* **2016,** *49*, 1985-2001.
(141) Cornel E. J.; Jiang, J.; Chen, S.; Du, J., Principles and Characteristics of Polymerization-Induced Self-Assembly with Various Polymerization Techniques. *CCS Chem.* **2020,** *3*, 2104-2125.
(142) Yeow J.; Boyer, C., Photoinitiated Polymerization-Induced Self-Assembly (Photo-PISA): New Insights and Opportunities. *Adv. Sci.* **2017,** *4*, 1700137.
(143) An N.; Chen, X.; Yuan, J., Non-thermally initiated RAFT polymerization-induced self-assembly. *Polym. Chem.* **2021,** *12*, 3220-3232.
(144) Chen S.-l.; Shi, P.-f.; Zhang, W.-q., In situ synthesis of block copolymer nano-assemblies by polymerization-induced self-assembly under heterogeneous condition. *Chinese J. Polym. Sci.* **2017,** *35*, 455-479.
(145) Cao J.; Tan, Y.; Chen, Y.; Zhang, L.; Tan, J., Expanding the Scope of Polymerization-Induced Self-Assembly: Recent Advances and New Horizons. *Macromol. Rapid Commun.* **2021,** *42*, 2100498.
(146) Wang X.; An, Z., New Insights into RAFT Dispersion Polymerization-Induced Self-Assembly: From Monomer Library, Morphological Control, and Stability to Driving Forces. *Macromol. Rapid Commun.* **2019,** *40*, 1800325.
(147) Zhang W.-J.; Hong, C.-Y.; Pan, C.-Y., Polymerization-Induced Self-Assembly of Functionalized Block Copolymer Nanoparticles and Their Application in Drug Delivery. *Macromol. Rapid Commun.* **2019,** *40*, 1800279.
(148) Zhang W.-J.; Kadirkhanov, J.; Wang, C.-H.; Ding, S.-G.; Hong, C.-Y.; Wang, F.; You, Y.-Z.,

Polymerization-induced self-assembly for the fabrication of polymeric nano-objects with enhanced structural stability by cross-linking. *Polym. Chem.* **2020,** *11*, 3654-3672.
(149) Xu J.; Jung, K.; Atme, A.; Shanmugam, S.; Boyer, C., A Robust and Versatile Photoinduced Living Polymerization of Conjugated and Unconjugated Monomers and Its Oxygen Tolerance. *J. Am. Chem. Soc.* **2014,** *136*, 5508-5519.
(150) Phommalysack-Lovan J.; Chu, Y.; Boyer, C.; Xu, J., PET-RAFT polymerisation: towards green and precision polymer manufacturing. *Chem. Commun.* **2018,** *54*, 6591-6606.
(151) Semsarilar M.; Ladmiral, V.; Blanazs, A.; Armes, S. P., Poly(methacrylic acid)-based AB and ABC block copolymer nano-objects prepared via RAFT alcoholic dispersion polymerization. *Polym. Chem.* **2014,** *5*, 3466-3475.
(152) Semsarilar M.; Jones, E. R.; Armes, S. P., Comparison of pseudo-living character of RAFT polymerizations conducted under homogeneous and heterogeneous conditions. *Polym. Chem.* **2014,** *5*, 195-203.
(153) Akpinar B.; Fielding, L. A.; Cunningham, V. J.; Ning, Y.; Mykhaylyk, O. O.; Fowler, P. W.; Armes, S. P., Determining the Effective Density and Stabilizer Layer Thickness of Sterically Stabilized Nanoparticles. *Macromolecules* **2016,** *49*, 5160-5171.
(154) Czajka A.; Armes, S. P., Time-Resolved Small-Angle X-ray Scattering Studies during Aqueous Emulsion Polymerization. *J. Am. Chem. Soc.* **2021,** *143*, 1474-1484.
(155) Huo M.; Zhang, Y.; Zeng, M.; Liu, L.; Wei, Y.; Yuan, J., Morphology Evolution of Polymeric Assemblies Regulated with Fluoro-Containing Mesogen in Polymerization-Induced Self-Assembly. *Macromolecules* **2017,** *50*, 8192-8201.
(156) Gao Y.; Li, X.; Hong, L.; Liu, G., Mesogen-Driven Formation of Triblock Copolymer Cylindrical Micelles. *Macromolecules* **2012,** *45*, 1321-1330.
(157) Huo M.; Zeng, M.; Li, D.; Liu, L.; Wei, Y.; Yuan, J., Tailoring the Multicompartment Nanostructures of Fluoro-Containing ABC Triblock Terpolymer Assemblies via Polymerization-Induced Self-Assembly. *Macromolecules* **2017,** *50*, 8212-8220.
(158) Huo M.; Zeng, M.; Wu, D.; Wei, Y.; Yuan, J., Topological engineering of amphiphilic copolymers via RAFT dispersion copolymerization of benzyl methacrylate and 2-(perfluorooctyl)ethyl methacrylate for polymeric assemblies with tunable nanostructures. *Polym. Chem.* **2018,** *9*, 912-919.
(159) Huo M.; Li, D.; Song, G.; Zhang, J.; Wu, D.; Wei, Y.; Yuan, J., Semi-Fluorinated Methacrylates: A Class of Versatile Monomers for Polymerization-Induced Self-Assembly. *Macromol. Rapid Commun.* **2018,** *39*, 1700840.
(160) Zhou J.; Yao, H.; He, R., Synthesis of fluorinated polyacrylate surfactant-free core-shell latex by RAFT-mediated polymerization-induced self-assembly: Effects of the concentration of hexafluorobutyl acrylate. *Adv. Polym. Technol.* **2018,** *37*, 3804-3812.
(161) Zhou J.; He, R.; Ma, J., RAFT-Mediated Polymerization-Induced Self-Assembly of Poly(Acrylic Acid)-b-Poly(Hexafluorobutyl Acrylate): Effect of the pH on the Synthesis of Self-Stabilized Particles. *Polymers* **2016,** *8*, 207.
(162) Shen L.; Guo, H.; Zheng, J.; Wang, X.; Yang, Y.; An, Z., RAFT Polymerization-Induced Self-Assembly as a Strategy for Versatile Synthesis of Semifluorinated Liquid-Crystalline Block

Copolymer Nanoobjects. *ACS Macro Lett.* **2018,** *7*, 287-292.
(163) Lv F., An, Z. Wu, P., Scalable preparation of alternating block copolymer particles with inverse bicontinuous mesophases. *Nat. Commun.* **2019,** *10*, 1397.
(164) Luo X.; An, Z., Polymerization-Induced Self-Assembly for the Preparation of Poly(N,N-dimethylacrylamide)- b-Poly (4-tert-butoxystyrene-co-pentafluorostyrene) Particles with Inverse Bicontinuous Phases. *Chin. J. Chem.* **2021,** *39*, 1819-1824.
(165) Busatto N.; Stolojan, V.; Shaw, M.; Keddie, J. L.; Roth, P. J., Reactive Polymorphic Nanoparticles: Preparation via Polymerization-Induced Self-Assembly and Postsynthesis Thiol–para-Fluoro Core Modification. *Macromol. Rapid Commun.* **2019,** *40*, 1800346.
(166) Zhao W.; Ta, H. T.; Zhang, C.; Whittaker, A. K., Polymerization-Induced Self-Assembly (PISA) - Control over the Morphology of (19)F-Containing Polymeric Nano-objects for Cell Uptake and Tracking. *Biomacromolecules* **2017,** *18*, 1145-1156.
(167) Xu A.; Lu, Q.; Huo, Z.; Ma, J.; Geng, B.; Azhar, U.; Zhang, L.; Zhang, S., Synthesis of fluorinated nanoparticles via RAFT dispersion polymerization-induced self-assembly using fluorinated macro-RAFT agents in supercritical carbon dioxide. *RSC Adv.* **2017,** *7*, 51612-51620.
(168) Chen Q.; Li, Y.; Liu, M.; Wu, X.; Shen, J.; Shen, L., Constructing helical nanowires via polymerization-induced self-assembly. *RSC Adv.* **2021,** *11*, 8986-8992.
(169) Liu D.; He, J.; Zhang, L.; Tan, J., 100th Anniversary of Macromolecular Science Viewpoint: Heterogenous Reversible Deactivation Radical Polymerization at Room Temperature. Recent Advances and Future Opportunities. *ACS Macro Lett.* **2019,** *8*, 1660-1669.
(170) Niu B.; Chen, Y.; Zhang, L.; Tan, J., Organic–inorganic hybrid nanomaterials prepared via polymerization-induced self-assembly: recent developments and future opportunities. *Polym. Chem.* **2022,** *13*, 2554-2569.
(171) Chai X.; Zhou, P.; Xia, Q.; Shi, B.; Wang, G., Fluorine-containing nano-objects with the same compositions but different segment distributions: synthesis, characterization and comparison. *Polym. Chem.* **2022,** *13*, 6293-6301.
(172) Couturaud B.; Georgiou, P. G.; Varlas, S.; Jones, J. R.; Arno, M. C.; Foster, J. C.; O'Reilly, R. K., Poly(Pentafluorophenyl Methacrylate)-Based Nano-Objects Developed by Photo-PISA as Scaffolds for Post-Polymerization Functionalization. *Macromol. Rapid Commun.* **2019,** *40*, 1800460.
(173) Gong H.; Gu, Y.; Zhao, Y.; Quan, Q.; Han, S.; Chen, M., Precise Synthesis of Ultra-High-Molecular-Weight Fluoropolymers Enabled by Chain-Transfer-Agent Differentiation under Visible-Light Irradiation. *Angew. Chem. Int. Ed.* **2020,** *59*, 919-927.
(174) Gu Y.; Wang, Z.; Gong, H.; Chen, M., Investigations into CTA-Differentiation-Involving Polymerization of Fluorous Monomers: Exploitation of Experimental Variances in Fine-Tuning of Molecular Weights. *Polym. Chem.* **2020,** *11*, 7402-7409.
(175) Gu Y.; Lin, P.; Zhou, C.; Chen, M., Machine Learning-Assisted Systematical Polymerization Planning: Case Studies on Reversible-Deactivation Radical Polymerization. *Sci. China: Chem.* **2021,** *64*, 1039-1046.
(176) Han S.; Gu, Y.; Ma, M.; Chen, M., Light-intensity switch enabled nonsynchronous growth of fluorinated raspberry-like nanoparticles. *Chem. Sci.* **2020,** *11*, 10431-10436.

(177) Shanmugam S.; Xu, J.; Boyer, C., Light-Regulated Polymerization under Near-Infrared/Far-Red Irradiation Catalyzed by Bacteriochlorophyll a. *Angew. Chem. Int. Ed.* **2016,** *55*, 1036-1040.
(178) Ma Q.; Wang, W.; Zhang, L.; Cao, H., RAFT Polymerization of Semifluorinated Monomers Mediated by a NIR Fluorinated Photocatalyst. *Macromol. Rapid. Commun.* **2022**, e2200122.
(179) Wan W.-M.; Pan, C.-Y., Atom Transfer Radical Dispersion Polymerization in an Ethanol/Water Mixture. *Macromolecules* **2007,** *40*, 8897-8905.
(180) Sugihara S.; Armes, S. P.; Lewis, A. L., One-Pot Synthesis of Biomimetic Shell Cross-Linked Micelles and Nanocages by ATRP in Alcohol/Water Mixtures. *Angew. Chem. Int. Ed.* **2010,** *49*, 3500-3503.
(181) Sugihara S.; Sugihara, K.; Armes, S. P.; Ahmad, H.; Lewis, A. L., Synthesis of Biomimetic Poly(2-(methacryloyloxy)ethyl phosphorylcholine) Nanolatexes via Atom Transfer Radical Dispersion Polymerization in Alcohol/Water Mixtures. *Macromolecules* **2010,** *43*, 6321-6329.
(182) Shi B.; Zhang, H.; Liu, Y.; Wang, J.; Zhou, P.; Cao, M.; Wang, G., Development of ICAR ATRP-Based Polymerization-Induced Self-Assembly and Its Application in the Preparation of Organic-Inorganic Nanoparticles. *Macromol. Rapid Commun.* **2019,** *40*, 1900547.
(183) Cordella D.; Ouhib, F.; Aqil, A.; Defize, T.; Jérôme, C.; Serghei, A.; Drockenmuller, E.; Aissou, K.; Taton, D.; Detrembleur, C., Fluorinated Poly(ionic liquid) Diblock Copolymers Obtained by Cobalt-Mediated Radical Polymerization-Induced Self-Assembly. *ACS Macro Lett.* **2017,** *6*, 121-126.
(184) Demarteau J.; Améduri, B.; Ladmiral, V.; Mees, M. A.; Hoogenboom, R.; Debuigne, A.; Detrembleur, C., Controlled Synthesis of Fluorinated Copolymers via Cobalt-Mediated Radical Copolymerization of Perfluorohexylethylene and Vinyl Acetate. *Macromolecules* **2017,** *50*, 3750-3760.
(185) Wang K.; Peng, H.; Thurecht, K. J.; Puttick, S.; Whittaker, A. K., pH-responsive star polymer nanoparticles: potential 19F MRI contrast agents for tumour-selective imaging. *Polym. Chem.* **2013,** *4*, 4480-4489.
(186) Wang K.; Peng, H.; Thurecht, K. J.; Puttick, S.; Whittaker, A. K., Biodegradable core crosslinked star polymer nanoparticles as19F MRI contrast agents for selective imaging. *Polym. Chem.* **2014,** *5*, 1760-1771.
(187) Zhang C.; Moonshi, S. S.; Wang, W.; Ta, H. T.; Han, Y.; Han, F. Y.; Peng, H.; Kral, P.; Rolfe, B. E.; Gooding, J. J.; Gaus, K.; Whittaker, A. K., High F-Content Perfluoropolyether-Based Nanoparticles for Targeted Detection of Breast Cancer by (19)F Magnetic Resonance and Optical Imaging. *ACS Nano* **2018,** *12*, 9162-9176.
(188) Koda Y.; Terashima, T.; Sawamoto, M., Fluorous microgel star polymers: selective recognition and separation of polyfluorinated surfactants and compounds in water. *J. Am. Chem. Soc.* **2014,** *136*, 15742-15748.
(189) Koda Y.; Terashima, T.; Sawamoto, M., Fluorinated Microgels in Star Polymers: From In-Core Dynamics to Fluorous Encapsulation. *Macromolecules* **2015,** *48*, 2901-2908.
(190) Koda Y.; Terashima, T.; Sawamoto, M., Fluorinated microgel star polymers as fluorous nanocapsules for the encapsulation and release of perfluorinated compounds. *Polym. Chem.* **2015,** *6*, 5663-5674.

(191) Zoppe J. O.; Ataman, N. C.; Mocny, P.; Wang, J.; Moraes, J.; Klok, H.-A., Surface-Initiated Controlled Radical Polymerization: State-of-the-Art, Opportunities, and Challenges in Surface and Interface Engineering with Polymer Brushes. *Chem. Rev.* **2017,** *117*, 1105-1318.
(192) Achilleos D. S.; Vamvakaki, M., End-Grafted Polymer Chains onto Inorganic Nano-Objects. *Materials* **2010,** *3*, 1981-2026.
(193) Hirai T.; Kobayashi, M.; Takahara, A., Control of the primary and secondary structure of polymer brushes by surface-initiated living/controlled polymerization. *Polym. Chem.* **2017,** *8*, 5456-5468.
(194) Terzić I.; Meereboer, N. L.; Mellema, H. H.; Loos, K., Polymer-based multiferroic nanocomposites via directed block copolymer self-assembly. *J. Mater. Chem. C* **2019,** *7*, 968-976.
(195) Bouharras F. E.; Raihane, M.; Ameduri, B., Recent progress on core-shell structured BaTiO3@polymer/fluorinated polymers nanocomposites for high energy storage: Synthesis, dielectric properties and applications. *Prog. Mater. Sci.* **2020,** *113*, 100670.
(196) Durand N.; Boutevin, B.; Silly, G.; Améduri, B., “Grafting From” Polymerization of Vinylidene Fluoride (VDF) from Silica to Achieve Original Silica–PVDF Core–Shells. *Macromolecules* **2011,** *44*, 8487-8493.
(197) Durand N.; Gaveau, P.; Silly, G.; Améduri, B.; Boutevin, B., Radical Grafting of Tetrafluoroethylene and Vinylidene Fluoride Telomers onto Silica Bearing Vinyl Groups. *Macromolecules* **2011,** *44*, 6249-6257.
(198) Durand N.; Mariot, D.; Améduri, B.; Boutevin, B.; Ganachaud, F., Tailored Covalent Grafting of Hexafluoropropylene Oxide Oligomers onto Silica Nanoparticles: Toward Thermally Stable, Hydrophobic, and Oleophobic Nanocomposites. *Langmuir* **2011,** *27*, 4057-4067.
(199) Zhang X.; Chen, H.; Ma, Y.; Zhao, C.; Yang, W., Preparation and dielectric properties of core–shell structural composites of poly(1H,1H,2H,2H-perfluorooctyl methacrylate)@BaTiO3 nanoparticles. *Appl. Surf. Sci.* **2013,** *277*, 121-127.
(200) Higaki Y.; Kobayashi, M.; Takahara, A., Direct Hydrophilic Modification of Polymer Surfaces via Surface-Initiated ATRP. In *Reversible Deactivation Radical Polymerization: Materials and Applications*, American Chemical Society: 2018; Vol. 1285, pp 157-168.
(201) Sakata H.; Kobayashi, M.; Otsuka, H.; Takahara, A., Tribological Properties of Poly(methyl methacrylate) Brushes Prepared by Surface-Initiated Atom Transfer Radical Polymerization. *Polym. J.* **2005,** *37*, 767-775.
(202) Huang H.; He, L., Silica-diblock fluoropolymer hybrids synthesized by surface-initiated atom transfer radical polymerization. *RSC Adv.* **2014,** *4*, 13108-13118.
(203) Chen S.; Lv, X.; Han, X.; Luo, H.; Bowen, C. R.; Zhang, D., Significantly improved energy density of BaTiO3 nanocomposites by accurate interfacial tailoring using a novel rigid-fluoro-polymer. *Polym. Chem.* **2018,** *9*, 548-557.
(204) Bouharras F. E.; Raihane, M.; Silly, G.; Totee, C.; Ameduri, B., Core–shell structured poly(vinylidene fluoride)-grafted-BaTiO3 nanocomposites prepared via reversible addition–fragmentation chain transfer (RAFT) polymerization of VDF for high energy storage capacitors. *Polym. Chem.* **2019,** *10*, 891-904.
(205) Laurent S.; Forge, D.; Port, M.; Roch, A.; Robic, C.; Vander Elst, L.; Muller, R. N., Magnetic

Iron Oxide Nanoparticles: Synthesis, Stabilization, Vectorization, Physicochemical Characterizations, and Biological Applications. *Chem. Rev.* **2008,** *108*, 2064-2110.
(206) Orel S. G.; Schnall, M. D., MR Imaging of the Breast for the Detection, Diagnosis, and Staging of Breast Cancer. *Radiology* **2001,** *220*, 13-30.
(207) Feng Z.; Li, Q.; Wang, W.; Ni, Q.; Wang, Y.; Song, H.; Zhang, C.; Kong, D.; Liang, X.-J.; Huang, P., Superhydrophilic fluorinated polymer and nanogel for high-performance 19F magnetic resonance imaging. *Biomaterials* **2020,** *256*, 120184.
(208) Xie D.; Yu, M.; Kadakia, R. T.; Que, E. L., 19F Magnetic Resonance Activity-Based Sensing Using Paramagnetic Metals. *Acc. Chem. Res.* **2020,** *53*, 2-10.
(209) Cho M. H.; Shin, S. H.; Park, S. H.; Kadayakkara, D. K.; Kim, D.; Choi, Y., Targeted, Stimuli-Responsive, and Theranostic 19F Magnetic Resonance Imaging Probes. *Bioconjugate Chem.* **2019,** *30*, 2502-2518.
(210) Krafft M. P., Fluorocarbons and fluorinated amphiphiles in drug delivery and biomedical research. *Adv. Drug Delivery Rev.* **2001,** *47*, 209-228.
(211) Modo M., 19F Magnetic Resonance Imaging and Spectroscopy in Neuroscience. *Neuroscience* **2021,** *474*, 37-50.
(212) Zhang C.; Yan, K.; Fu, C.; Peng, H.; Hawker, C. J.; Whittaker, A. K., Biological Utility of Fluorinated Compounds: from Materials Design to Molecular Imaging, Therapeutics and Environmental Remediation. *Chem. Rev.* **2022,** *122*, 167-208.
(213) Hendrick R. E.; Kneeland, J. B.; Stark, D. D., Maximizing signal-to-noise and contrast-to-noise ratios in flash imaging. *Magn. Reson. Imaging* **1987,** *5*, 117-127.
(214) Zhang C.; Moonshi, S. S.; Han, Y.; Puttick, S.; Peng, H.; Magoling, B. J. A.; Reid, J. C.; Bernardi, S.; Searles, D. J.; Král, P.; Whittaker, A. K., PFPE-Based Polymeric 19F MRI Agents: A New Class of Contrast Agents with Outstanding Sensitivity. *Macromolecules* **2017,** *50*, 5953-5963.
(215) Zhang C.; Sanchez, R. J. P.; Fu, C.; Clayden-Zabik, R.; Peng, H.; Kempe, K.; Whittaker, A. K., Importance of Thermally Induced Aggregation on 19F Magnetic Resonance Imaging of Perfluoropolyether-Based Comb-Shaped Poly(2-oxazoline)s. *Biomacromolecules* **2019,** *20*, 365-374.
(216) Kolouchova K.; Sedlacek, O.; Jirak, D.; Babuka, D.; Blahut, J.; Kotek, J.; Vit, M.; Trousil, J.; Konefał, R.; Janouskova, O.; Podhorska, B.; Slouf, M.; Hruby, M., Self-Assembled Thermoresponsive Polymeric Nanogels for 19F MR Imaging. *Biomacromolecules* **2018,** *19*, 3515-3524.
(217) Fu C.; Tang, J.; Pye, A.; Liu, T.; Zhang, C.; Tan, X.; Han, F.; Peng, H.; Whittaker, A. K., Fluorinated Glycopolymers as Reduction-responsive 19F MRI Agents for Targeted Imaging of Cancer. *Biomacromolecules* **2019,** *20*, 2043-2050.
(218) Munkhbat O.; Canakci, M.; Zheng, S.; Hu, W.; Osborne, B.; Bogdanov, A. A.; Thayumanavan, S., 19F MRI of Polymer Nanogels Aided by Improved Segmental Mobility of Embedded Fluorine Moieties. *Biomacromolecules* **2019,** *20*, 790-800.
(219) Szatrowski T. P.; Nathan, C. F., Production of Large Amounts of Hydrogen Peroxide by Human Tumor Cells1. *Cancer Res.* **1991,** *51*, 794-798.
(220) Couturaud B.; Houston, Z. H.; Cowin, G. J.; Prokeš, I.; Foster, J. C.; Thurecht, K. J.; O'Reilly,

R. K., Supramolecular Fluorine Magnetic Resonance Spectroscopy Probe Polymer Based on Passerini Bifunctional Monomer. *ACS Macro Lett.* **2019,** *8*, 1479-1483.
(221) Huang P.; Guo, W.; Yang, G.; Song, H.; Wang, Y.; Wang, C.; Kong, D.; Wang, W., Fluorine Meets Amine: Reducing Microenvironment-Induced Amino-Activatable Nanoprobes for 19F-Magnetic Resonance Imaging of Biothiols. *ACS Appl. Mater. Interfaces* **2018,** *10*, 18532-18542.
(222) Taylor N. G.; Chung, S. H.; Kwansa, A. L.; Johnson Iii, R. R.; Teator, A. J.; Milliken, N. J. B.; Koshlap, K. M.; Yingling, Y. G.; Lee, Y. Z.; Leibfarth, F. A., Partially Fluorinated Copolymers as Oxygen Sensitive 19F MRI Agents. *Chem. Eur. J.* **2020,** *26*, 9982-9990.
(223) Reis M.; Gusev, F.; Taylor, N. G.; Chung, S. H.; Verber, M. D.; Lee, Y. Z.; Isayev, O.; Leibfarth, F. A., Machine-Learning-Guided Discovery of 19F MRI Agents Enabled by Automated Copolymer Synthesis. *J. Am. Chem. Soc.* **2021,** *143*, 17677-17689.
(224) Fu C.; Zhang, C.; Peng, H.; Han, F.; Baker, C.; Wu, Y.; Ta, H.; Whittaker, A. K., Enhanced Performance of Polymeric 19F MRI Contrast Agents through Incorporation of Highly Water-Soluble Monomer MSEA. *Macromolecules* **2018,** *51*, 5875-5882.
(225) Rolfe B. E.; Blakey, I.; Squires, O.; Peng, H.; Boase, N. R.; Alexander, C.; Parsons, P. G.; Boyle, G. M.; Whittaker, A. K.; Thurecht, K. J., Multimodal polymer nanoparticles with combined 19F magnetic resonance and optical detection for tunable, targeted, multimodal imaging in vivo. *J. Am. Chem. Soc.* **2014,** *136*, 2413-2419.
(226) Elnakat H.; Ratnam, M., Distribution, functionality and gene regulation of folate receptor isoforms: implications in targeted therapy. *Adv. Drug Delivery Rev.* **2004,** *56*, 1067-1084.
(227) Boase N. R. B.; Blakey, I.; Rolfe, B. E.; Mardon, K.; Thurecht, K. J., Synthesis of a multimodal molecular imaging probe based on a hyperbranched polymer architecture. *Polym. Chem.* **2014,** *5*, 4450-4458.
(228) Ardana A.; Whittaker, A. K.; Thurecht, K. J., PEG-Based Hyperbranched Polymer Theranostics: Optimizing Chemistries for Improved Bioconjugation. *Macromolecules* **2014,** *47*, 5211-5219.
(229) Wallat J. D.; Czapar, A. E.; Wang, C.; Wen, A. M.; Wek, K. S.; Yu, X.; Steinmetz, N. F.; Pokorski, J. K., Optical and Magnetic Resonance Imaging Using Fluorous Colloidal Nanoparticles. *Biomacromolecules* **2017,** *18*, 103-112.
(230) Thurecht K. J.; Blakey, I.; Peng, H.; Squires, O.; Hsu, S.; Alexander, C.; Whittaker, A. K., Functional Hyperbranched Polymers: Toward Targeted in Vivo 19F Magnetic Resonance Imaging Using Designed Macromolecules. *J. Am. Chem. Soc.* **2010,** *132*, 5336-5337.
(231) Moonshi S. S.; Zhang, C.; Peng, H.; Puttick, S.; Rose, S.; Fisk, N. M.; Bhakoo, K.; Stringer, B. W.; Qiao, G. G.; Gurr, P. A.; Whittaker, A. K., A unique 19F MRI agent for the tracking of non phagocytic cells in vivo. *Nanoscale* **2018,** *10*, 8226-8239.
(232) Yang J.; Zhang, Q.; Chang, H.; Cheng, Y., Surface-engineered dendrimers in gene delivery. *Chem. Rev.* **2015,** *115*, 5274-300.
(233) Riess J. G.; Krafft, M. P., Fluorinated materials for in vivo oxygen transport (blood substitutes), diagnosis and drug delivery. *Biomaterials* **1998,** *19*, 1529-1539.
(234) Cametti M.; Crousse, B.; Metrangolo, P.; Milani, R.; Resnati, G., The fluorous effect in biomolecular applications. *Chem. Soc. Rev.* **2012,** *41*, 31-42.

(235) Lostalé-Seijo I.; Montenegro, J., Synthetic materials at the forefront of gene delivery. *Nat. Rev. Chem.* **2018,** *2*, 258-277.
(236) Wang H.; Miao, W.; Wang, F.; Cheng, Y., A Self-Assembled Coumarin-Anchored Dendrimer for Efficient Gene Delivery and Light-Responsive Drug Delivery. *Biomacromolecules* **2018,** *19*, 2194-2201.
(237) Chang H.; Zhang, J.; Wang, H.; Lv, J.; Cheng, Y., A Combination of Guanidyl and Phenyl Groups on a Dendrimer Enables Efficient siRNA and DNA Delivery. *Biomacromolecules* **2017,** *18*, 2371-2378.
(238) Mastrobattista E.; Hennink, W. E., Charged for success. *Nat. Mater.* **2012,** *11*, 10-12.
(239) Wang M.; Liu, H.; Li, L.; Cheng, Y., A fluorinated dendrimer achieves excellent gene transfection efficacy at extremely low nitrogen to phosphorus ratios. *Nat. Commun.* **2014,** *5*, 3053.
(240) Guo X.; Yuan, Z.; Xu, Y.; Wei, M.; Fang, Z.; Yuan, W.-E., A fluorinated low-molecular-weight PEI/HIF-1α shRNA polyplex system for hemangioma therapy. *Biomater. Sci.* **2020,** *8*, 2129-2142.
(241) Wang M.; Cheng, Y., Structure-activity relationships of fluorinated dendrimers in DNA and siRNA delivery. *Acta Biomater.* **2016,** *46*, 204-210.
(242) Shen W.; Wang, H.; Ling-hu, Y.; Lv, J.; Chang, H.; Cheng, Y., Screening of efficient polymers for siRNA delivery in a library of hydrophobically modified polyethyleneimines. *J. Mater. Chem. B* **2016,** *4*, 6468-6474.
(243) Chen G.; Wang, Y.; Wu, P.; Zhou, Y.; Yu, F.; Zhu, C.; Li, Z.; Hang, Y.; Wang, K.; Li, J.; Sun, M.; Oupicky, D., Reversibly Stabilized Polycation Nanoparticles for Combination Treatment of Early- and Late-Stage Metastatic Breast Cancer. *ACS Nano* **2018,** *12*, 6620-6636.
(244) Li L.; Li, X.; Wu, Y.; Song, L.; Yang, X.; He, T.; Wang, N.; Yang, S.; Zeng, Y.; Wu, Q.; Qian, Z.; Wei, Y.; Gong, C., Multifunctional Nucleus-targeting Nanoparticles with Ultra-high Gene Transfection Efficiency for in vivo Gene Therapy. *Theranostics* **2017,** *7*, 1633-1649.
(245) Eldredge A. C.; Johnson, M. E.; Cao, Y.; Zhang, L.; Zhao, C.; Liu, Z.; Yang, Q.; Guan, Z., Dendritic peptide bolaamphiphiles for siRNA delivery to primary adipocytes. *Biomaterials* **2018,** *178*, 458-466.
(246) Zhang T.; Huang, Y.; Ma, X.; Gong, N.; Liu, X.; Liu, L.; Ye, X.; Hu, B.; Li, C.; Tian, J.-H.; Magrini, A.; Zhang, J.; Guo, W.; Xing, J.-F.; Bottini, M.; Liang, X.-J., Fluorinated Oligoethylenimine Nanoassemblies for Efficient siRNA-Mediated Gene Silencing in Serum-Containing Media by Effective Endosomal Escape. *Nano Lett.* **2018,** *18*, 6301-6311.
(247) Li L.; Song, L.; Yang, X.; Li, X.; Wu, Y.; He, T.; Wang, N.; Yang, S.; Zeng, Y.; Yang, L.; Wu, Q.; Wei, Y.; Gong, C., Multifunctional “core-shell” nanoparticles-based gene delivery for treatment of aggressive melanoma. *Biomaterials* **2016,** *111*, 124-137.
(248) Wang H.; Wang, Y.; Wang, Y.; Hu, J.; Li, T.; Liu, H.; Zhang, Q.; Cheng, Y., Self-Assembled Fluorodendrimers Combine the Features of Lipid and Polymeric Vectors in Gene Delivery. *Angew. Chem. Int. Ed.* **2015,** *54*, 11647-11651.
(249) Nuhn L.; Hirsch, M.; Krieg, B.; Koynov, K.; Fischer, K.; Schmidt, M.; Helm, M.; Zentel, R., Cationic Nanohydrogel Particles as Potential siRNA Carriers for Cellular Delivery. *ACS Nano* **2012,** *6*, 2198-2214.
(250) Tan E.; Lv, J.; Hu, J.; Shen, W.; Wang, H.; Cheng, Y., Statistical versus block fluoropolymers

in gene delivery. *J. Mater. Chem. B* **2018,** *6*, 7230-7238.
(251) Zha Z.; Hu, Y.; Mukerabigwi, J. F.; Chen, W.; Wang, Y.; He, C.; Ge, Z., Thiolactone Chemistry-Based Combinatorial Methodology to Construct Multifunctional Polymers for Efficacious Gene Delivery. *Bioconjugate Chem.* **2018,** *29*, 23-28.
(252) Kretzmann J. A.; Evans, C. W.; Feng, L.; Lawler, N. B.; Norret, M.; Higgins, M. J.; Iyer, K. S., Surface Diffusion of Dendronized Polymers Correlates with Their Transfection Potential. *Langmuir* **2020,** *36*, 9074-9080.
(253) Chang H.; Lv, J.; Gao, X.; Wang, X.; Wang, H.; Chen, H.; He, X.; Li, L.; Cheng, Y., Rational Design of a Polymer with Robust Efficacy for Intracellular Protein and Peptide Delivery. *Nano Lett.* **2017,** *17*, 1678-1684.
(254) Lee K. Y.; Yuk, S. H., Polymeric protein delivery systems. *Prog. Polym. Sci.* **2007,** *32*, 669-697.
(255) Cheng Y., Design of Polymers for Intracellular Protein and Peptide Delivery. *Chin. J. Chem.* **2021,** *39*, 1443-1449.
(256) Gu Z.; Biswas, A.; Zhao, M.; Tang, Y., Tailoring nanocarriers for intracellular protein delivery. *Chem. Soc. Rev.* **2011,** *40*, 3638-3655.
(257) Pisal D. S.; Kosloski, M. P.; Balu-Iyer, S. V., Delivery of Therapeutic Proteins. *J. Pharm. Sci.* **2010,** *99*, 2557-2575.
(258) Yu M.; Wu, J.; Shi, J.; Farokhzad, O. C., Nanotechnology for protein delivery: Overview and perspectives. *J. Controlled Release* **2016,** *240*, 24-37.
(259) Lv J.; He, B.; Yu, J.; Wang, Y.; Wang, C.; Zhang, S.; Wang, H.; Hu, J.; Zhang, Q.; Cheng, Y., Fluoropolymers for intracellular and in vivo protein delivery. *Biomaterials* **2018,** *182*, 167-175.
(260) Lv J.; Fan, Q.; Wang, H.; Cheng, Y., Polymers for cytosolic protein delivery. *Biomaterials* **2019,** *218*, 119358.
(261) Ren L.; Lv, J.; Wang, H.; Cheng, Y., A Coordinative Dendrimer Achieves Excellent Efficiency in Cytosolic Protein and Peptide Delivery. *Angew. Chem. Int. Ed.* **2020,** *59*, 4711-4719.
(262) Lv J.; Wang, C.; Li, H.; Li, Z.; Fan, Q.; Zhang, Y.; Li, Y.; Wang, H.; Cheng, Y., Bifunctional and Bioreducible Dendrimer Bearing a Fluoroalkyl Tail for Efficient Protein Delivery Both In Vitro and In Vivo. *Nano Lett.* **2020,** *20*, 8600-8607.
(263) Fu C.; Demir, B.; Alcantara, S.; Kumar, V.; Han, F.; Kelly, H. G.; Tan, X.; Yu, Y.; Xu, W.; Zhao, J.; Zhang, C.; Peng, H.; Boyer, C.; Woodruff, T. M.; Kent, S. J.; Searles, D. J.; Whittaker, A. K., Low-Fouling Fluoropolymers for Bioconjugation and In Vivo Tracking. *Angew. Chem. Int. Ed.* **2020,** *59*, 4729-4735.
(264) Gong P.; Zhao, Q.; Dai, D.; Zhang, S.; Tian, Z.; Sun, L.; Ren, J.; Liu, Z., Functionalized Ultrasmall Fluorinated Graphene with High NIR Absorbance for Controlled Delivery of Mixed Anticancer Drugs. *Chem. Eur. J.* **2017,** *23*, 17531-17541.
(265) Hu Q.; Sun, W.; Wang, C.; Gu, Z., Recent advances of cocktail chemotherapy by combination drug delivery systems. *Adv. Drug Deliv. Rev.* **2016,** *98*, 19-34.
(266) Mohammadi M. R.; Nojoomi, A.; Mozafari, M.; Dubnika, A.; Inayathullah, M.; Rajadas, J., Nanomaterials engineering for drug delivery: a hybridization approach. *J. Mater. Chem. B* **2017,** *5*, 3995-4018.

(267) Vonarbourg A.; Passirani, C.; Saulnier, P.; Benoit, J.-P., Parameters influencing the stealthiness of colloidal drug delivery systems. *Biomaterials* **2006,** *27*, 4356-4373.
(268) Parveen S.; Misra, R.; Sahoo, S. K., Nanoparticles: a boon to drug delivery, therapeutics, diagnostics and imaging. *Nanomedicine* **2012,** *8*, 147-166.
(269) Zhang C.; Liu, T.; Wang, W.; Bell, C. A.; Han, Y.; Fu, C.; Peng, H.; Tan, X.; Král, P.; Gaus, K.; Gooding, J. J.; Whittaker, A. K., Tuning of the Aggregation Behavior of Fluorinated Polymeric Nanoparticles for Improved Therapeutic Efficacy. *ACS Nano* **2020,** *14*, 7425-7434.
(270) Xu D.; Li, A.; Lin, W.; Zou, Q.; Wu, S.; Mondal, A. K.; Xiao, W.; Huang, F., Preparation and characterization of pH and thermally responsive perfluoropolyether acrylate copolymer micelles and investigation its drug-loading properties. *J. Appl. Polym. Sci.* **2023,** *140*, e53805.
(271) Du W.; Xu, Z.; Nyström, A. M.; Zhang, K.; Leonard, J. R.; Wooley, K. L., 19F- and Fluorescently Labeled Micelles as Nanoscopic Assemblies for Chemotherapeutic Delivery. *Bioconjugate Chem.* **2008,** *19*, 2492-2498.
(272) Fu C.; Bongers, A.; Wang, K.; Yang, B.; Zhao, Y.; Wu, H.; Wei, Y.; Duong, H. T. T.; Wang, Z.; Tao, L., Facile synthesis of a multifunctional copolymer via a concurrent RAFT-enzymatic system for theranostic applications. *Polym. Chem.* **2016,** *7*, 546-552.
(273) Dolmans D. E. J. G. J.; Fukumura, D.; Jain, R. K., Photodynamic therapy for cancer. *Nat. Rev. Cancer* **2003,** *3*, 380-387.
(274) Castano A. P.; Mroz, P.; Hamblin, M. R., Photodynamic therapy and anti-tumour immunity. *Nat. Rev. Cancer* **2006,** *6*, 535-545.
(275) Lovell J. F.; Liu, T. W. B.; Chen, J.; Zheng, G., Activatable Photosensitizers for Imaging and Therapy. *Chem. Rev.* **2010,** *110*, 2839-2857.
(276) Abrahamse H.; Hamblin, Michael R., New photosensitizers for photodynamic therapy. *Biochem. J.* **2016,** *473*, 347-364.
(277) Yuan P.; Ruan, Z.; Jiang, W.; Liu, L.; Dou, J.; Li, T.; Yan, L., Oxygen self-sufficient fluorinated polypeptide nanoparticles for NIR imaging-guided enhanced photodynamic therapy. *J. Mater. Chem. B* **2018,** *6*, 2323-2331.
(278) Dias A. M. A.; Bonifácio, R. P.; Marrucho, I. M.; Pádua, A. A. H.; Costa Gomes, M. F., Solubility of oxygen in n-hexane and in n-perfluorohexane. Experimental determination and prediction by molecular simulation. *Phys. Chem. Chem. Phys.* **2003,** *5*, 543-549.
(279) Lu K.; He, C.; Lin, W., Nanoscale Metal–Organic Framework for Highly Effective Photodynamic Therapy of Resistant Head and Neck Cancer. *J. Am. Chem. Soc.* **2014,** *136*, 16712-16715.
(280) Wallat J. D.; Wek, K. S.; Chariou, P. L.; Carpenter, B. L.; Ghiladi, R. A.; Steinmetz, N. F.; Pokorski, J. K., Fluorinated polymer–photosensitizer conjugates enable improved generation of ROS for anticancer photodynamic therapy. *Polym. Chem.* **2017,** *8*, 3195-3202.
(281) Aricò A. S.; Bruce, P.; Scrosati, B.; Tarascon, J.-M.; van Schalkwijk, W., Nanostructured materials for advanced energy conversion and storage devices. *Nat. Mater.* **2005,** *4*, 366-377.
(282) Zhang X.; Shen, Y.; Zhang, Q.; Gu, L.; Hu, Y.; Du, J.; Lin, Y.; Nan, C.-W., Ultrahigh Energy Density of Polymer Nanocomposites Containing BaTiO3@TiO2 Nanofibers by Atomic-Scale Interface Engineering. *Adv. Mater.* **2015,** *27*, 819-824.

(283) Chu B.; Zhou, X.; Ren, K.; Neese, B.; Lin, M.; Wang, Q.; Bauer, F.; Zhang, Q. M., A Dielectric Polymer with High Electric Energy Density and Fast Discharge Speed. *Science* **2006,** *313*, 334-336.

(284) Prateek; Thakur, V. K.; Gupta, R. K., Recent Progress on Ferroelectric Polymer-Based Nanocomposites for High Energy Density Capacitors: Synthesis, Dielectric Properties, and Future Aspects. *Chem. Rev.* **2016,** *116*, 4260-4317.

(285) Tang H.; Sodano, H. A., Ultra High Energy Density Nanocomposite Capacitors with Fast Discharge Using Ba0.2Sr0.8TiO3 Nanowires. *Nano Lett.* **2013,** *13*, 1373-1379.

(286) Yang K.; Huang, X.; Huang, Y.; Xie, L.; Jiang, P., Fluoro-Polymer@BaTiO3 Hybrid Nanoparticles Prepared via RAFT Polymerization: Toward Ferroelectric Polymer Nanocomposites with High Dielectric Constant and Low Dielectric Loss for Energy Storage Application. *Chem. Mater.* **2013,** *25*, 2327-2338.

(287) Zhou J.; Hou, D.; Cheng, S.; Zhang, J.; Chen, W.; Zhou, L.; Zhang, P., Recent advances in dispersion and alignment of fillers in PVDF-based composites for high-performance dielectric energy storage. *Mater. Today Energy* **2023,** *31*, 101208.

(288) Varun S.; George, N. M.; Chandran, A. M.; Varghese, L. A.; Mural, P. K. S., Multifaceted PVDF nanofibers in energy, water and sensors: A contemporary review (2018 to 2022) and future perspective. *J. Fluor. Chem.* **2023,** *265*, 110064.

(289) Bouharras F. E.; Labardi, M.; Tombari, E.; Capaccioli, S.; Raihane, M.; Améduri, B., Dielectric Characterization of Core-Shell Structured Poly(vinylidene fluoride)-grafted-BaTiO3 Nanocomposites. *Polymers* **2023,** *15*, 595.

(290) Améduri B., *Perfluoroalkyl Substances: Synthesis, Properties, Applications and Regulations*. Royal Society of Chemistry: Oxford, 2022.

(291) Lehmler H.-J., Synthesis of environmentally relevant fluorinated surfactants—a review. *Chemosphere* **2005,** *58*, 1471-1496.

(292) Hu X. C.; Andrews, D. Q.; Lindstrom, A. B.; Bruton, T. A.; Schaider, L. A.; Grandjean, P.; Lohmann, R.; Carignan, C. C.; Blum, A.; Balan, S. A.; Higgins, C. P.; Sunderland, E. M., Detection of Poly- and Perfluoroalkyl Substances (PFASs) in U.S. Drinking Water Linked to Industrial Sites, Military Fire Training Areas, and Wastewater Treatment Plants. *Environ. Sci. Technol. Lett.* **2016,** *3*, 344-350.

(293) Kotthoff M.; Müller, J.; Jürling, H.; Schlummer, M.; Fiedler, D., Perfluoroalkyl and polyfluoroalkyl substances in consumer products. *Environ. Sci. Pollut. Res.* **2015,** *22*, 14546-14559.

(294) Lohmann R.; Cousins, I. T.; DeWitt, J. C.; Glüge, J.; Goldenman, G.; Herzke, D.; Lindstrom, A. B.; Miller, M. F.; Ng, C. A.; Patton, S.; Scheringer, M.; Trier, X.; Wang, Z., Are Fluoropolymers Really of Low Concern for Human and Environmental Health and Separate from Other PFAS? *Environ. Sci. Technol.* **2020,** *54*, 12820-12828.

(295) Ameduri B., Fluoropolymers: A special class of per- and polyfluoroalkyl substances (PFASs) essential for our daily life. *J. Fluor. Chem.* **2023,** *267*, 110117.

(296) Henry B. J.; Carlin, J. P.; Hammerschmidt, J. A.; Buck, R. C.; Buxton, L. W.; Fiedler, H.; Seed, J.; Hernandez, O., A critical review of the application of polymer of low concern and regulatory criteria to fluoropolymers. *Integr. Environ. Assess. Manag.* **2018,** *14*, 316-334.

(297) Korzeniowski S. H.; Buck, R. C.; Newkold, R. M.; kassmi, A. E.; Laganis, E.; Matsuoka, Y.; Dinelli, B.; Beauchet, S.; Adamsky, F.; Weilandt, K.; Soni, V. K.; Kapoor, D.; Gunasekar, P.; Malvasi, M.; Brinati, G.; Musio, S., A critical review of the application of polymer of low concern regulatory criteria to fluoropolymers II: Fluoroplastics and fluoroelastomers. *Integr. Environ. Assess. Manag.* **2023,** *19*, 326-354.

(298) European Chemicals Agency (ECHA), "ECHA receives PFASs restriction proposal from five national authorities" can be found under https://echa.europa.eu/fr/-/echa-receives-pfass-restriction-proposal-from-five-national-authorities

(299) Lindstrom A. B.; Strynar, M. J.; Libelo, E. L., Polyfluorinated Compounds: Past, Present, and Future. *Environ. Sci. Technol.* **2011,** *45*, 7954-7961.

(300) Interstate Technology & Requlatory Council (ITRC) online document, "PFAS Technical and Regulatory Guidance Document" and "Fact Sheets PFAS-1", can be found under https://pfas-1itrcweb.org/.

(301) Kumarasamy E.; Manning, I. M.; Collins, L. B.; Coronell, O.; Leibfarth, F. A., Ionic Fluorogels for Remediation of Per- and Polyfluorinated Alkyl Substances from Water. *ACS Cent. Sci.* **2020,** *6*, 487-492.

(302) Tan X.; Sawczyk, M.; Chang, Y.; Wang, Y.; Usman, A.; Fu, C.; Král, P.; Peng, H.; Zhang, C.; Whittaker, A. K., Revealing the Molecular-Level Interactions between Cationic Fluorinated Polymer Sorbents and the Major PFAS Pollutant PFOA. *Macromolecules* **2022,** *55*, 1077-1087.

(303) Choudhary A.; Bedrov, D., Interaction of Short-Chain PFAS with Polycationic Gels: How Much Fluorination is Necessary for Efficient Adsorption? *ACS Macro Lett.* **2022,** *11*, 1123-1128.

(304) Verduzco R.; Wong, M. S., Fighting PFAS with PFAS. *ACS Cent. Sci.* **2020,** *6*, 453-455.

(305) Koda Y.; Terashima, T.; Nomura, A.; Ouchi, M.; Sawamoto, M., Fluorinated Microgel-Core Star Polymers as Fluorous Compartments for Molecular Recognition. *Macromolecules* **2011,** *44*, 4574-4578.

(306) Manning I. M.; Guan Pin Chew, N.; Macdonald, H. P.; Miller, K. E.; Strynar, M. J.; Coronell, O.; Leibfarth, F. A., Hydrolytically Stable Ionic Fluorogels for High-Performance Remediation of Per- and Polyfluoroalkyl Substances (PFAS) from Natural Water. *Angew. Chem. Int. Ed.* **2022,** *61*, e202208150.

(307) Xiao L.; Ling, Y.; Alsbaiee, A.; Li, C.; Helbling, D. E.; Dichtel, W. R., β-Cyclodextrin Polymer Network Sequesters Perfluorooctanoic Acid at Environmentally Relevant Concentrations. *J. Am. Chem. Soc.* **2017,** *139*, 7689-7692.

(308) DiStefano R.; Feliciano, T.; Mimna, R. A.; Redding, A. M.; Matthis, J., Thermal destruction of PFAS during full-scale reactivation of PFAS-laden granular activated carbon. *Remediation* **2022,** *32*, 231-238.

(309) Sathe D.; Zhou, J.; Chen, H.; Schrage, B. R.; Yoon, S.; Wang, Z.; Ziegler, C. J.; Wang, J., Depolymerizable semi-fluorinated polymers for sustainable functional materials. *Polym. Chem.* **2022,** *13*, 2608-2614.

(310) Oh M. S.; Jeon, M.; Jeong, K.; Ryu, J.; Im, S. G., Synthesis of a Stretchable but Superhydrophobic Polymer Thin Film with Conformal Coverage and Optical Transparency. *Chem. Mater.* **2021,** *33*, 1314-1320.

(311) Ouhib F.; Dirani, A.; Aqil, A.; Glinel, K.; Nysten, B.; Jonas, A. M.; Jerôme, C.; Detrembleur, C., Transparent superhydrophobic coatings from amphiphilic-fluorinated block copolymers synthesized by aqueous polymerization-induced self-assembly. *Polym. Chem.* **2016,** *7*, 3998-4003.
(312) Pera-Titus M.; Leclercq, L.; Clacens, J.-M.; De Campo, F.; Nardello-Rataj, V., Pickering Interfacial Catalysis for Biphasic Systems: From Emulsion Design to Green Reactions. *Angew. Chem. Int. Ed.* **2015,** *54*, 2006-2021.
(313) Boissenot T.; Bordat, A.; Fattal, E.; Tsapis, N., Ultrasound-triggered drug delivery for cancer treatment using drug delivery systems: From theoretical considerations to practical applications. *J. Controlled Release* **2016,** *241*, 144-163.
(314) Paefgen V.; Doleschel, D.; Kiessling, F., Evolution of contrast agents for ultrasound imaging and ultrasound-mediated drug delivery. *Front. Pharmacol.* **2015,** *6*, 197.
(315) Zhong Z.-R.; Chen, Y.-N.; Zhou, Y.; Chen, M., Challenges and Recent Developments of Photoflow-Reversible Deactivation Radical Polymerization (RDRP). *Chinese J. Polym. Sci.* **2021,** *39*, 1069-1083.
(316) Wang Z.; Zhou, Y.; Chen, M., Computer-Aided Living Polymerization Conducted under Continuous-Flow Conditions. *Chin. J. Chem.* **2022,** *40*, 285-296.
(317) Ma M.; Shao, F.; Wen, P.; Chen, K.; Li, J.; Zhou, Y.; Liu, Y.; Jia, M.; Chen, M.; Lin, X., Designing Weakly Solvating Solid Main-Chain Fluoropolymer Electrolytes: Synergistically Enhancing Stability toward Li Anodes and High-Voltage Cathodes. *ACS Energy Lett.* **2021,** *6*, 4255-4264.
(318) Zeng Y.; Quan, Q.; Wen, P.; Zhang, Z.; Chen, M., Organocatalyzed Controlled Radical Copolymerization toward Hybrid Functional Fluoropolymers Driven by Light. *Angew. Chem. Int. Ed.* **2022,** *61*, e202215628.
(319) Huang Z.; Choudhury, S.; Gong, H.; Cui, Y.; Bao, Z., A Cation-Tethered Flowable Polymeric Interface for Enabling Stable Deposition of Metallic Lithium. *J Am Chem Soc* **2020,** *142*, 21393-21403.
(320) Pester C. W.; Narupai, B.; Mattson, K. M.; Bothman, D. P.; Klinger, D.; Lee, K. W.; Discekici, E. H.; Hawker, C. J., Engineering surfaces through sequential stop-flow photopatterning. *Adv. Mater.* **2016,** *28*, 9292-9300.
(321) Discekici E. H.; Pester, C. W.; Treat, N. J.; Lawrence, J.; Mattson, K. M.; Narupai, B.; Toumayan, E. P.; Luo, Y.; McGrath, A. J.; Clark, P. G.; Read de Alaniz, J.; Hawker, C. J., Simple Benchtop Approach to Polymer Brush Nanostructures Using Visible-Light-Mediated Metal-Free Atom Transfer Radical Polymerization. *ACS Macro Lett.* **2016,** *5*, 258-262.
(322) Cai T.; Neoh, K.-G.; Kang, E.-T., Functionalized and Functionalizable Fluoropolymer Membranes. In *Handbook of Fluoropolymer Science and Technology*, Smith, D. W.; Iacono, S. T.; Iyer, S. S., Eds. 2014; pp 149-181.
(323) Cui Z.; Drioli, E.; Lee, Y. M., Recent progress in fluoropolymers for membranes. *Prog. Polym. Sci.* **2014,** *39*, 164-198.